



Institute for Water
and Energy Sciences
(incl. Climate Change)



PAN-AFRICAN UNIVERSITY
INSTITUTE FOR WATER AND ENERGY SCIENCES
(including CLIMATE CHANGE)

Master Dissertation

Submitted in partial fulfillment of the requirements for the Master's degree in
[CLIMATE CHANGE ENGINEERING]

Presented by

Tafara Chikosha

**Powering through uncertainty. Assessing the impact of climate change on
hydropower generation: A case study of Kariba South Hydropower Station,
Kariba subbasin, Zimbabwe.**

Defended on 16/04/2025 Before the Following Committee:

Chair: Dr Anabella Ferral, The Mario Gulich Institute, Argentina (UNC)

Supervisor: Dr. Amos T. Kabo-bah, University of Energy and Natural Resources (UENR)

External Examiner: Pr. Hamouda Boutaghane, University of Badji Mokhtar-Annaba

Internal Examiner: Dr Tayeb Hocine, University Abou Bekr Belkaid-Tlemcen

DECLARATION

I hereby declare that the research is original and has not been submitted to other universities for the award of any degree.



Signature:

Date:25/03/2025

Name: Tafara Chikosha

Tack: Climate Change Engineering

University: Pan African University Institute of Water and Energy Sciences, Including Climate Change.

University of Tlemcen, Algeria

Supervisor

RECOMMENDATION

This master's research thesis was conducted by the candidate independently, with my help and direction. For this reason, I approve this work for examination.

Signature:

Date:25/03/2025

Name: Dr. Amos T. Kabo-bah

Dedication

This piece is a heartfelt tribute to my beloved grandmother, Rina Eustina Chigwendere. Her steadfast belief in my dreams, which she instilled in me with her unwavering support, inspires me daily. Although she's no longer by my side, her selfless love has been the foundation of my academic journey. I celebrate this achievement with immense gratitude, honouring her wish for my success. I hold her memory close and cherish the thought of her finding peace in heaven, watching over me with pride.

ACKNOWLEDGMENT

First and foremost, I would like to express my deepest gratitude to Prof Amos Kabo-bah for his invaluable guidance, encouragement, and support throughout this research process. His expertise and mentorship have been instrumental in shaping this thesis and helping me navigate the challenges I encountered.

I am profoundly thankful to the Zambezi River Authority for granting me access to crucial data on river discharge, effective storage, and water level. Of particular mention is Mr Pherry Mwiinga, a hydrologist at the Zambezi River Authority, whose dedication and assistance were pivotal in securing the hydrological data promptly. Your efforts and generosity with your time and knowledge are deeply appreciated.

I am equally grateful to the Meteorological Service Department of Zimbabwe for their assistance in providing me with the climate data for my study area. I wish to particularly thank Mr Chawaguta a meteorologist at the Meteorological Service Department, who supervised me during my internship and played a significant role in facilitating access to the climate data.

I want to express sincere gratitude to the Algerian government for making my stay in Algeria possible, as well as to the African Union Commission (AUC) through the Pan African University Institute of Water and Energy Sciences, including Climate Change (PAUWES) for providing me with the scholarship that allowed me to pursue my postgraduate studies. I was able to pursue and finish this study thanks to your assistance.

I am deeply grateful to all the individuals and organizations who have contributed in one way or another to the successful completion of this work. Thank you for your support, encouragement, and trust in my potential.

Tafara Chikosha

ABSTRACT

The Intergovernmental Panel on Climate Change (IPCC) AR5 highlights that climate change already impacts water resources, leading to extreme precipitation, floods, cyclones, decreased runoff in water-stressed regions, and expanding drought areas. These effects are evident in the Zambezi River Basin, Africa's fourth-largest river system. This study assesses the impact of climate change on the hydropower generation capacity of the Kariba South Hydropower Station (KSHS) in Zimbabwe's Kariba Subbasin over the past three decades. As hydropower remains Zimbabwe's primary renewable electricity source, with KSHS currently contributing 185 MW to the national grid, understanding climate-induced hydrological changes is crucial for the energy security of Zimbabwe. The research examines historical trends in precipitation, temperature, river flow, and effective live storage from 1990 to 2019 using data from the Meteorological Services Department of Zimbabwe (MSD) and the Zambezi River Authority (ZRA). Data analysis was conducted using XLSTAT version 2024.4.

Preliminary findings indicate a slight increase in annual mean maximum temperature at both Binga and Kariba stations over the study period. The annual mean minimum temperature exhibited a slight increase from 1990 to 1998 at Binga and from 1990 to 1997 at Kariba, followed by a slight decrease from 1999 to 2019 at Binga and from 1998 to 2019 at Kariba. However, these temperature trends were not statistically significant. Precipitation trends varied across the stations, with Binga slightly experiencing increasing annual and seasonal total rainfall, while Kariba exhibited a decreasing trend. However, neither trend was statistically significant. River flow patterns at three gauging stations along the Zambezi River also revealed notable variations. Chavuma Gauging Station recorded a decline in discharge from 1990 to 1997, followed by an increasing trend from 1998 to 2019. Similarly, flow at the Victoria Falls Gauging Station declined from 1990 to 1997 but increased afterward. In contrast, the Ngonye Hydro Gauging Station exhibited a consistent decline in discharge across the study period, 2005-2019. These river flow changes directly impact water availability into Lake Kariba's inflows, influencing the hydropower generation capacity at KSHS.

These findings highlight Zimbabwe's hydropower sector's vulnerability to climate change, emphasizing the need for adaptive strategies to enhance energy security. The study provides critical insights for policymakers and energy planners to develop climate-resilient hydropower infrastructure in the Middle Zambezi River Basin.

Keywords: Climate Change, Hydropower, Water resources, Kariba Subbasin

TABLE OF CONTENTS

DECLARATION AND RECOMMENDATIONS	(i)
DECLARATION	(i)
RECOMMENDATIONS	(i)
Dedication	(ii)
Acknowledgment	(iii)
Abstract	(iv)
List of Tables	(V)
List of Figures	(vi)
List of Abbreviations	(vii)
CHAPTER ONE	1
INTRODUCTION	1
1.1Background Information	1
1.2Statement of the problem	4
1.3Objectives	5
1.4Research questions	6
1.5Hypothesis	6
1.6 Justification of study	6
1.7 Scope of the Study and Limitations	7
1.8 Structure of the thesis	8
CHAPTER TWO	10
LITERATURE REVIEW	10
2.1 Climate Change A Global Perspective	10
2.2 Overview of climate in Zimbabwe	11
2.3 Overview of hydropower	13
2.4 Hydropower in Zimbabwe	15

2.5 Hydropower generation in the Zambezi River Basin and climate change	16
2.6 Climate Change in the Zambezi River Basin	19
2.7 Impact of climate change on water resources.....	21
2.8 Impact of climate change on river flow	23
2.9 Climate Change Modelling.....	25
2.10 Downscaling global Climate models to regional Scales	26
2.11 Bias correction	28
2.12 Climate Scenarios.....	29
CHAPTER THREE	32
METHODOLOGY AND MATERIALS.....	32
3.1 Study area	32
3.1.1 Location.....	32
3.1.2 Climate of study area	33
3.1.2 Topography.....	34
3.1.3 Geology and Soils	36
3.1.4 Land use and Land cover	39
3.2 Methodology Flow Chart.....	41
3.2.1 Data collection and preprocessing	41
3.2.2 Soil and soil texture data	44
3.2.3 Data cleaning and standardisation	45
3.2.4 Homogeneity test and trend analysis.....	45
3.2.5 Homogeneity test	46
3.2.6 The Mann-Kendall test for monotonic trends	47
3.2.7 The magnitude of the trend (Sens slope estimator).....	49
3.2.8 Determination of precipitation and temperature trends.....	50
3.2.9 Determination of Discharge Trends	51
CHAPTER FOUR.....	52

Results and Discussion	52
4.0 Temperature and precipitation trends from 1990-2019	52
4.1 Binga and Kariba annual mean maximum temperature	54
4.1.1 Homogeneity test for Binga and Kariba annual mean maximum temperature.....	54
4.1.2 Trend analysis for Binga and Kariba annual mean maximum temperature	55
4.2 Binga and Kariba annual mean minimum temperature	58
4.2.1 Homogeneity test for Binga and Kariba annual mean minimum temperature	58
4.2.2 Trend Analysis for Binga and Kariba Annual Mean Minimum Temperature.....	59
4.3 Binga and Kariba Annual Total precipitation	63
4.3.1 Homogeneity test for Binga and Kariba for Annual total precipitation.....	66
4.3.2 Trend Analysis for Binga and Kariba Annual total Precipitation	70
4.5 River flow	73
4.5.1 Ngonye Rapids (Sioma Falls) gauging station	74
4.5.1.2 Homogeneity test for Ngonye River flow	74
4.5.1.3 Trend analysis for Ngonye River flow.....	75
4.5.2 Chavuma Mission Gauging Station.....	76
4.5.2.1 Homogeneity test for Chavuma station discharge	76
4.5.2.2 Trend analysis for Chavuma station	77
4.5.3 Victoria Falls (Big Tree Station)	79
4.5.3.1 Homogeneity test for Victoria Falls River flow	80
4.5.3.2. Trend analysis for Victoria Falls River flow.....	80
4.5.4 Lake Kariba reservoir level.....	83
4.5.4.1 Homogeneity test for total Annual mean Lake level.....	84
4.5.4.2 Mann-Kendall test for Annual mean lake level	84
4.5.5 Effective live storage	85
4.5.6 Future Projections.....	87
4.5.6.1 Projected Annual mean maximum temperature	87

4.5.6.2 Projected Annual Mean Minimum Temperature.....	88
4.5.6.3 Projected Annual total precipitation	90
CHAPTER FIVE.....	92
CONCLUSION AND RECOMMENDATIONS	92
5.1 CONCLUSION.....	92
5.2 RECOMMENDATIONS.....	94
REFERENCES.....	96

List of Tables

Table 2.1: Hydropower Potential Capacity.....	14
Table 2.2: Kariba South Hydropower Station (KSHS) generators.....	16
Table 2.3: List of selected GCMs used in this study.....	26
Table 3.1: Data Used and Corresponding Sources.....	42
Table 3.2: List of meteorological stations used for this study.....	43
Table 3.3: List of Hydro gauging stations used for this study.....	43
Table 4.1: Climate change indicators of Kariba Subbasin (Binga station)	52
Table 4.2: Climate change indicators of Kariba Subbasin (Kariba station).....	53
Table 4.3: Homogeneity test for Binga and Kariba annual mean maximum temperature (°C)	58
Table 4.4: Trend analysis for Binga and Kariba annual mean maximum temperature (°C).....	58
Table 4.5: Homogeneity test for Binga and Kariba annual mean minimum temperature (°C)	62
Table 4.6: Trend analysis for Binga and Kariba annual mean minimum temperature (°C)	63
Table 4.7: Binga and Kariba annual total precipitation and seasonal precipitation (NDJFM) Homogeneity test from 1990-2019.....	69
Table 4.8: Binga and Kariba seasonal and annual total precipitation Mann-Kendall and Sens Slope trend analysis from 1990-2019.....	69
Table 4.9: Results of the Pettitt’s homogeneity test, Mann-Kendall, and Sens slope trend tests on annual mean maximum temperature.....	71
Table 4.10: Results of the Pettitt’s homogeneity test, Mann-Kendall and Sens slope trend tests on annual mean maximum temperature	72
Table 4.11: Results of the Pettitt’s homogeneity test, Mann-Kendall and Sens slope trend tests on annual total and seasonal precipitation.....	74
Table 4.12: Annual mean discharge at Chavuma Mission, Ngonye (Sioma Falls), and Victoria Falls stations.....	81
Table 4.13: Homogeneity test for Chavuma Mission,	

Ngonye Rapids (Sioma Falls), and Victoria Falls (Big Tree Station) 1990-2019.....	82
Table 4.14: MK trend test for annual mean river flow for Chavuma , Ngonye, and Victoria Falls.....	82
Table 4.15: Sen’s slope test for annual mean river flow for, Ngonye Rapids, Chavuma, and Victoria Falls	82
Table 4.16: Lake Kariba Pettitt’s homogeneity test, Mann-Kendall , and Sens slope trend test.....	85

List of Figures

Figure 2.1: Schematic layout of the Zambezi River’s existing and potential hydroelectric power sites. Source.....	17
Figure 2.2: Predicted atmospheric CO ₂ concentration for different shared socioeconomic pathways (SSPs) across the 21 st century	31
Figure 3.1: Study area map of the Kariba subbasin.....	33
Figure 3.2: Kariba subbasin topographical map.....	35
Figure 3.3: Soil map of Kariba subbasin.....	37
Figure 3.4: Major soil texture of Kariba subbasin.....	38
Figure 3.5: Land Use Land Cover Map of 2023 Kariba subbasin.....	40
Figure 3.6: Methodological flow chart.....	41
Figure 3.7 :Locations of Hydro gauging and meteorological stations used for the study.....	44
Figure 4.1: Binga annual mean maximum temperature 1990-2019.....	55
Figure 4.2: Kariba annual mean maximum temperature 1990-2019.....	55
Figure 4.3: Binga annual mean maximum temperature 1990-2019.....	56
Figure 4.4: Kariba annual mean maximum temperature 1990-1997.....	57
Figure 4.5: Kariba annual mean maximum temperature 1998-2019.....	57
Figure 4.6: Binga homogeneity test annual mean minimum temperature 1990-2019.....	59
Figure 4.7: Kariba homogeneity test annual mean minimum temperature (1990-2019).....	59
Figure 4.8: Binga annual mean minimum temperature (°C) 1990-1998.....	60
Figure 4.9: Binga annual mean minimum temperature (°C) 1999-2019.....	61
Figure 4.10: Kariba annual mean minimum temperature (°C) 1990-1997.....	61
Figure 4.11: Kariba annual mean minimum temperature (°C) 1998-2019.....	62
Figure 4.12: Binga seasonal precipitation homogeneity test 1990-2019.....	64
Figure 4.13: Kariba seasonal precipitation homogeneity test 1990-2019.....	64
Figure 4.14: Binga total annual precipitation 1990-2019.....	65
Figure 4.15: Kariba total annual precipitation 1990-2019.....	65
Figure 4.16: Binga seasonal total precipitation (NDJFM) 1990-2019.....	65
Figure 4.17: Binga total annual precipitation 1990-2019.....	66

Figure 4.18: Kariba seasonal (NDJFM) total precipitation 1990-2019.....	67
Figure 4.19: Kariba total annual precipitation 1990-1995.....	68
Figure 4.20: Kariba total annual precipitation 1996-2019.....	68
Figure 4.21: Annual mean maximum temperature for NASA Power meteorological stations in the Kariba subbasin.....	72
Figure 4.22: Annual mean minimum temperature for NASA POWER meteorological stations in the Kariba subbasin.....	73
Figure 4.23: Annual total precipitation for NASA POWER meteorological stations in the Kariba subbasin.....	73
Figure 4.24: Homogeneity test for Ngonye (Sioma Falls) annual mean discharge 2005-2019.....	75
Figure 4.25: Trend analysis for Ngonye (Sioma Falls) annual mean discharge 2005-2019.....	76
Figure 4.26: Homogeneity test for Chavuma Mission annual mean discharge 1990-2019.....	77
Figure 4.27: Trend analysis for Chavuma Mission station annual mean discharge 1990-1997.....	78
Figure 4.28: Chavuma Mission station annual mean discharge 1998 -2019.....	78
Figure 4.29: Homogeneity test for Victoria Falls (Big Tree Station annual mean discharge 1990-2019.....	79
Figure 4.30: Victoria Falls (Big Tree station) annual mean discharge (m ³ /s) 1990-2019.....	80
Figure 4.31: Homogeneity test for Lake Kariba mean annual water level.....	81
Figure 4.32: Mann-Kendall trend test for Lake Kariba mean annual water level (1990-1998).....	83
Figure 4.33: Mann-Kendall trend test for Lake Kariba mean annual water level (1999-2019).....	84
Figure 4.34: Kariba Effective live storage in billion cubic meters BCM 1990-2023.....	85
Figure 4.35: Projected annual mean maximum temperature (°C) SSP245 2041-2065.....	86
Figure 4.36: Projected annual mean maximum temperature (°C) SSP585 2041-2065.....	88
Figure 4.37: Projected annual mean minimum temperature (°C) SSP245 2041-2065.....	88
Figure 4.38: Projected annual mean minimum temperature (°C) SSP585 2041-2065.....	89
Figure 4.39: Figure 4.37: Projected future precipitation for the Kariba	

subbasin under 4 GCM SSP 245 models for the future 2041-2065.....89
Figure 4.40: Figure 4.37: Projected future precipitation for the Kariba
subbasin under 4 GCM models SSP 585 future 2041-2065.....90

List of Abbreviations

BCM - Billion Cubic Meters

CC - Climate Change

CH₄ – Methane

CMIP6 - Coupled Model Intercomparison Project

GHGs - Greenhouse Gases

GWh - Gigawatt Hours

IPCC - Intergovernmental Panel for Climate Change

LULC - Land Use Land Cover

MK - Mann-Kendall

MSD - Meteorological Services Department of Zimbabwe

MW - Megawatts

NDJFM - November December January February March

RoR - Run-of-River

SADC - Southern African Development Community

SAPP - Southern African Power Pool

ZRA - Zambezi River Authority

ZRB - Zambezi River Basin

CHAPTER ONE

INTRODUCTION

1.1 Background Information

The United Nations Framework Convention on Climate Change (UNFCCC, 1992), in its Article 1, defines climate change as "a change of climate that is attributed directly or indirectly to human activity that alters the composition of the global atmosphere and which is in addition to natural climate variability observed over comparable periods". Climate variability, according to the Intergovernmental Panel on Climate Change (IPCC, 2014), refers to "the variations in the mean state and other statistics (such as standard deviations and the occurrence of extremes) of the climate on all spatial and temporal scales beyond that of individual weather events." Climate change (CC) and climate variability are both anticipated to significantly influence precipitation and runoff patterns in various regions, which serve as inflows to surface reservoirs at hydropower facilities. Subsequently, this will impact the prospective contribution of these assets to the total portfolio of power generation.

The development of hydropower and other renewable energy sources is becoming increasingly important for meeting electricity generation targets and climate mitigation initiatives due to the sharp increase in global energy demands and greenhouse gas emissions. Hydropower is essential to worldwide initiatives aimed at fulfilling Sustainable Development Goal (SDG) 7, which seeks to ensure access to affordable, dependable, sustainable, and modern energy for all, with hydropower being a pivotal component of this agenda (Kamal et al., 2021). Climate change poses a significant threat to global energy systems, particularly hydropower generation, which is highly susceptible to precipitation patterns and water availability variations. This vulnerability underscores the urgent need for adaptive strategies. The impacts of climate change are increasingly jeopardizing the operational effectiveness and contribution of existing water infrastructures, particularly hydropower plants, to the national energy portfolios. The availability and accessibility of vital natural resources are significantly impacted by climate change and variability, which also shapes ecosystems and human activity. Since temperature variations, precipitation patterns, and extreme weather events affect hydrological cycles, water availability, and water quality, water resources are especially at risk. The phenomenon alters the natural availability of water, groundwater levels, and streamflow patterns, leading to significant implications for ecosystems and human activities

(Teweldebrihan & Dinka, 2024). In most parts of the world, climate change is already affecting the physical processes, leading to changes in precipitation patterns, with some areas or regions receiving less rainfall and others receiving more rainfall, increased surface temperatures, and the increased frequency of extreme events such as floods, droughts, heatwaves, and cyclones (Ebi et al., 2020).

Africa's high sensitivity, exposure, and limited capacity for adaptation make it a continent considered highly vulnerable to the effects of climate change. One of Africa's most vulnerable regions is considered to be Southern Africa (Davis-Reddy & Vincent, 2017). Climate projections suggest that Southern Africa will face heightened effects on water resources, potentially worsening existing stress (Gan et al., 2016). A significant source of electricity in Southern Africa, hydropower is highly susceptible to changes in water availability brought on by climate change and hydrological fluctuations. The capacity of hydropower generation can be significantly impacted by variations in temperature, precipitation patterns, and extreme weather events, which could pose problems for the region's energy security. Regional studies on the impact of climate change on water resources and hydropower generation review that, while some regions may experience increased hydropower generation due to climate-induced changes in water availability, others may see significant reductions (Oyerinde et al., 2016; Spalding-Fecher et al., 2016; Tarroja et al., 2016). The increasing energy demand across the African continent, where hydropower contributes significantly to the energy mix and the need for sustainable energy system development, necessitates a comprehensive understanding of these systems and the challenges climate change poses. A key component of the Southern African Power Pool's (SAPP) long-term growth prospects and security is the hydropower resources of the Zambezi River Basin (ZRB).

The ZRB comprises 13 subbasins and is the largest river basin in the Southern African Development Community (SADC) and the fourth largest in Africa (Ndhlovu & Woyessa, 2021). The Zambezi River is a critical source of hydropower, containing several significant dams that act as reservoirs that generate electricity for various countries across Southern Africa. Hydropower is an important contributor to the Southern African Power Pool (SAPP), contributing 24 % as per the 2021 annual report of the SAPP installed generation mix (SAPP, 2021). The region's hydropower infrastructure comprises several significant dams, including the Cahora Dam, Kafue Gorge Upper Dam, Kafue Gorge Lower Dam, Itezhi-Tezhi Dam, and the Kariba Dam. The Kariba dam is the largest, holding up to 160,000 million m³, and the

Cahora Bassa is the second largest, holding up to 150,000 million m³ of water (Hamududu & Killingtveit, 2016). The Kariba dam hosts two adjacent hydropower plants, the Kariba North and South Hydropower Plants, which are essential for supplying electricity to Zambia and Zimbabwe. One of the 13 distinct subbasins of the ZRB is the Kariba subbasin, which is home to critical infrastructure for Zimbabwe's energy sector, specifically the Kariba South Hydropower Station (KSHS).

The 1,050 MW Kariba South Hydropower Station (KSHS) is located in Mashonaland West, Zimbabwe, at the Kariba Gorge on the southern bank of Kariba Dam. The Kariba South Hydropower Station (KSHS) has been a pillar of Zimbabwe's energy industry since it was built. It continues to be an essential part of its energy mix (Kariba South Power Station, Zambezi River, Zimbabwe, 2020). Hydropower contributes a great part of Zimbabwe's renewable energy to the national grid, followed by solar energy. It also plays a key role in supporting the country's mitigation efforts in the energy sector, which is the country's major contributor to GHG emissions (Government of Zimbabwe, 2020) . The KSHS and the Hwange coal-fired power station provide Zimbabwe with the largest electricity needs, providing 35% and 55% of Zimbabwe's electricity, respectively. However, recent climate-induced droughts across Southern Africa have heightened concerns over KSHS's vulnerability to climate change.

Considering the importance of energy and energy security to the socioeconomic well-being of Zimbabwe, this study seeks to address this critical gap. A clear understanding of the impact of climate change on hydropower generation at the Kariba South Hydropower Station is crucial for developing adaptation strategies and ensuring a sustainable energy supply in the face of environmental uncertainty. Kariba South Hydropower Plant is a cornerstone of the national electric grid. Understanding climate change effects on hydropower at the Kariba South Hydropower Station is essential in informing clear energy policies and effective adaptation strategies. The central research question guiding this study is, "To what extent will climate change impact the hydropower generation capacity of the Kariba South Hydropower Station (KSHS)?".

1.2 Statement of the Problem

Kariba South Hydropower Station (KSHS) contributes heavily to Zimbabwe's energy balance. However, its electricity generation capacity has become relatively more unpredictable over the years due to the effects of climate change, which have strained the functionality of KSHS. The middle Zambezi River Basin (ZRB), where the KSHS is located, has experienced noticeable shifts in temperature and precipitation patterns, leading to altered river flow. These changes raise concerns about the long-term sustainability of hydropower generation at the KSHS, particularly given the predicted future climate scenarios. The IPCC (2007) identified the Zambezi as the river basin with the most severe potential impacts of climate change among 11 major African river basins, attributed to the combined effects of rising temperatures and declining rainfall in the Zambezi River Basin.

Hydropower relies on water inflows, making it crucial to consider the impact of climate change on water resources. This study aims to assess how climate change has affected and will continue to affect the electricity generation capacity of the KSHS. By analysing historical data on precipitation, temperature, river flow, and effective live storage from 1980 to 2019. The results will offer valuable insights into how climate-induced changes in the Lower ZRB's hydrological patterns affect the operational reliability of the KSHS, providing a foundation for developing strategies to mitigate the expected adverse effects.

The Kariba South Hydropower Station (KSHS) is a vital part of Zimbabwe's energy infrastructure, supplying a significant amount of the nation's electricity. However, in recent decades, the hydropower generation capacity of the KSHS has become increasingly uncertain, mainly due to the impacts of climate change. The middle ZRB, where the KSHS is located, has experienced noticeable shifts in temperature and precipitation patterns, leading to altered river flow patterns. This shift in precipitation patterns and increased temperature has decreased the lake level at Kariba Dam, a crucial infrastructure for hydropower generation for Zimbabwe, Zambia, and the Southern African Power Pool (SAPP). These changes raise concerns about the long-term sustainability of hydropower generation at the KSHS, particularly given the predicted future climate scenarios. The IPCC (2007) has categorized the Zambezi as the river basin exhibiting the worst potential effects of climate change among 11 major African river basins due to the resonating effect of an increase in temperature and a decrease in rainfall along the ZRB.

Hydropower relies on water inflows, making it crucial to consider the impact of climate change on water resources. This study aims to assess how climate change has affected and will continue to affect the electricity generation capacity of the KSHS. The goal of analysing historical data on precipitation, temperature, and river flow from 1990 to 2019. The results will offer valuable insights into how climate-induced changes in the Lower ZRB's hydrological patterns affect the operational reliability of the KSHS, providing a foundation for developing strategies to mitigate the expected adverse effects.

Identified research gaps include:

The majority of studies conducted in the ZRB regarding the effects of climate change on hydropower establish a foundation for assessing more detailed impact studies at specific hydropower sites within the ZRB. Existing studies on the impacts of climate change on hydropower in the ZRB have a limited specific focus on KSHS. (Hamududu & Killingveit, 2016).

Linking water and power sectors is essential to assessing the effects of climate change on hydropower plants in the ZRB and its implications for the national electricity systems of significant riparian states.

1.3 Objectives

1.3.1 Main objective

This research aims to assess climate change's impact on water flow in the middle Zambezi River basin, specifically the Kariba subbasin, and its implications for hydropower generation at the Kariba South Hydropower Station (KSHS).

1.3.2 Specific objectives

- i) To analyse historical trends in precipitation and temperature, in the Kariba subbasin from 1990 to 2019.
- ii) To examine historical river flow trends in the Kariba Subbasin, using data from Victoria Falls (Big Tree Station), Chavuma Mission, and Ngonye Rapids gauging stations.

iii) To assess the variability of Kariba Dam's live storage levels and its impact on hydropower generation at Kariba South Hydropower Station.

1.4 Research questions

- i) How have temperature and precipitation patterns in the Kariba Subbasin changed from 1990 to 2019?
- ii) What are the historical trends in river flow for the Kariba Subbasin between 1990 and 2019?
- iii) What is the relationship between the variability of Kariba Dam's live storage levels and hydropower generation at the Kariba South Hydropower Station?
- iv) **What are the projected future impacts of climate change on hydropower generation at the Kariba South Hydropower Station (KSHS)?**

1.5 Hypothesis

1.5.1 Primary Hypothesis:

H1: Climate change has a significant negative impact on the hydropower generation capacity of the KSHS, primarily due to reduced streamflow in the lower ZRB.

1.5.2 Secondary Hypothesis:

H2: Changes in precipitation patterns and increased temperature associated with climate change are directly correlated with decreased water availability in the Zambezi River and Kariba dam catchment area, affecting the KSHS's ability to generate electricity consistently.

H3: The variability in hydropower generation at the KSHS over the study period can be attributed more to climate-related factors than to operational or infrastructural issues.

1.6 Justification of the study

The Kariba South Hydropower Station (KSHS) is crucial to Zimbabwe's energy infrastructure as it provides a significant portion of its electricity. However, due to the impact of climate change on global weather patterns, hydropower stations like KSHS face threats to their reliability and efficiency. The middle Zambezi River Basin (ZRB), which supplies water to the KSHS, has already seen precipitation and temperature changes, leading to river flow pattern modifications. The anticipated changes will likely exacerbate risks to the sustainability of hydropower generation in Zimbabwe.

Given the critical role of the Kariba South Hydroelectric Station (KSHS) in Zimbabwe's energy mix, it is essential to understand the impact of climate change on its operation. This research is justified for three main reasons:

1. National Energy Security: The Kariba South Hydroelectric Station (KSHS) is essential for maintaining a stable and dependable electricity supply in Zimbabwe. Any substantial decrease in its generation capacity due to climate change could result in widespread energy shortages, with significant economic and social consequences. This research will offer valuable insights essential for national energy planning and security.

2. Contribution to Climate Change Research: This study aims to expand our understanding of the effects of climate change on hydropower, especially in African river basins. It will offer empirical data that researchers and practitioners can utilize to gain insight into and tackle the challenges of climate change in similar regions.

3. Economic and Environmental Sustainability: Hydropower is a crucial renewable energy source, and ensuring its sustainability is vital for reducing Zimbabwe's carbon footprint and fulfilling international climate obligations. This study aims to support the sustainable management of water resources in the ZRB, guaranteeing that hydropower continues to be a viable and eco-friendly energy source in the future.

1.7 Scope of study and limitations

This study aims to assess the impact of climate change on hydropower generation at the KSHS, located on the southern shore of Lake Kariba, along the middle ZRB. The KSHS on the Zambezi River, specifically within the Kariba subbasin ZRB, serves as the geographical confinement for the study. The study restricts its geographical scope to the KSHS located on the Zambezi River, specifically within the Kariba subbasin ZRB. The focus will be on the Kariba subbasin, which feeds into this hydropower facility. The study covers the period from 1990 to 2019. This timeframe allows for a comprehensive analysis of long-term trends and variations in climate, river flow, and hydropower generation. The study will explore historical and current hydrological and climate data, including temperature, precipitation, river flow patterns, and their impact on hydropower generation. In addition to understanding past and present impacts, the study will project future scenarios based on climate models to anticipate potential challenges

for hydropower generation. The research relies on hydropower data from the Zimbabwe Power Company and meteorological data, including precipitation, evaporation, and temperature records from different stations across the study area from the Meteorological Service Department of Zimbabwe. The Zambezi River Authority provided the hydrological data, which included river flow, Kariba reservoir data, and lake levels.

This study acknowledges limitations, notably that power generation is affected by multiple factors, especially government policy, which was not addressed in this research. We could not obtain hydropower generation data from the Zimbabwe Power Company on time, which is the institute responsible for overseeing the Kariba South Hydropower Station. This study primarily focused on the effects of climate change on water resources. Furthermore, a comprehensive examination of supplementary factors influencing river flow, including population dynamics, land use alterations, and sedimentation, was not performed. The study primarily examined the implications of climate change on river flow. A further limitation of this study is the considerable cost of obtaining climate data, which constrained the quantity of historical observed data from stations that could be utilized for our analysis.

1.8 Structure of the Thesis

1.8.1 Summary of thesis outline

The thesis is structured as follows: Chapter One introduces the study, while Chapter Two comprehensively reviews the relevant literature. Chapter Three details the general methodology utilized in the research. Chapter Four discusses the results and their implications, and Chapter Five concludes with recommendations based on the findings.

Chapter 1 serves as an introductory overview, providing essential background information and analysing the challenges faced in the Zambezi River Basin (ZRB) and the broader Southern African region. This chapter articulates the problem statement and justifies undertaking this study. Furthermore, it identifies existing research gaps within the inquiry area and outlines the significance of the research endeavour. In addition, Chapter 1 delineates the thesis's overall objectives and specific aims.

Chapter 2 reviews the relevant literature on the impact of climate change on hydrology and water resources. It includes reviewing hydrological modelling, hydrological models, regional

climate modelling in Southern Africa, downscaling techniques, bias correction, and water resources management.

Chapter 3 outlines the research methodology employed in the study and presents an overview of the materials and methods utilized throughout the research. This study delineates the research area in which it was conducted.

Chapter 4 provides an in-depth presentation and analysis of the findings, exploring the implications and significance of the results in detail.

Chapter 5 offers a comprehensive summary of the findings and presents thoughtful recommendations based on the analysis conducted throughout the study

CHAPTER 2

LITERATURE REVIEW

2.1 Climate change: a global perspective

Global warming and climate change are core environmental issues in the 21st century that significantly affect ecosystems, human societies, and crucial infrastructures. Globally, human activities have elevated the rate of greenhouse gases, leading to global warming. Such gases raise global temperatures, melting the polar ice caps, rising sea levels, and altering the general climate system (Post et al., 2019). The steady increase in global temperature over the past years or decades has led to the emergence of climate change, a manifestation of gradual changes in temperature, seasonal characteristics, and annual precipitation (Rebecca Lindsey & Luann Dahlman, 2023). Climate change, which results in flood disasters, droughts, heat waves, cyclones, and other extremes, poses new and higher risks to climate-sensitive sectors such as agriculture and food security, water resources, and energy.

Climate change can occur due to internal variability within the climate system and external factors (both natural and anthropogenic). Researchers have identified and proved human-induced climate forcing as the leading cause of climate change during the twentieth century, while natural-induced forcing factors helped correct the warming of the earlier part of the century (Chan & Wu, 2015; Gillett et al., 2021). Climate variations originate in the internal conditions of the climate system or external factors impacting it, both natural and anthropogenic. More specifically, natural drivers are changes in solar activity, volcanic activity, and orbital parameters. For example, climate change can result from warming due to increased solar activity or cooling due to reduced sun activity. A volcanic eruption puts substantial amounts of aerosols like sulphur dioxide into the Earth's atmosphere, preventing some solar warming or radiating heat back into space, causing cooling of the Earth's surface temperatures. Additionally, changes in Earth's orbit, axial tilt, and precession, also known as Milankovitch cycles, operate on a timescale of thousands of years, causing shifts in the distribution of solar radiation received across the planet (Meyers & Malinverno, 2018).

While greenhouse gases are perhaps the most central influence of humankind on future climate in terms of radiative forcing, there is a wide range of additional influences, including

anthropogenic aerosols(Hoesly et al., 2018). Anthropogenic drivers of climate change are predominantly linked to human activities that increase greenhouse gas (GHG) atmospheric concentrations. Anthropogenic increases in atmospheric greenhouse gas concentrations are the primary driver of current and future climate change. Carbon dioxide (CO₂), methane (CH₄), and nitrous oxide (N₂O) mostly come from the burning of fossil fuels for energy, transport, and industrial uses. Deforestation and respective changes in land usage increase pressure on GHG emissions since the Earth's capacity to absorb CO₂ decreases. CO₂ emissions from fossil fuel burning and industrial activities accounted for approximately 78% of the overall increase in GHG emissions from 1970 to 2010. Worldwide, economic and population expansion remained the primary catalysts for the rise in CO₂ emissions from fossil fuel use (IPCC, 2014). The majority of the scientific body in our world overwhelmingly agrees that these human activities are the primary drivers of the accelerated warming rates experienced since the middle of the twentieth century (IPCC, 2021a; Perkins, 2015; Trenberth, 2018).

Emissions of greenhouse gases from human activities have been responsible for approximately 1.1°C of warming since 1850-1900 and averaged over the next 20 years; global temperatures are expected to reach or exceed 1.5°C of warming. Anthropogenic forcings have likely significantly contributed to surface temperature rises throughout all continental regions, excluding Antarctica, since the mid-20th century (IPCC, 2021a). The amount of greenhouse gases that humans are currently indiscriminately releasing into the atmosphere has the potential to aggravate global warming and change weather conditions globally (Yoro & Daramola, 2020). Although warming has not been evenly spread globally, the increasing trend in the average global temperature shows that warming dominates over cooling in most areas (Rebecca et al., 2023). Mitigating climate change necessitates significant and continuous reductions in greenhouse gas emissions, which, in conjunction with adaptation, can limit climate change risks.

2.2 Overview of climate in Zimbabwe

The landlocked nation of Zimbabwe is situated in the southern part of Africa. The nation lies between latitudes 15° -23° South and longitudes 25° - 34° East of the Greenwich meridian. Zimbabwe is bordered by four neighbouring countries: South Africa to the South, Botswana to the west, Zambia to the north, and Mozambique to the East and northeast. The country has a total land area of 390,757 square kilometers and a total population of 15,178,957 as of 2023

(World Bank Group, 2021; ZimStat, 2024). There are four distinct seasons in Zimbabwe. The hot and dry season, which lasts from August to October, is distinguished by high temperatures. A post-rainy season from mid-March to mid-May follows the hot and wet seasons. Which lasts from mid-November to mid-March and produces the more significant part of the nation's precipitation. The incredibly dry and cool season, also called winter, commences between mid-May and July and is distinguished by lower temperatures, particularly during June and July, accompanied by minimal rainfall (Sanger et al., 2024).

The annual rainfall ranges from below 400 mm in the South to over 1000 mm in the East (Ministry of Environment Climate Tourism and Hospitality Industry, 2020). The country receives most of its rainfall between November to March. Rainfall decreases from north to South and East to west due to various factors, including altitude, topography, and proximity to weather systems like the Intertropical Convergence Zone (ITCZ), affecting rainfall distribution across different regions. The nation can be categorized into three principal geographical rainfall zones: the Eastern Highlands, adjacent to the Mozambique border, which receives annual precipitation ranging from 1000 mm to 2000 mm, characterized by a wet, temperate climate with year-round rainfall; the Central and Northern Highveld, which obtains 600 mm to 1000 mm of rainfall, encompassing the central plateau and northern areas such as Kariba, influenced by the Zambezi River; and the Lowveld and western region, which experiences annual rainfall of 300 mm to 600 mm, marked by hot and arid conditions with sparse, highly variable, and unreliable precipitation (FAO, 2016).

The mean monthly temperature of Zimbabwe ranges between 15 °C and 25 °C. The East and the Highveld high-elevation areas are generally more remarkable than the lower areas. Temperatures in the highveld (a central plateau) during the summer months typically fluctuate between 25 °C and 30 °C; however, in winter, they can drop to a range of 7 °C to 22 °C. Conversely, in the low veld regions (the southern and western low-lying areas), summer temperatures can soar from 30 °C to 40 °C, but in winter, they generally fall between 10 °C and 25 °C. In the Eastern Highlands (the mountainous areas to the East), summer temperatures often range from 18 °C to 25 °C, although during winter, they can dip to between 5 °C and 20 °C (Government of Zimbabwe, 2016). On average, October and November are the warmest months of the year in Zimbabwe, with variations related to altitude. These temperature variations are significant for understanding the climate dynamics of these regions (Bailey & Dorothy, 2020).

2.3 Overview of hydropower

Hydropower plants generate electricity by converting water's kinetic energy into mechanical and electrical energy (Anaza et al., 2017). Hydropower is determined by the product of the hydraulic head and water flow, but the technical installed capacity limits it (Wan et al., 2021). Dams or lakes used as reservoirs are filled with water through the natural flow of rivers and snowmelt. Run-of-river hydropower plants generate hydroelectricity from the river's natural flow, and they do not require dam construction to act as a reservoir. They depend on precipitation, groundwater flow, and runoff, which are dynamic and can change frequently. Run-of-River (RoR) hydropower plants are considered socially and environmentally acceptable because the water volumes diverted are released back to the river relatively close to the intake (Kuriqi et al., 2019). Storage hydropower plants consist of a dam that impounds water in a reservoir. The water from the reservoir feeds the turbines and generators, usually located within the dam itself. When the middle reaches of a waterway system experience large fluctuations in water flow, storage hydropower plants are frequently constructed. In the case of pumped storage systems, previously released water is pumped back artificially into storage during periods of low energy prices (Turner & Voisin, 2022).

Hydropower is one of the most widely used renewable energy sources globally, accounting for a significant share of electricity generation sources in many countries, with 16% of the world's electricity coming from hydropower. Hydropower accounts for 61% of the total energy derived from renewable sources (IEA, 2020). Hydropower is a mature technology widely used in over 150 countries, and more than 1416 GW of hydro capacity has been installed globally (World Energy Council, 2015). Hydropower ranks among the most efficient technological options for generating renewable electrical energy using "water-to-wire" technologies with efficiencies as high as 90% or even more (Killingveit, 2018). Hydropower forms part of different countries' current and future renewable energy mix as of 2021, China was the largest global hydropower producer and remains the largest hydropower producer, boasting a total installed capacity of 391 gigawatts (GW) (IHA, 2022).

Hydropower constitutes a significant part of the energy portfolio in numerous African nations, with an installed capacity of 38 GW, as shown in Table 2.1. Hydropower offers substantial prospects for economic advancement and might establish the continent as a frontrunner in renewable energy consumption; moreover, around 90% of its hydropower potential still needs to be explored. Furthermore, the advancement of hydropower aligns with the objectives set forth by the United Nations Development Goals, contributing to sustainable growth and

environmental stewardship (IHA, 2022). Ethiopia is the foremost hydropower generator in Africa, with a substantial share of its electricity generation coming from the Grand Ethiopian Renaissance Dam (GERD). This infrastructure initiative addresses the nation’s energy requirements and fosters regional advancement. Dependence on hydropower is high in Central and East Africa, while it is low in North Africa due to its limited river systems. Southern and West Africa have a moderate reliance on hydropower. Sub-Saharan Africa (excluding South Africa) currently relies on hydropower for 60% of its electricity generation, with many individual countries being even more dependent; such countries include Malawi, Ethiopia, Mozambique, Namibia, the Democratic Republic of the Congo (DRC), and Zambia, hydropower accounts for more than 90% of electricity generation (Arnell et al., 2019). In 2021, 24% of all energy used came from hydropower (SAPP, 2021).

Table 2.1: Hydropower Potential Capacity (IHA, 2022)

Region	Installed capacity (GW)	Pipeline (GW)	Remaining (GW)
Global	1250	500	2000
North and Central America	205	28	387
South America	177	48	275
Europe	254	23	73
Africa	38	118	474
South and Central Asia	154	91	355
East Asia and the Pacific	501	240	350

2.4 Hydropower in Zimbabwe

Zimbabwe's energy mix comprises both renewable and non-renewable energy sources, with hydropower providing the most significant proportion of electricity generated from renewable energy sources and coal forming the most important source of electricity generated from fossil fuels. Zimbabwe relies on a combination of hydropower (68.17%), coal, and renewable energy sources (31.83%) in 2022, as per the Zimbabwe Energy Regulatory Authority. The country's electricity supply is primarily managed by government-owned institutions, the Zimbabwe Power Company (ZPC) and the Zimbabwe Electricity and Distribution Company (ZETDC). Hydropower plays a crucial role in the national energy mix, with the Kariba South Hydropower Station (KSHS) being a major contributor to the country's electricity needs. In 2021, the Kariba hydropower station in Zimbabwe served as the country's primary source of electrical energy, fulfilling 57% of its energy requirements (ZERA, 2016). Zimbabwe has some small hydroelectric power stations also like Duru hydroelectric power station in Honde Valley in the Eastern Highlands along the river Duru with an installed capacity of 2.2 MW, Nyamhingura Hydroelectric power station in the Eastern highlands along the Nyamhingura River with an installed capacity of 1.1 MW, Kupinga hydroelectric power station in Chipinge District with an installed capacity of 1.6MW provides a third of electricity in Chipinge town (Republic of Zimbabwe, 2021).

The Kariba catchment is crucial for Zimbabwe, Zambia, and the broader southern Africa region, as it contains the two hydroelectric facilities, Kariba South and Kariba North, which are integral components of the Southern African Power Pool (SAPP) (Mwangala et al., 2024). The Kariba South Hydropower Station is on the Zambezi Gorge in the Mashonaland West province of Zimbabwe. The Kariba South hydropower Station is a 1,050 MW hydroelectric station. At construction, the Kariba South hydropower Station consisted of 6 vertical-shaft Francis's turbines units, each with a capacity of 125MW; in 2018, two units, each with a capacity of 150MW, were added in the expansion of the KSHS. Table 2.1 below shows the years in which the KSHS generators were commissioned (Ivey, 2018). Table 1.1 provides an overview of the Kariba South Hydropower Station generators, detailing their total output and the year or years they were commissioned. This power station harnesses water from the Kariba Dam reservoir and is characterized as a reservoir-based hydropower facility.

The two 150MW units are housed in a 24m wide, 36m high, and 94m long underground powerhouse. The design head of the expansion is 89m. The expansion of the Kariba South

Hydropower Station included building a surge chamber that was 25 m in diameter and 60 m high, along with two vertical shafts measuring 7 m in diameter each. Additionally, two steel-lined penstocks with a diameter of 6.5m were constructed, as well as a single tailrace tunnel that was 12 m in diameter. The operational efficiency of this station is approximately 90% (Kariba South Power Station, n.d.). The electricity produced by the Kariba South Hydropower Station is then transferred to the national grid of Zimbabwe through a 330 kV switching station.

Table 2.2: Kariba South Hydropower Station (KSHS) generators

Source	Output (MW)	Count	Total Output (MW)	Year Commissioned
Hydro	125	6	750	1959-1962
Hydro	150	2	300	2018

Source, (Basson, 2011) .<https://www.esi-africa.com/wp-content/uploads/>.

The Kariba South Hydropower Station plays a pivotal role in Zimbabwe’s energy sector; however, the reliance on river flow for energy generation makes the Kariba Hydropower Station particularly vulnerable to fluctuations in water availability, which can be exacerbated by climate change. Changes in water availability along the Zambezi River, resulting from decreased precipitation, increased evaporation rates, and increased water demand, modifying runoff patterns, will significantly affect hydropower potential, including that of the Kariba South Hydro Station (KSHS). This impact is particularly critical in light of the rising electricity demand in Zimbabwe (Chilkoti et al., 2017; Van Vliet et al., 2016).

2.5 Hydropower generation in the ZRB and climate change

Zambezi River is a keystone in hydroelectric power generation for African countries that share this valued water resource. Multiple hydropower stations are located along the Zambezi River and its tributaries (Fanaian et al., 2015). Some are RoR plants, mainly the Victoria Falls hydroelectric plant on its tributaries, where water flows through the station without any storage. In contrast, others, like the Kariba hydropower stations, are impoundments where large quantities of water are stored in reservoirs. The hydropower resources of the Zambezi River Basin (ZRB) are central to the long-term growth prospects and security of the Southern African Power Pool (SAPP) (Sanchez, 2018). The demand for power in the Southern African Development Community (SADC) region is rapidly increasing due to ongoing industrialization and efforts to enhance human development. The electricity sector is vital for driving regional

integration and economic growth, making energy security increasingly important for sustained development across the SADC.

The ZRB has nearly 5,000MW of installed hydropower generation capacity; 45% of the basin’s installed capacity is in Mozambique, 36% in Zambia, 14% in Zimbabwe, and 5% in Malawi. The hydropower resources of the ZRB are central to the long-term growth prospects and security of the Southern African Power Pool (SAPP); the hydropower resource potential of ZRB of 15,000MW-20,000MW in generation potential (Caron & Markusen, 2016; Spaldingfecher et al., 2017). Numerous hydroelectric projects have been proposed along the Zambezi River Basin (ZRB). The Mupata Gorge Hydroelectric Scheme (HES) is one such project, and it is located downstream of Mupata Gorge, which is located between the two existing dams in the region, Kariba and Cahora Bassa dams, with a planned installed capacity of 1200megawatt (MW). Batoka Gorge HES is located downstream of Victoria Falls with an anticipated capacity of (2400 MW); the Devil’s Gorge Hydropower Plant, located further downstream from Batoka Gorge, also has a planned capacity of 1,250 MW. The Ngonye HES, projected to have a capacity of 180 MW, is located near the constructed Ngonye Falls upstream in the Zambezi. Furthermore, plans exist to develop several additional smaller hydroelectric schemes in the area. Figure 2.1 below shows existing and potential hydroelectric power sites along the Zambezi River.

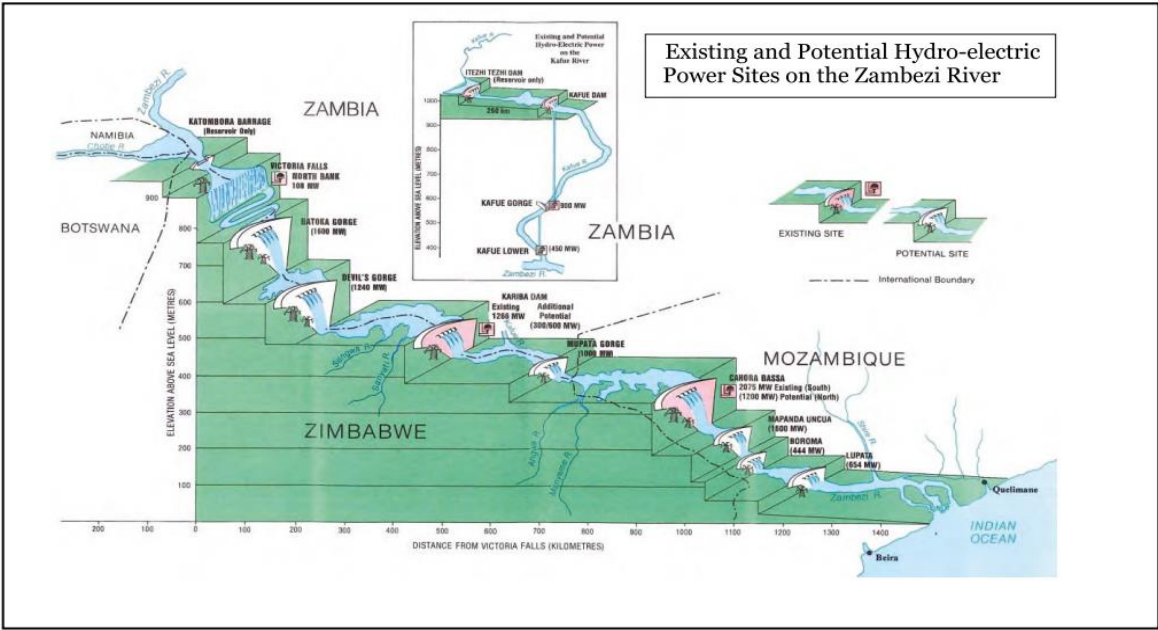


Figure 2.1: Schematic layout of the Zambezi River’s existing and potential hydroelectric power sites. Source : (Zambezi River Authority, 2021).

Climate change impacts hydropower production by altering total annual inflow volumes and modifying the seasonal distribution of water resources. Regions experiencing increased precipitation and runoff will likely have enhanced potential for hydropower production, whilst regions with diminished precipitation and runoff may encounter a decline in hydropower potential (Mukheibir, 2013). Climate change affects the ZRB's resource potential due to variations in river flow (runoff), which are linked to variations in local or regional climate parameters like temperature and precipitation in the catchment area. These modifications result in altered runoff volumes, immediately affecting hydropower production. Zimbabwe is among the countries affected by the impact of climate change on its water resources. The Kariba South Hydropower Station, the country's biggest hydropower generation station with a stored capacity of 1050MW, only produces 184 MW on average due to water rationing, resulting in low inflows into Lake Kariba. Reduced water in the lake has resulted in power cuts of up to 12 or more hours daily. Researchers have studied the impact of climate change/climate variability on hydropower in the ZRB to have an idea or predict the future outlook of hydroelectric power potential.

Most researchers concur that anticipated future dry years, floods, and rising water demand will adversely affect the current hydroelectric plants along the ZRB (Cahora Bassa, Kariba, Kafue Gorge, and Itzhi Tezhi), a dry climate will reduce average electricity generation by 10-20% with the Kariba station being the most affected showing great sensitivity to climate compared to other plants, a wetter climate is projected to increase generation at Kariba and most new plants, though a wetter climate will have a less significant impact on generation at Cahora Bassa and Kafue Gorge upper due to increased reservoir evaporation, vegetation evapotranspiration and increase in water demand, e.g., for irrigation in the catchments (Spalding-Fecher et al., 2016, 2017; Yamba et al., 2011). A study by Spalding-Fecher, Senatla, et al. (2017) indicates that under drying conditions, the Kariba Hydroelectric Scheme (HES) is the most vulnerable existing hydropower plant, while the Batoka Gorge project is the most vulnerable among new plants, showing greater sensitivity to climate change than other downstream plants. Under wetter climate scenarios, hydropower generation at Kariba and most new power plants is expected to increase.

Climate change is expected to adversely impact future hydropower output in the ZRB. Rising air temperatures will lead to heightened evaporation and diminished rainfall, contributing to

decreased inflows and higher reservoir evaporation. Reducing water resources will diminish hydropower generation capacity. (Hamududu & Killingtveit, 2016). The Kariba South Hydropower Station has declined in electricity generation due to reduced water inflows into the Kariba catchment area and low rainfall over the past years. In 2022, the Kariba South hydropower station was wholly suspended due to low water levels on the bank. El Niño events are primarily linked to droughts in Southern Africa; generally, in El Niño years, the region receives below-average rainfall. In Zimbabwe, the El Niño phenomenon in some areas resulted in up to 21 hours without electricity daily.

2.6 Climate Change in the ZRB

The Zambezi River Basin, which spreads from Angola, Botswana, Malawi, Mozambique, Namibia, Tanzania, Zambia, and Zimbabwe, has been subject to climate change. These impacts have complex implications for the ecosystems, living standards, and economies of the countries in the region. The region within Southern Africa is among some of the most sensitive regions within the globe in terms of climate change impacts. Average temperatures have been observed to increase in the ZRB, leading to high evaporation rates that impact the river flow. Forecasting of this region reveals a potential rise in temperatures by 2050, which ranges from no change to a rise of 3.5°C in the winter and 4°C in the summer. Climate change affects the African arid communities, especially those inhabiting land located in international river basins. On the African continent, one of these regions is the Zambezi River Basin (ZRB), which is estimated to be the most affected by climate change impacts of the eleven river basins in Africa (Kling et al., 2014). The impacts of climate change on the African continent are in light of the expected temperature rise and reduced rainfall in the area (IPCC, 2021b) .

The Zambezi River Basin has experienced increased variability in rainfall patterns due to climate change. While some areas have seen an increase in rainfall, other regions have been exposed to more frequent and intense drought situations (Schlosser & Strzepek, 2015) . The fluctuations in rainfall significantly impact the amount of water available for agriculture, industries, and household use. The changes in rainfall and the growing demand for water in the Zambezi River Basin are, at the same time, diminishing the potential for hydroelectric power generation in this region, which can lead to a decline in current and future projects.

Changes in temperature and precipitation patterns have brought about challenges in keeping a stable river flow, hence impacting water availability for human consumption, economic uses, and various ecosystems. However, increased flow events result in flooding, which may cause significant loss of life and property damage. On the other hand, decreased flow events result in decreased water availability and increased salinity levels, adversely affecting ecosystems, especially aquatic organisms, and agricultural productivity. Changes in temperature, precipitation, and river flow significantly impact ecosystems and, therefore, biodiversity in the Zambezi River Basin. The impacts on the ecosystem comprise changes in the distribution and quantitative composition of different species of plants and animals, including fish populations, together with adjustments of the wetlands and flood plains. The manifestation of climate change includes climate variability; there are now indications that there will be a stronger, increased frequency, and widening occurrence of such natural catastrophes as droughts, floods, and cyclones, all felt particularly within the Zambezi River Basin (Hughes & Farinosi, 2020).

However, increased flow events result in flooding, which may cause significant loss of life and property damage. On the other hand, decreased flow events result in decreased water availability and increased salinity levels, adversely affecting ecosystems, especially aquatic organisms, and agricultural productivity (Sabater et al., 2023). Changes in temperature, precipitation, and river flow significantly impact ecosystems and, therefore, biodiversity in the Zambezi River Basin. The impacts on the ecosystem comprise changes in the distribution and quantitative composition of different species of plants and animals, including fish populations, and adjustments of the wetlands and flood plains. The manifestation of climate change includes climate variability; there are now indications that there will be a more substantial, increased frequency, and widening occurrence of such natural catastrophes as droughts, floods, and cyclones, all felt particularly within the Zambezi River Basin.

Climate change-induced droughts, particularly the severe droughts caused by El Niño in the Zambezi River Basin, impact various sectors that rely on water, such as agriculture, energy, domestic water supply, and tourism. Hydroelectric power generation is particularly significant for the countries that share the Basin. The reduction in water levels in the reservoirs along the Basin has led to reduced power generation, and in some cases, a complete shutdown of operations at hydropower stations. One notable instance is the Kariba Hydropower Station, which experienced a complete halt in power generation in September 2024. This was the second time that power generation had to be suspended on the world's largest artificial lake since its

creation in 1959; the first occurrence was in November 2022 when power generation on the Zimbabwe side was halted due to low water levels (Cyril Zenda, 2024). Reduced hydropower generation from the Kariba hydropower station during the 1991–1992 drought led to a decrease in export earnings of US\$36 million, a reduction in GDP, and the loss of 3000 jobs in Zimbabwe

Droughts, floods, and cyclones are among the natural disasters that are more intense, frequent, and widely distributed in the Zambezi River Basin, which is a clear indication of climate change due to climate variability (Kling et al., 2014). There have been some of the worst floods in the Zambezi River Basin in 1999 and 2001, droughts in 1986–1987, 1991–1995, 1997–1998, 2003–2004, and the worst drought in 2015–2016. The drought of 2015–2016 caused livestock losses, poor harvests, infrastructure damage, and the spread of waterborne illnesses. To address the effects of the 2015–16 drought, the governments of Malawi and Angola needed US\$380 million and US\$261 million, respectively (ZAMCOM, 2016). Angola's upper Zambezi, Botswana's Cuando/Chobe River confluence, Namibia's Zambezi Region, Zambia's Kafue Flats, and Malawi's lower Shire are among the flood-prone regions along the Zambezi River Basin. Due to the increased likelihood of water-borne illnesses and population displacement, these flood events heavily burden public health, infrastructure, and energy infrastructure, such as hydropower plants in the Zambezi River Basin.

2.7 Impact of climate change on water resources

Zimbabwe is classified as a semi-arid nation, which encounters significant issues in water resource management owing to its low mean annual precipitation and the ephemeral or non-perennial characteristics of most rivers in its arid areas. The challenges are exacerbated by the impacts of climate change, which are expected to be more pronounced in Southern Africa than in some other regions in Africa regions (Hamududu & Killingtveit, 2016; Serdeczny et al., 2017). Water is an essential resource for Zimbabwe's economy, supporting vital sectors, including agriculture, industry, and energy. More than 70% of the population depends on rainfed agriculture for their sustenance, underscoring the importance of water in agricultural and livestock production (Mabhaudhi et al., 2018). Moreover, water facilitates industrial operations, cooling in thermal power plants, and hydropower production, a vital component of the country's energy portfolio.

Climate Change intensifies preexisting weaknesses in Zimbabwe's hydrological infrastructure and water supplies. Forecasts for Southern Africa suggest a reduction in total annual precipitation and an escalation in consecutive dry days, leading to prolonged aridity (Umugwaneza et al., 2021). Rising temperatures intensify the alterations, increasing evaporation and reducing water availability. Consequently, surface and groundwater resources are expected to decline, intensifying water scarcity and threatening the sustainability of water-dependent sectors.

Reduction in precipitation directly affects the water supply to reservoirs essential for storing water required for hydropower generation. Decreased precipitation directly affects the water supply to reservoirs essential for storing water required for hydropower generation. Decreased streamflow impairs hydroelectric facilities' operational efficiency, such as the Kariba South Hydroelectric Station. Moreover, alterations in rainfall patterns due to climate change are expected to enhance rainfall intensity during wet seasons, resulting in more severe flooding events (Diop, S., Scheren, P., & Niang, 2021). Such extremes can destabilize aquatic ecosystems, degrade water quality, and present additional issues for irrigation, agriculture, and energy generation.

The occurrence and severity of extreme climate events are anticipated to increase markedly across Southern Africa, including Zimbabwe. These extremes, including floods and droughts, affect water resource management by taxing existing infrastructure and exacerbating risks to economic and environmental systems. Heavy rainfall events can lead to significant flooding, inundating reservoirs, and deteriorating water quality, whereas extended droughts intensify water scarcity, reducing water levels in reservoirs (Frischen et al., 2020). Zimbabwe is one of the countries most adversely affected by drought, where drought consequences have resulted in water scarcity, reduced agricultural yields, and episodes of food poverty, coupled with economic decline. Rainfall is projected to be more variable and erratic, with rainy season onset dates projected to be later or irregular and dry periods more frequent and longer. The agricultural industry, primarily consisting of smallholder rainfed systems, is significantly vulnerable to drought. The anticipated rise in extreme events by 2050 will likely produce cascade consequences on aquatic ecosystems, agriculture, and hydropower generation, requiring adaptive management techniques to alleviate their impact (Government of Zimbabwe, 2016).

Climate variability poses a significant problem to water management in Zimbabwe. Rainfall patterns are erratic and unpredictable, exhibiting significant fluctuations driven by global and regional climatic systems. These variances result in divergent situations, including extended droughts in certain areas and severe flooding in others. Natural climatic variability significantly influences worldwide weather patterns. The El Niño phase of the El Niño/Southern Oscillation (ENSO) significantly increases the likelihood of severe droughts (Mosley, 2015; Nguyen et al., 2021). Droughts are defined by a substantial drop in streamflow, a fall in groundwater levels, and a reduction in lake levels. These factors can significantly affect the ecology and water accessibility. Recent developments indicate that Zimbabwe has achieved a notable 63% implementation rate of water management practices, as measured by United Nations indicators. These water management practices present a significant opportunity to enhance these practices further, yielding even more excellent outcomes.

2.8 Impact of climate change on river flow

River flow remains a resource where water abstraction is important to riparian communities for different activities, including agricultural activities and energy production. Climate change impacts precipitation patterns, changing their frequency and intensity and affecting river water flows. A reduction or a decrease in precipitation reduces river water flow, affecting aquatic ecosystems and all infrastructures that depend on water flow, e.g., hydropower stations (Moran et al., 2018). The erratic nature of river flow during the wet and dry seasons affects the development of hydropower sites (Ajiboye, 2013). Warmer temperatures due to climate change cause a significant melt in snow melt, thus significantly increasing river flow during spring. The increase in snowmelt is associated with extremes such as floods and, in some cases, erosion. Conversely, cooler temperatures can also reduce snowmelt and river flow, affecting the general water supply for riparian communities. Climate change impacts the renewal rates of groundwater stored in aquifers that underlie rivers and streams, hence the base flow rates. A deficit in groundwater recharge may result in reduced river flow, while an increment in recharge may propel river flow rates (Meixner et al., 2016).

At any time and place, the flow of a river is composed of a mixture of surface water, soil water, and groundwater, and precipitation is the ultimate source of all river flow, each contributing to

the overall hydrology of the river system. Precipitation is the key driver of river flow, providing the necessary water that enters the river channel. The process in which precipitation reaches the channel is affected by climate, geology, topography, soils, and vegetation. The geology and topography affect how water is absorbed and how quickly it runs into the river; steep topography permits rapid runoff and reduced infiltration, increasing river flow. Spatial and temporal variation of precipitation (amount: rain vs. snow, timing, and duration), along with the effects of topography, soil texture, and plant evapotranspiration on the hydrologic cycle, generate localized and regional flow paths.

One of the key components of establishing hydrological variability is identifying changes in river flow; when sufficient records are obtained, streamflow variability may be used to create a trend of a river system at various monitoring stations and determine whether stream flow is increasing or decreasing (Gumbo et al., 2021). Applying the SWAT hydrologic model, streamflow simulations in the ZRB were conducted under two climate scenarios (RCP 4.5 and RCP 8.5) using multi-global climate projections. The results indicate a minor reduction in annual stream flow of less than 3% under RCP 4.5 and an increase of approximately 6% using RCP 8.5. Simulations suggested that interannual and interannual streamflow variability will rise in the future under RCP 8.5 and decrease under the RCP 4.5 scenario (Ndhlovu & Woyessa, 2021).

River flow variability and its temporal fluctuations can be analysed using several methods, including statistical analysis, which encompasses regression analysis, analysis of variance, and time series analysis, which are diverse statistical methodologies employed to examine streamflow data for identifying trends and patterns (Jiang & Wang, 2019). Hydrological modelling enables evaluating and predicting alterations in a river's stream flow regime due to climate change, land development, or water management techniques. Satellite-based remote sensing data can provide information on river flow, variability, and land use and cover alterations that may influence stream flow (Silvestro et al., 2015). Assessing river flow, water quality, and other hydrological characteristics in the stream may provide insights into the source. Hydrological data may be gathered during a study to elucidate the primary elements of stream flow variations and for model calibration and validation (Sirisena et al., 2020).

2.9 Climate Change Modelling

Climate change models are mathematical representations of the climate system's physical, biological, and chemical fundamentals (Edwards, 2011; Gettelman & Rood, 2016). Climate models are important tools for understanding the Earth's climate, predicting future changes, and informing decision-making. Many climate models have been developed to conduct climate projections. They simulate and help us understand climate change in response to the emission of greenhouse gases and aerosols (Goosse et al., 2010). The results obtained from these models are averages over regions. The coverage relies on the model's specific times and resolutions. There are different types of climate models, which include Energy Balance Models (EBMs), Radiative Convective (RC) Models, Statistical Dynamical (SD) Models, and Global Circulation Models (GCMs) (Bhardwaj, 2015). Climate modeling is achieved through two primary methods: Global Climate Modelling and Regional Climate Modeling.

The most common and widely used tools for understanding historical climatic factors like temperature, precipitation, and atmospheric circulation patterns and projecting possible future climate changes under different emission scenarios are global circulation models (GCMs) (Kusangaya et al., 2014). Global climate models (GCMs) are the primary tools used to simulate and predict the impacts of climate change on hydrological variables and to project future climate conditions (Goharian et al., 2016; Karamouz et al., 2013). While GCMs provide valuable insights, they often operate at a coarse spatial resolution (they simulate the climate over large grid cells, typically around 100 to 200 km on each side), which may not capture the finer details needed for regional studies (Demory et al., 2020).

However, to study the impact of climate change, it is necessary to predict changes on much finer scales. RCMs come into play since they downscale GCM outputs to a finer spatial resolution (typically 5-50 Km grids). RCMs offer a more detailed representation of extreme events, which is critical for assessing the potential impacts of climate change at a regional and country level. Global Climate Models (GCM) can replicate the global circulation's response to large-scale forcings, such as greenhouse gases or changes in solar irradiance. In contrast, Regional Climate Models (RCM) consider sub-GCM scale forcings and processes, including topographic elevation, coastlines, inland water bodies, and the distribution of vegetation and other surfaces, as well as mesoscale dynamic processes (Giorgi, 2019). For this study, we used four GCMs (CNRM-CM6, IPSL-CM6A-LR, MIROC6, MPI-ESM1-2-LR) for the period (2040-2070) relative to the present climate (1990-2019) shown in Table 2.3, these GCMS have

been used in previous studies conducted around the Zambezi River basin,(Almazroui et al., 2020; Hamududu & Killingveit, 2016; Ndhlovu & Woyessa, 2021).

Table 2.3 List of selected GCMs used in this study

GCM Name	Institute/Developer	Horizontal resolution (lon.by lat. in degrees)	Country
CNRM-CM6-1	National Center for Meteorological Research Climate Model, version 6	1.4°×1.4°	France
IPSL-CM6A-LR (France)	Institute Pierre-Simon Laplace Climate Model, version 6A, Low Resolution	2.5°×1.3°	France
MPI-ESM1-2-LR	Max Planck Institute Earth System Model, version 1.2, Low Resolution	1.9°×1.9°	Germany
MIROC6	Model for Interdisciplinary Research on Climate, version 6	1.4°×1.4°	Japan

2.10 Downscaling GCMs Projections to Regional Scales

Downscaling is a fundamental procedure in assessing the future impact of climate change at regional scales. Downscaling, also known as one-way nesting, involves the flow of information from the large-scale driving conditions to the RCM, but not vice versa (Giorgi, 2019). Downscaling helps enhance the accuracy of climate projections by incorporating regional-specific characteristics like topography and land use. For the assessment of the impact of climate change at a regional scale, the GCM data are spatially too coarse (~100–200 km); hence, these GCMs require downscaling to regional or local (Kusangaya et al., 2014; Smitha et al., 2018).

Two fundamental downscaling approaches, statistical downscaling and dynamical downscaling (RCMs), resolve the scale discrepancy between GCM climate projection outputs and the spatial resolution required for the local climate impact studies (Jang & Kavvas, 2015).

Statistical downscaling (SD) entails the formulation of statistical correlations between large-scale atmospheric variables (predictors) from General Circulation Models (GCMs) and local or regional climate variables, precisely temperature and precipitation (predictands); these relationships are then used to downscale the GCM outputs (Zorita & Von Storch, 1999). Statistical Downscaling techniques are more computationally efficient and more straightforward to use. There must be adequate long-term observed data to apply SD and generate strong statistical connections for regions of interest (Bhowmik et al., 2017; Kattsov et al., 2013; Schoof, 2013). Delta changes statistical downscaling method was used to downscale the GCM data in this study. The Delta change method has been used in many studies to downscale GCM climate data. The future climate in the basin was projected by downscaling the GCM results using statistical downscaling using the Delta change method. This method entails reduced computational demands and a more straightforward model formulation (Maraun et al., 2010).

Dynamical downscaling uses information from GCMs to high-resolution Regional Climate Models (RCMs), which are nested within GCMs, simulating a smaller region at a higher resolution to derive physically consistent regional weather and climate parameters with sufficient details (Teutschbein & Seibert, 2012). They incorporate physical processes not explicitly resolved in GCMs, providing more detailed regional climate information. The availability of RCM simulations constrains the dynamical approach, so statistical downscaling is a popular alternative for impact studies because of its relative ease of use and a general performance comparable with output from RCMs (Eden & Widmann, 2014). Copernicus, the Earth Observation program of the European Union, was essential in facilitating access to CMIP6 climate projections. The outputs from CMIP6 provide an opportunity to improve our understanding of climate change's past, present, and future, arising from natural, unforced variability or in response to changes in radiative forcing. Compared to previous versions, improvements in the CMIP6 model (e.g., CMIP3 and CMIP5) have been used to understand historical and future changes in precipitation and temperature under different scenarios in Africa (Aloysius et al., 2016; Jury, 2019). These improvements on CMIP6 include high spatial and temporal resolution and improved representation of microphysics, aerosols, and ocean dynamics; CMIP6 uses a new set of emission scenarios and Shared Social economic Pathways

(SSPs), which integrate socio-economic trends with climate projections (Eyring et al., 2016). We obtained the four GCMs for this research from the user-friendly interface of the Copernicus data store. It enabled us to download the GCM datasets for historical and future precipitation and minimum and maximum temperature for our study period, which we then downscaled and bias-corrected.

2.11 Bias Correction

Bias correction involves adjusting for systematic biases between the modeled properties of the climate system and the corresponding real property that can distort results and interpretation (Kotlarski et al., 2014; Teutschbein & Seibert, 2013). Climate models – global (GCMs) and regional (RCMs) simulations of temperature, precipitation, and wind patterns through globally interacting systems between the atmosphere, oceans, and land- represent another area where output from various sources could be used. Climate models are reliable for simulating regional and local fine-scale climates but suffer from serious systematic errors, notably in small-scale patterns of daily precipitations that primarily rely on model resolution and selected parameters.

However, these models exhibit significant systematic errors or biases compared to observed historical climate information. Regional Climate Models (RCMs), downscaled from General Circulation Models (GCMs), often suffer from significant biases and have a horizontal resolution that is frequently coarser than what is required that is frequently coarser than what is required. The sources of these biases can include low spatial resolution, incomplete physical processes, and parameterization within the models (Teutschbein & Seibert, 2012). Direct utilization of simulations as an input to impact models, such as hydrological models, leads to unrealistic outcomes. Considering the above, RCMs are inadequate for direct use in climate change impact and adaptation assessment studies. Therefore, the impact models are often driven by the corrected GCMs/RCMs outputs having characteristics statistically similar to observed data (Hagemann et al., 2013).

Bias correction techniques have overcome the challenge of using direct RCM outputs in impact studies. Bias correction ensures that the outputs are suitable for analysis. Bias correction readjusts model outputs to reflect historical observations better and thus make them more reliable for future projection. Several bias correction methods have been developed to refine model outputs to make them more applicable to specific locations or regions, ensuring local

relevance in impact assessments. Most bias correction methods use monthly statistics to derive correction factors (Smitha et al., 2018). Among bias correction methods, one is called the delta change, which can be either a multiplicative or an additive. Additive correction means adding a constant value to the simulated data based on the difference between observed and modelled historical data and is suitable for climatic variables like temperature. Multiplicative correction means that the simulated data are multiplied by a correction factor based on the observed data and is suitable for climatic variables such as precipitation (Räty et al., 2014). The mean bias correction was used for this research due to its simplicity and ease of use (Zhao et al., 2017).

2.12 Climate Scenarios

Climate scenarios play a pivotal role in climate change research and assessment. They allow us to project how driving forces, such as human activities, environmental policies, economic trends, and technological changes, will shape future emissions and the associated uncertainty. This understanding is crucial for assessing the urgency of climate change and the need for mitigation and adaptation measures. Climate scenarios assist in climate change analysis, including climate modelling and assessing impacts, adaptation, and mitigation (Pedersen et al., 2022) .

Emissions and climate emissions have been key components of the IPCC's research in climate change evaluation. The IPCC has evolved its scenarios over time, starting with the SA90 used in early assessments of the potential impacts of greenhouse gas emissions on the global climate. The commonly known IS92 scenarios were released in 1992 to drive global circulation models. After evaluating the performance of IS92 scenarios, in 2000, the Special Report on Emission Scenarios (SRES) was released, marking a significant milestone in climate change research. The SRES informed the third Assessment Report (AR3) in 2001 and the fourth Assessment Report (AR4) in 2007. The SRES provided a set of emission scenarios, divided among four main storylines (A1, A2, B1, and B2), each with a marked scenario that serves as an illustration. The A1 storyline has three scenario groups, which are A1F1 (fossil fuel-intensive), A1T (non-fossil energy sources), and A1B (a balanced mix of energy sources) (Davidson, 2014; IPCC, 1990; Leggett et al., 1992). The SRES scenarios cover the primary drivers of future emissions, from population growth to technological and economic advancement (IPCC, 2014a; Riahi et al., 2017).

Recent emission scenarios were produced independently of the IPCC, although they were extensively utilized in IPCC publications, including the Fifth Assessment Report (AR5) and the Sixth Assessment Report (AR6), the Representative Concentration Pathways (RCPs), and Shared Socioeconomic Pathways (SSPs). RCPs are designated trajectories for greenhouse gas and atmospheric concentration, air pollutant emissions, and land use aerosol concentrations, formulated to guide the Fifth Assessment Report (AR5). These routes are defined by the radiative force generated by the conclusion of the 21st century. Four Representative Concentration Pathways (RCPs) have been established: RCP 2.6, representing a low-emission scenario; RCP 4.5 and RCP 6.0, both of which are stabilization scenarios, with RCP 6.0 exhibiting a higher radiative forcing level than RCP 2.6; and RCP 8.5, characterized as a high baseline emission scenario (Jubb et al., 2013). Figure 2.2 below shows the projected atmospheric CO₂ concentration expressed in CO₂-equivalents (ppm) for different shared socioeconomic pathways (SSPs) across the 21st century. The pathways correspond to different levels of radiative forcing (energy imbalance in the Earth system) by 2100.

Compared to the representative concentration pathways (RCPs), the five primary shared socioeconomic paths (SSPs: SSP1-1.9, SSP1-2.6, SSP2-4.5, SSP3-7.0, and SSP5-8.5) are more uniformly distributed and project lower radiative forcing and temperatures by 2100 (Meinshausen et al., 2020). This research utilized SSP245 (middle of the road) and SSP585 (fossil-fuel development), as they offer both an upper and moderate boundary for climate effect forecasts, so ensuring a comprehensive range of potential futures is addressed (Bobde et al., 2024). SSP245 concentration pathway is a moderate scenario for future greenhouse gas emission; it represents a “middle of the road” approach where societal, economic, and technological trends do not drastically deviate from historical patterns. Conversely, SSP585 represents a high-emission, fossil fuel-driven society where global greenhouse gas emissions continue to rise strongly throughout the 21st century (Welch, 2024).

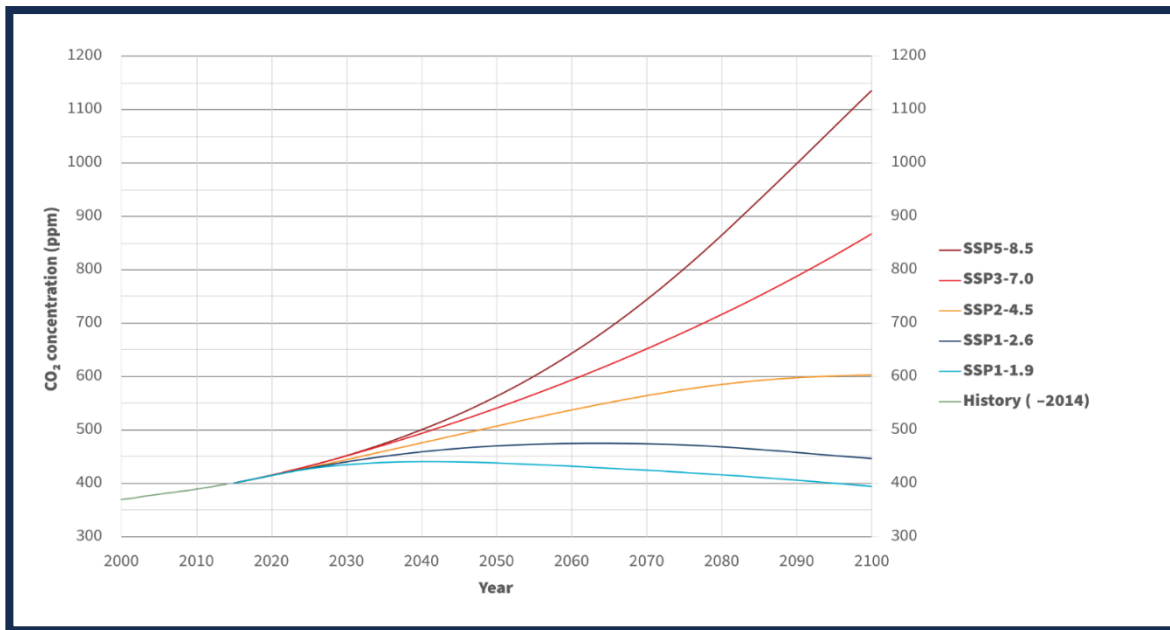


Fig 2.2: predicted atmospheric CO₂ concentration for different shared socioeconomic pathways (SSPs) across the 21st century (Wikipedia contributors, 2024).

CHAPTER THREE

METHODOLOGY AND MATERIALS

3.1 Study area

3.1.1 Location

This study specifically aims to investigate the Kariba subbasin, one of the 13 essential subbasins of the ZRB. The Kariba catchment encompasses an area of 663,848 square kilometers, extending from Lake Kariba, situated at coordinates 18° 04' S and 26° 42' E, to the Kariba Gorge at 16° 31' S and 28° 45' E. Zambia borders the region to the north and Zimbabwe to the south. Lake Kariba, created by the damming of the Kariba Gorge, stands as the world's largest artificial reservoir by volume. It features a surface area of 5,577 square kilometers and possesses a live storage volume of 564,800 million cubic meters. This reservoir regulates runoff from an upstream catchment area of approximately 687,535 square kilometers, representing around 47% of the Zambezi River catchment area. The Kariba catchment lies between 400 and 1600 meters above sea level. Figure 3 below illustrates the Zambezi River Basin, highlighting the location of the Kariba subbasin. Additionally, it shows the position of the Kariba subbasin within the context of the map of Zimbabwe.

Study Area Map

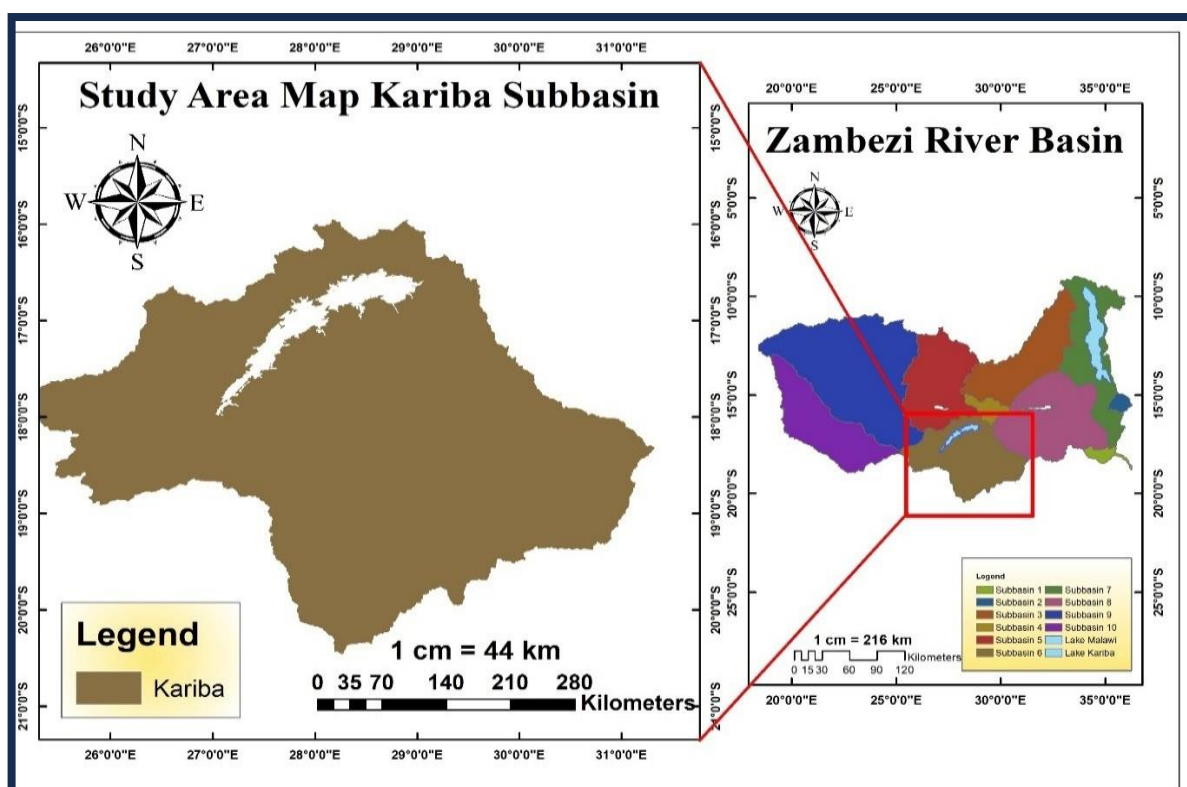


Figure 3.1: Study area map of the Kariba subbasin

3.1.2 Climate of the study area

Kariba is a lake in the Gwebe Valley, within the Kariba subbasin in the Middle Zambezi basin. The prevailing climatic conditions in this area are warm, tropical, and semi-arid, with variations in climate throughout the two main seasons. The movements of air masses with the ITCZ are the basin's most important causes of climate and rainfall distribution. There are three primary seasons in the area surrounding Lake Kariba. Warm and dry season: The first season is from September to October. During the warm and dry seasons, these are the hottest months of the year, and rainfall levels are low compared to the rest of the year. Warm and Wet Season: The region receives most rainfall from November to March when temperatures are relatively high. The movement of the ITCZ, which favours moist air from the Indian Ocean to the region, is responsible for this. Cool and dry seasons, from April to August, have relatively low temperatures with almost no monthly rainfall. The catchment area experiences an average annual rainfall of approximately 970 mm. Mwangala et al. (2024) project an average rainfall of approximately 500mm in the southern part of the catchment area, compared to a projected 1200mm in the northern region. This precipitation makes the mean annual discharge 372,490

mm³, or an average flow rate of 1,181 m³/s (Muchuru et al., 2015). Topographic barriers, vegetation cover that regulates air circulation patterns, and precipitation in different parts of the catchment area explain these differences.

3.1.3 Topography

Kariba subbasin varies from 363 m near the Kariba Dam to over 1592 m in the adjacent escarpments and highlands. The topography of the Kariba Subbasin catchment, with its diverse landscapes, is a powerful force influencing the region's hydrology. The significant highland regions, such as the Muchinga Escarpment in Zambia and the Zambezi Escarpment in Zimbabwe, play a crucial role in shaping rainfall patterns and surface runoff. Steep slopes facilitate swift drainage during rainfall and showcase the potency of natural forces. Rolling plains characterize certain basin areas below the escarpments that regulate water flow. Topography influences the development of tributaries contributing to the Zambezi River, such as the Kafue River, the Sengwa River, the Ruziruhuru River, the Luangwa River, and various smaller streams in the region. Differences in elevation increase the river's flow speed, influencing sediment transport and water storage in the Kariba Reservoir. Figure 3.2 illustrates the topographic map of the Kariba subbasin.

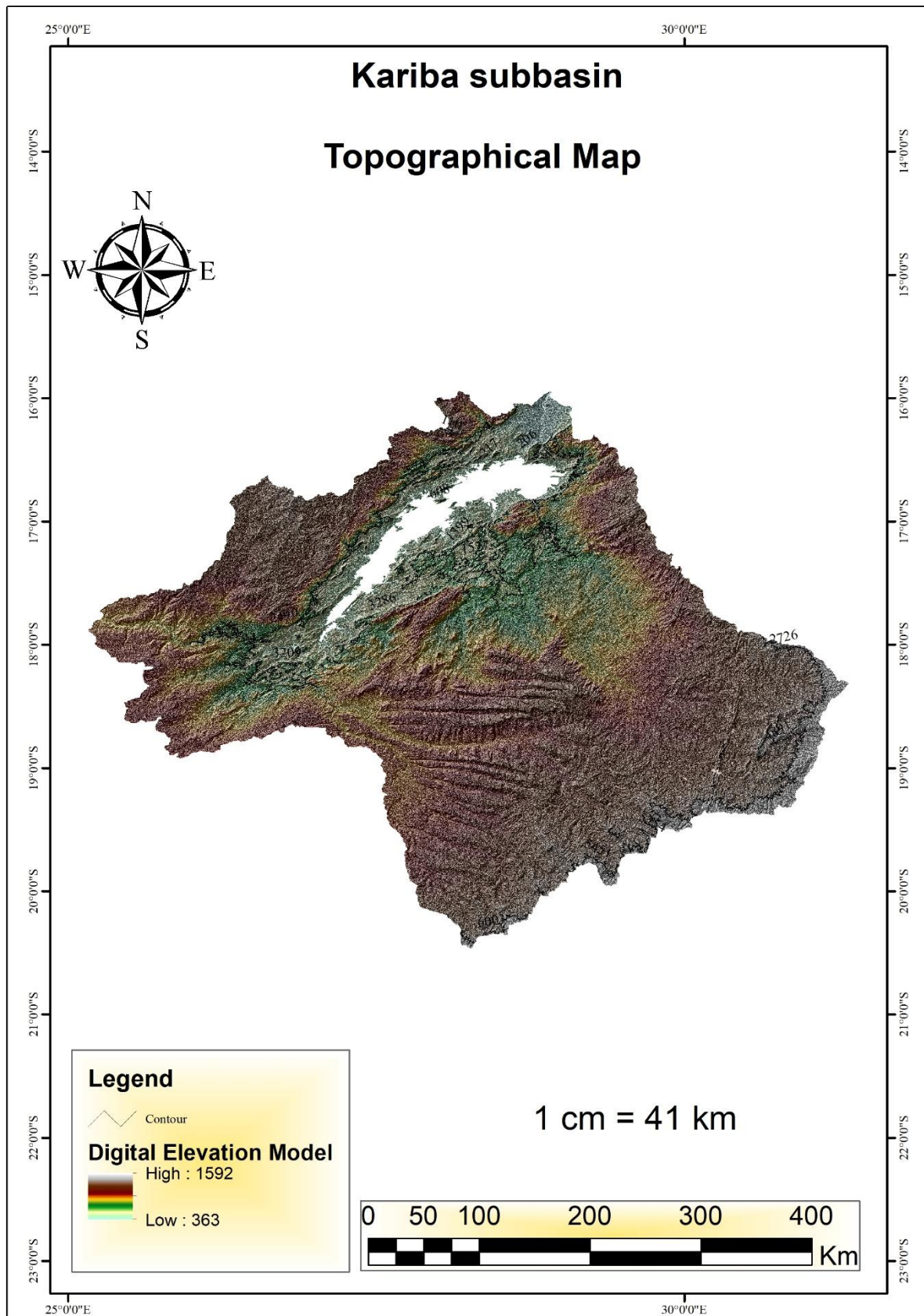


Figure 3.2: Kariba subbasin topographical map

3.1.4 Geology and Soils

The geological nature of the Kariba subbasin presents varied soil types and complex geological topography. Much of this subbasin comprises old Precambrian basement rocks, including granites and gneisses that are mostly impermeable and control groundwater movement and storage dynamics. In the southern part of the subbasin, sedimentary rocks like sandstones, coal seams, and shales are found, and sediments of the Karoo Supergroup predominate. In the western and southern regions, one can observe the presence of Kalahari sands, which consist of fine-grained particles. In the Kariba subbasin, twelve predominant soil classes according to FAO classification have been identified: Vertic Cambisols, Orthic Ferrasols, Lithosols, Eutric Fluvisols, Chromic Luvisols, Ferric Luvisols, Gleyric Luvisols, Eutric Nitosols, Cambic Arenosols, Luvic Arenosols, Vertisols, and Pellic Vertisols. The dominant soil types in this subbasin are Lithosols, Chromic Luvisols, and Ferric Luvisols (see Figure 3.3). In addition, 5 (five) soil textures were found according to FAO classification: Clay, Sandy Clay Loam, Sandy Loam, Loam, and Clay Loam. Thus, the dominant soil textures are Sandy Loam, Clay, and Sandy Clay Loam, respectively (see Figure 3.4). As a result, infiltration dominates in the Kariba subbasin due to high infiltration soils (Sandy loam and Loam). In contrast, infiltration is generally higher, and the presence of significant Clay soils and Clay Loam indicates localized areas with high runoff potential, especially during intense rainfall events.

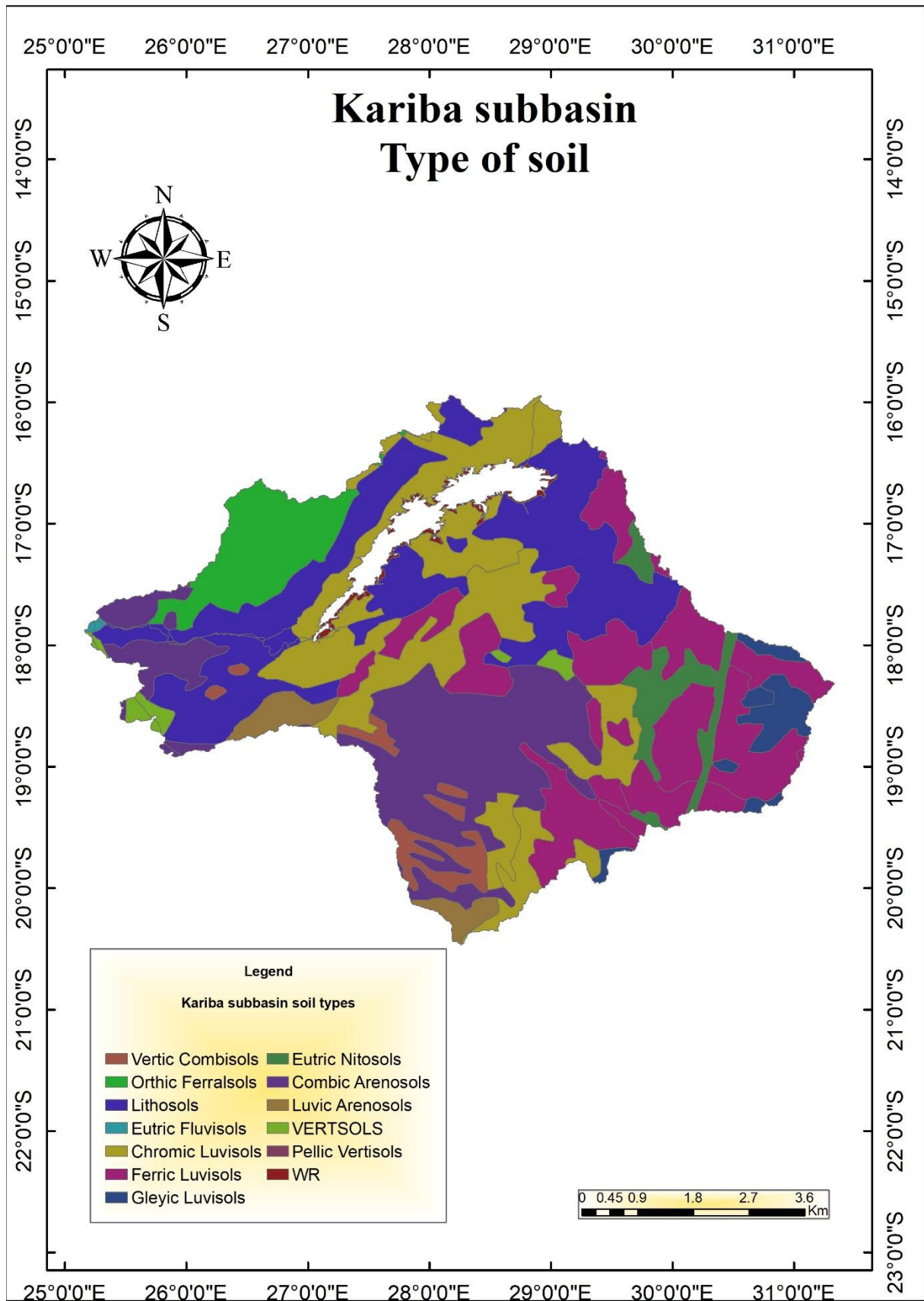


Figure 3.3: Soil map of Kariba subbasin

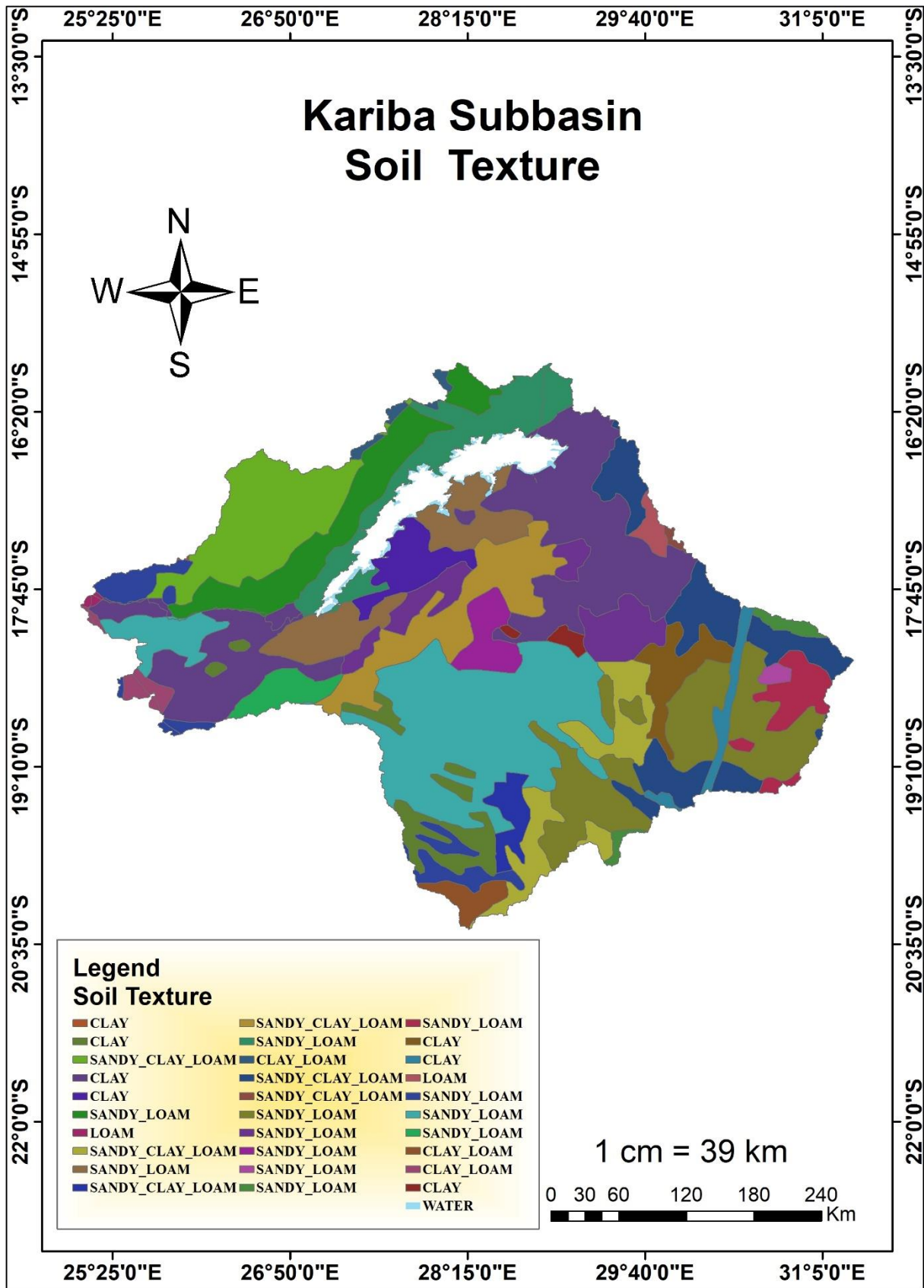


Figure 3.4: Major soil texture of Kariba subbasin

3.1.5 Land Use/Land Cover (LULC)

Assessing runoff, infiltration, and sedimentation—all of which affect Lake Kariba's water availability for hydropower generation is made easier with an understanding of land use and land cover of a particular area. The 2023 LULC map of the Kariba subbasin in Figure 3.5 below offers a visual representation of the spatial distribution of different land cover types within the region. Rangeland (54.86 %) and trees (37.03 %) predominate on the map. This natural vegetation is essential to the ecosystem of the subbasin because it provides cover, which lessens erosion and helps promote biodiversity. Agricultural lands are scattered throughout the subbasin, as evidenced by crops (7.21%). The presence of crops shows that communities staying within the subbasin are actively engaged in farming and depend on local produce for their consumption. The basin's sparse build-up areas suggest that infrastructure development and human settlement are concentrated in certain areas rather than occurring widely. River networks exist within the subbasin. Some of the rivers include the Zambezi River, which is the primary river draining into Lake Kariba; the Bumi River; the Sebungwe River; the Sengwa River; Ruziruhuru River, and the Gwayi River, a major tributary of the Zambezi River. Major water bodies like Lake Kariba also exist in the subbasin; Lake Kariba serves multiple purposes, from domestic to industrial water supply to providing livelihood opportunities through fishing and commercial fish farming. One purpose of great importance to this research is the use of Kariba in hydropower generation for Zambia and Zimbabwe. Build-up areas within the basin are sparse, indicating that human settlement and infrastructure development are concentrated in specific locations rather than widespread. These built areas in the subbasin are found in towns and cities, including Kariba, Victoria Falls, Gweru, and Bulawayo, all found in Zimbabwe, and Livingstone in Zambia.

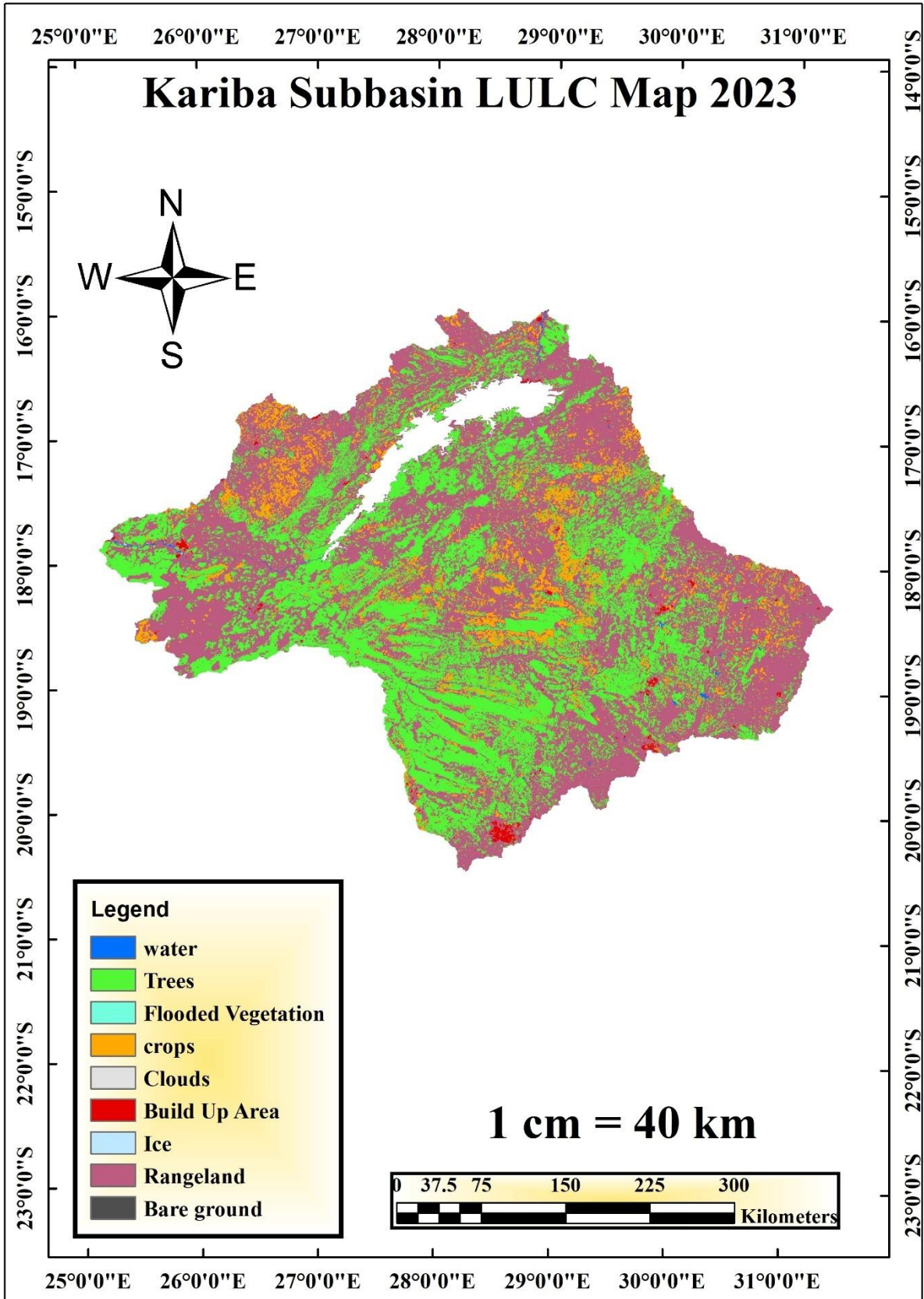


Figure 3.5: Land Use Land Cover Map of 2023 Kariba subbasin

3.2 Methodological Flowchart

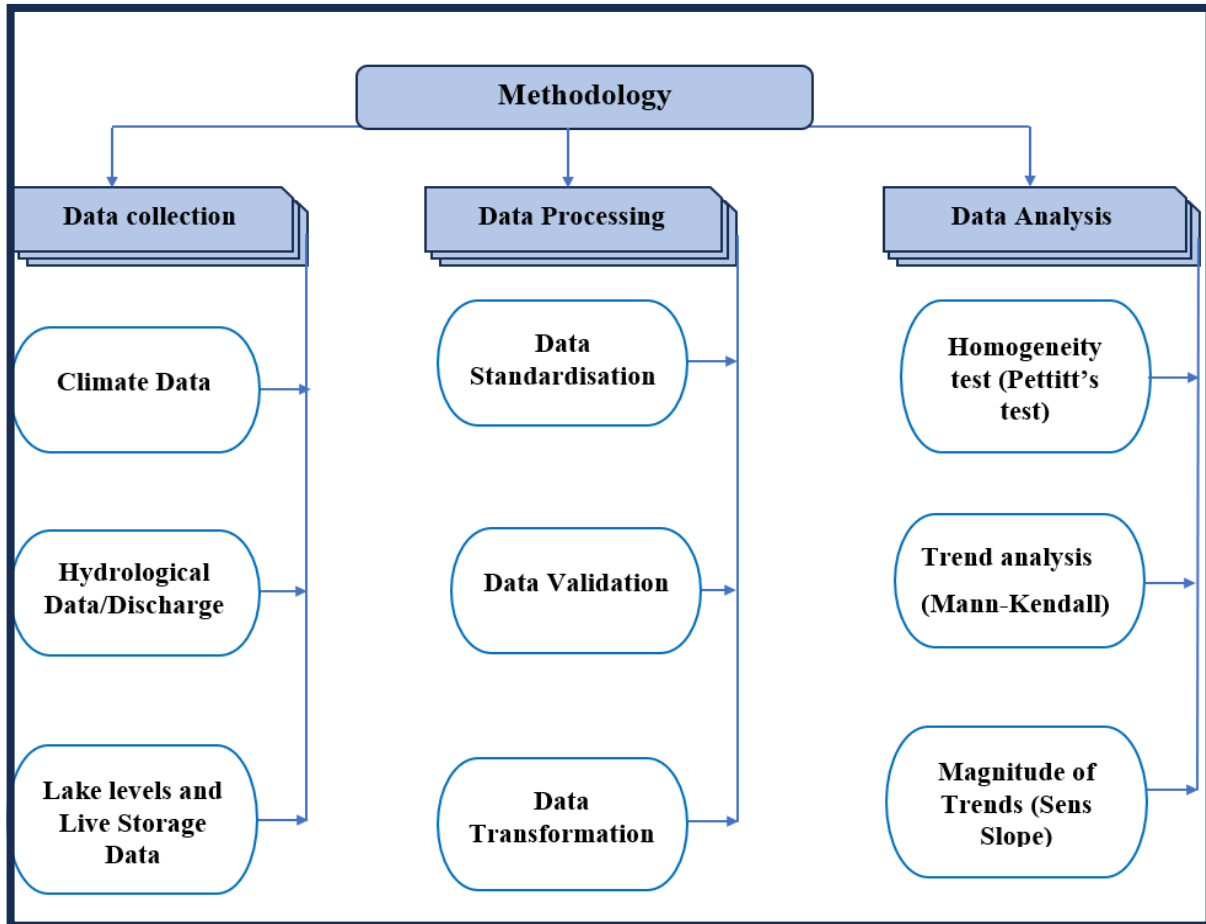


Figure 3.6: Methodological flow chart

3.2.1 Data collection and preprocessing

The study focused on assessing the impact of climate change on hydropower generation. This research selected, processed, and used data from 1990 to 2019. We obtained observed climate data relevant to the study area from the Meteorological Services of the Department of Zimbabwe (MSD). This climate dataset contains records of precipitation (mm), minimum temperature (°C), and maximum temperature (°C) for the period 1990 to 2019. We also downloaded satellite data from NASA Power to increase the number of meteorological stations we could use for trend analysis for our basin, as shown in Tables 3.2 and 3.3. We selected these monitoring stations to detect trends in river flow/discharge for two reasons: (1) the discharge recorded at Chavuma and Ngonye Falls substantially contributes to the discharge at Victoria Falls, forming the predominant input into Kariba Dam. Monitoring these stations is essential for understanding long-term patterns and assessing the effects of climate change on water availability at Kariba Dam for hydropower production. (2) The availability of high-quality,

complete daily measurements over a long period, from 1990 to 2019, except for the Ngonye station, where data collection began in 2005 after the station. Figure 3.7 represents the locations of the meteorological and hydro gauging stations used in this research. Additionally, we collected water level measurements for Kariba Dam from the Zambezi River Authority from 1990 to 2019. Table 3.1 below shows the data sets used for this research and the corresponding sources from which the data sets were collected.

Table 3.1: Data Used and Corresponding Sources

Data	Source	Spatial-temporal /resolution
DEM	SRTM 1-Arc	30m
Soil map	FAO	1:5 000 000
Land Cover map	ESA Sentinel-2	10m
Meteorological data (observed)	Meteorological Service Department of Zimbabwe	monthly
Hydrological data	Zambezi River Authority	monthly
GCM (historical and future) data	Copernicus	monthly
Tmax and Tmin	NASA Power	monthly

Table 3.2: List of meteorological stations on the Kaiba subbasin used for the study

Station_id	Station	Country	Latitude	Longitude	Elevation_(m)
Ghcnd: ZI000067755	Binga,	Zimbabwe	-17.617	27.333	620
Ghcnd: ZI000067965	Bulawayo airport,	Zimbabwe	-20.017	28.617	1326
Ghcnd: ZI000067861	Gokwe,	Zimbabwe	-18.217	28.933	1282
Ghcnd: ZI000067867	Gweru,	Zimbabwe	-19.45	29.85	1429
Ghcnd: ZI000067853	Hwange National Park	Zimbabwe	-18.633	27	1077
Ghcnd: ZI000067761	Kariba,	Zimbabwe	-16.517	28.883	518
Ghcnd: BC012192590	Kasane,	Botswana	-17.817	25.15	1002
Ghcnd: ZI000067865	Kwekwe,	Zimbabwe	-18.1	29.833	1215
Ghcnd: ZA000067743	Livingstone	Zambia	-17.817	25.817	986
Ghcnd: ZI000067843	Victoria Falls	Zimbabwe	-18.1	25.85	1062

Table 3.3: Hydro Gauging stations used for this study

Station Name	Location		Period of Records	Country	Data Collected	Type of gauge
	Latitude	Longitude				
Chavuma Mission	-13.08	22.68	1990-2019	Zambia	discharge data	Manual+SADC HYCOS Telemetry
Ngonye Rapids (Sioma Falls)	-16.64	23.56	2005-2019	Zambia	discharge data	Manual+WAR MA GSM Telemetry
Victoria Falls (Big Tree station)	-17.91	25.85	1990-2019	Zimbabwe	discharge data	Manual

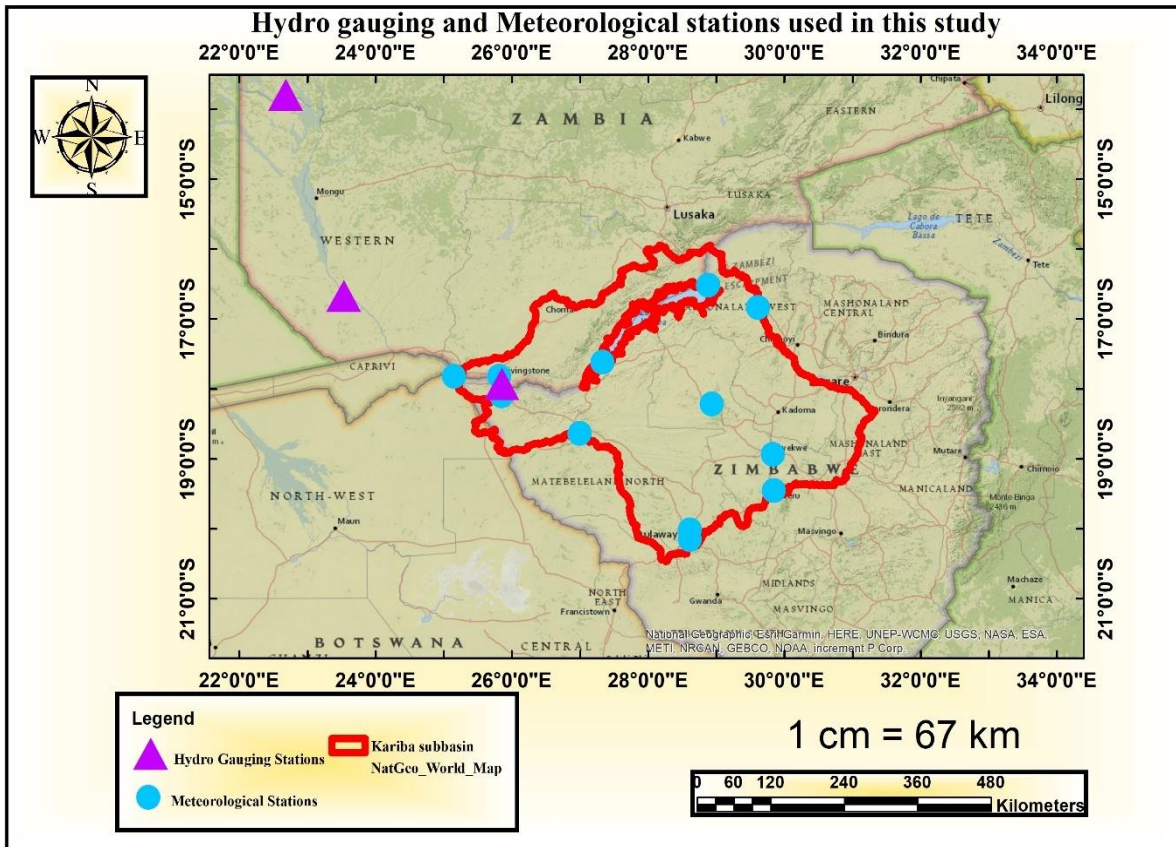


Figure 3.7: Locations of Hydro gauging and meteorological stations used for the study

3.2.2 Soil and soil texture data

The World Digital Soil Map (DSMW) dataset, developed by FAO/UNESCO, was downloaded in ZIP format and processed to extract relevant soil data for Zimbabwe, Zambia, and Botswana. The DSMW shapefile (SHP) was imported into ArcMap, where soil data specific to these three countries were extracted and exported as individual shapefiles for further processing.

To focus on the Kariba Subbasin, the Kariba Subbasin soil profile shapefile was integrated into ArcMap and spatially cropped to align with the country-specific soil files. The resulting soil map was subsequently reclassified to generate :

- Figure 3.2: Soil Map of the Kariba Subbasin, representing the spatial distribution of soil types within the subbasin.
- Figure 3.3: Main Soil Texture of the Kariba Subbasin, which classifies soil textures across the study area.

FAO datasets, including Africa, are widely recognized and utilized in scientific research due to their comprehensive global spatial coverage. The FAO/UNESCO soil classification system is

internationally standardized, ensuring consistency in soil mapping and interpretation. The FAO/UNESCO World Soil Map, which has a scale of 1:500,000, made an accurate spatial representation and classification of soil properties within the Kariba Subbasin possible. The map served as a dependable data source for this study.

3.2.3 Data cleaning and standardisation

A thorough data cleaning and standardization procedure was implemented to guarantee the precision and consistency of hydrological, climatic, and hydropower data. Finding and fixing outliers, missing values, and inconsistencies in all datasets used in this research work was part of this data-cleaning process. The Meteorological Services Department of Zimbabwe (MSD) provided the temperature, precipitation, and climate records. These datasets were methodically analysed to find extreme outliers, missing values, and measurement irregularities. To improve data reliability, appropriate data correction methods were used where needed, such as statistical validation and interpolation. The Zambezi River Authority (ZRA) provided hydrological data, mainly river discharge records, for three important gauging stations: Victoria Falls (Big Tree Station), Ngonye (Sioma Falls), and Chavuma Mission. A comparative study was conducted among these stations to guarantee data uniformity and standardization. A solid dataset for hydrological trend analysis was ensured by identifying and correcting errors and outliers in discharge records. Effective live storage data was obtained from the Zambezi River Authority and this Data was important in determining the water that was set for hydropower generation These records were validated to remove inconsistencies and verify data integrity by cross-referencing them with documented water availability and operational conditions. The study made sure that all datasets were trustworthy by going through this thorough cleaning and standardization process.

3.2.4 Homogeneity test and Trend analysis

The analysis of climatic parameters (precipitation, maximum temperature, and minimum temperature) for Binga and Kariba stations, as well as river flow data from three hydro-gauging stations (Chavuma Mission, Ngonye (Sioma Falls), and Victoria Falls (Big Tree Station)), was conducted using statistical methods to assess homogeneity and trends in the time series data.

Pettitt's test was used to identify possible time series change points to assess the dataset's homogeneity. Furthermore, the direction and magnitude of trends in hydrological and climatic data over time were evaluated using the Mann-Kendall trend analysis and Sen's slope estimator. Microsoft Excel was used to perform the homogeneity and trend analyses using the

XLSTAT program (version 2024.4). 0, build 1424). By accepted statistical practice for identifying significant trends and changes in datasets about climate and hydrology, the significance level was set at 5% or a 95 percent confidence level.

3.2.5 Homogeneity test

A homogeneity test evaluates the statistical consistency of time series data, including temperature, precipitation, and streamflow, over time or across regions. Therefore, adjusting time series data that exhibit changes unrelated to weather, climate, or hydrology is crucial. Several factors, such as (a) sensor instrumentation (upgrading from analog to digital instruments), (b) observation practices (shifting from morning to afternoon), and (c) modification of environmental conditions (overall changes in land use and land cover), among others, may cause these inconsistencies (Muchuru et al., 2015). Several approaches have been developed to perform the homogeneity test, the Cumulative deviations test, which detects changes or shifts in the mean of a dataset over time, and the cumulative deviations test, which evaluates the sum of deviations of a variable from its mean to identify potential inhomogeneities or structural breaks in time series data. Statistical tests are also used in homogeneity tests involving parametric and non-parametric methods. Pettitt's non-parametric test was used for this work's homogeneity test. It does not require any assumption about the distribution of data. Pettitt's test allows one to detect a time at which a shift occurred (Pettitt, 1979).

H_0 : the dataset is homogeneous (there is no change point in the dataset)

H_1 : the dataset is inhomogeneous (there is a change point in the dataset)

Detection of change point methods is crucial for identifying dates when time series data is altered, which can be linked to climate change. (Palaniswami & Muthiah, 2018).

Test statistics

For a time, series $X = (x_1, x_2, \dots, x_T)$, the Pettitt test calculates rank-based statistics $U_{t,T}$ for each point t , T (potential change point) in the dataset shown in Equation 1 below.

(1)

$$U_{t,T} = \sum_{i=1}^t \sum_{j=t+1}^T \text{sgn}(X_i - X_j), \quad 1 \leq t < T$$

Were

(2)

$$\text{sgn}(x) = \begin{cases} 1, & \text{if } x > 0 \\ 0, & \text{if } x = 0 \\ -1, & \text{if } x < 0 \end{cases}$$

Maximum test statistics:

(3)

The maximum absolute value of $U_{t,T} K = \max|U_k|, 1 \leq t < T$

Significance:

(4)

$$p \approx 2 \exp\left(\frac{-6K_{\tau}^2}{T^3 + T^2}\right)$$

At a significance level α , $p < \alpha$, the null hypothesis, H_0 is rejected.

The annual mean minimum temperature, annual mean maximum temperature, annual total precipitation, and total seasonal precipitation (NDJFM) were analysed for homogeneity before the trend analysis test was applied, with a significance level of 5% and a 95% confidence level of the p-value.

3.2.6 The Mann-Kendall test for monotonic trends

The Mann-Kendall (MK) test, also called the MK test, is employed in environmental, hydrological, or climate data to statistically evaluate the presence of a monotonic upward or downward trend in the variable of interest over time (Mann, 1945). A monotonic trend, whether upward or downward, signifies that the variable consistently increases or decreases over time, regardless of linearity. The MK's strength lies in its non-parametric nature, allowing the application to any distribution without the necessity for normality assumptions and less sensitivity to outliers while being straightforward and interpretable (Moses, 2024). The MK test has been utilised in hydro-meteorological time series to detect significant trend patterns

(Mazvimavi & Wolski, 2006; Mphale et al., 2018; Muchuru et al., 2015). The data should exhibit no autocorrelation; however, normal distribution and linearity are unnecessary.

How the test works

The MK test tests whether to reject the null hypothesis H_0 and accept the alternative hypothesis

H_1 where:

H_0 : No monotonic trend

H_1 : A monotonic trend is present in the two-sided Test, or there is an upward trend (or downward trend) in the one-sided Test.

For the time series x_1, \dots, x_n , the MK test uses the following statistics S is calculated using Equation (1) as follows:

(1)

$$S = \sum_{i=1}^{n-1} \sum_{j=i+1}^n \text{sign}(x_j - x_i)$$

Where:

S is the test statistic

Sign $(X_j - X_i)$ is the sign function:

- +1 if $X_j > X_i$
- 0 if $X_j = X_i$
- -1 if $X_j < X_i$

If $S > 0$, then later observations in the time series tend to be larger than those that appear earlier in the time series, while the reverse is also true if $S < 0$.

The variance of S is given by using Equation (2):

(2)

$$\text{var} = \frac{1}{18} \left[n(n-1)(2n+5) - \sum_t f_t(f_t-1)(2f_t+5) \right]$$

Where t varies over the set of tied ranks and f_t is the number of times (i.e. frequency) that the rank t appears.

Standard Normal Z -statistics as indicated in Equation (3):

(3)

$$z = \begin{cases} (S - 1)/se, & S > 0 \\ 0, & S = 0 \\ (S + 1)/se, & S < 0 \end{cases}$$

se is the square root of the variance

3.2.7 The magnitude of the trend (Sen's slope estimator)

Sen initially designed this test to assess statistical linear relationships. This analysis quantifies the magnitude of trends in long-term temporal data. Sen's slope is considered one of the best methods for detecting linear relationships as it remains unaffected by outliers in the data (Ray et al., 2021). This study employs the Sens slope to quantify the magnitude of trends in temperature, total rainfall, and water flow data.

The individual slope (Q_i) is estimated using Equation (4):

(4)

$$T_i = \frac{x_j - x_k}{j - k} \quad \text{for } i = 1, 2, \dots, N$$

X_j and X_k are considered data values or variables at time j and k ($j > k$), respectively. N is the number of observations, and j and k are indices. Sen's slope is then calculated as the median for all slopes

Equation (5) provides Sen's estimator of slope, which is the median of these N values of T_i :

(5)

$$Q_i = \begin{cases} \frac{T_{N+1}}{2} & N \text{ is odd} \\ \frac{1}{2} \left(\frac{T_N}{2} + \frac{T_{N+1}}{2} \right) & N \text{ is even} \end{cases}$$

Q_{med} is computed by a two-sided test at $100(1-\alpha)$ % confidence interval.

The positive (Q_i) indicates an increased trend, while negative Q_i values indicate a negative trend in the temporal data.

3.2.8 Determination of precipitation and Temperature trends

We computed the homogeneity and trend tests using add-ins XLSTAT 2024.4.0. We analysed historical precipitation and temperature trends by obtaining monthly average precipitation and temperature data from 1990 to 2019 from stations within the study area provided by the Meteorological Services Department of Zimbabwe (MSD). We computed and graphed the annual mean maximum, annual mean minimum temperature, seasonal total, and annual precipitation over time, observing and analysing the resulting trends. Precipitation and temperature trends served as indicators of climate change in the Kariba Subbasin of the middle ZRB. We used the nonparametric homogeneity Pettitt test for homogeneity at a 5% significance level. We then used the MK test to examine the behaviour of the monotonic trends in temperature and precipitation, and we used the Sens slope estimation to gauge the trends' magnitude. The MK trend test was used to detect trends of historical annual mean minimum temperature ($^{\circ}\text{C}$), annual mean maximum temperature ($^{\circ}\text{C}$), total seasonal (wet season) precipitation, annual total precipitation (mm), and mean annual precipitation (mm) data (1990-2019).

To assess historical precipitation and temperature trends, we obtained monthly average precipitation and temperature data from 1990 to 2019 for stations within the study area, as provided by the Meteorological Services Department of Zimbabwe (MSD). These datasets were analysed to identify long-term climate patterns in the Kariba Subbasin of the Middle Zambezi River Basin (ZRB).

We conducted homogeneity and trend analyses using XLSTAT 2024.4.0 add-ins in Microsoft Excel. The analysis involved computing and graphing :

- Annual mean maximum temperature ($^{\circ}\text{C}$)
- Annual mean minimum temperature ($^{\circ}\text{C}$)

- Total seasonal precipitation (wet season)
- Annual total precipitation (mm)

These climatic parameters were evaluated as indicators of climate change impacts on the hydrological system within the Kariba Subbasin.

We applied Pettitt's 5% significance level test for the homogeneity assessment to detect potential change points in the time series data. We used the Mann-Kendall (MK) test to analyse monotonic trends, which is widely applied in climate trend analysis due to its robustness against non-normally distributed data and outliers. Furthermore, the Sen's Slope Estimator was employed to quantify the magnitude of detected trends, providing a robust, nonparametric measure of the rate of change over time.

This approach ensured a comprehensive evaluation of historical climate trends, enabling a better understanding of temperature and precipitation variability in the study area.

3.2.9 Determination of River Flow /Discharge

Historical river flow data were analysed for the Chavuma Mission, Ngonye (Sioma Falls), and Victoria Falls (Big Tree) hydrological monitoring stations. Monthly discharge records from 1990 to 2019 were obtained from the Zambezi River Authority (ZRA) to assess long-term hydrological trends within the Kariba Subbasin of the Middle Zambezi River Basin (ZRB).

A nonparametric Mann-Kendall (MK) test was applied to the discharge data from the three monitoring stations to evaluate river discharge trends. The MK test was chosen due to its ability to reliably identify monotonic patterns in time series data, even in cases where the datasets are not normally distributed or contain missing values. The size and direction of the found river discharge trends were also measured using Sen's Slope Estimator. By reducing the impact of outliers, this nonparametric estimator offers a trustworthy indicator of trend magnitude, which makes it especially appropriate for hydrological time series analysis.

This analysis aims to understand the hydrological response to climate variability and its consequences for hydropower production at Kariba South Hydropower Station.

CHAPTER FOUR

RESULTS AND DISCUSSION

4.0 Temperature and precipitation trends from 1990 to 2019.

Tables 4.1 and 4.2 below summarise specific climate change indicators for our study area, including the annual mean minimum temperature, the annual mean maximum temperature in degrees Celsius, and annual total precipitation in millimetres. These parameters were important for analysing the trends of these climatic parameters (temperature and precipitation) for our study area from 1990 to 2019.

Table 4.1: Climate change indicators of Kariba subbasin (Binga station)

Year	Annual Mean Min Temperature (°C)	Annual Mean Max Temperature (°C)	Annual total Precipitation (mm)
1990	19.62	29.17	365.00
1991	19.38	30.10	571.70
1992	19.80	29.63	470.10
1993	19.97	30.94	648.70
1994	19.83	29.62	349.30
1995	20.25	31.33	366.60
1996	20.54	30.33	738.10
1997	20.02	30.07	1198.10
1998	20.56	31.22	479.00
1999	20.63	30.79	462.00
2000	21.11	32.08	1012.80
2001	20.86	30.62	1029.00
2002	20.33	30.92	458.70
2003	21.07	32.21	490.30
2004	20.07	30.41	885.30
2005	20.36	30.00	355.30

2006	20.88	31.23	1107.80
2007	20.59	30.17	846.10
2008	20.39	30.02	946.50
2009	20.27	30.33	733.70
2010	19.99	30.07	1107.30
2011	20.93	31.22	800.30
2012	20.33	30.79	564.00
2013	21.58	32.08	675.50
2014	20.53	30.62	697.60
2015	20.45	30.89	416.50
2016	21.22	32.15	504.30
2017	19.97	30.41	899.80
2018	20.28	30.00	655.80
2019	20.95	31.23	378.10

Table 4.2: Climate change indicators of Kariba subbasin (Kariba station)

Year	Annual Mean Min Temperature (°C)	Annual Mean Max Temperature (°C)	Annual total Precipitation (mm)
1990	17.81	30.11	586.80
1991	17.46	29.46	480.30
1992	18.68	30.81	582.00
1993	18.17	29.87	524.80
1994	18.60	30.48	497.80
1995	18.05	30.47	311.50
1996	17.82	30.33	819.40
1997	18.85	31.20	912.20
1998	20.08	32.18	899.30
1999	19.88	31.75	627.70
2000	18.70	30.76	663.40
2001	17.81	30.36	693.80

2002	19.56	32.44	594.60
2003	19.54	31.21	692.30
2004	18.85	30.75	875.80
2005	19.12	31.15	667.10
2006	19.16	31.30	699.60
2007	19.85	32.44	828.00
2008	19.36	31.21	817.20
2009	18.87	31.81	862.10
2010	20.11	32.63	760.50
2011	18.55	32.01	672.90
2012	18.09	31.33	758.30
2013	19.41	32.16	778.40
2014	18.83	31.27	743.20
2015	19.22	31.19	492.40
2016	19.03	31.40	746.00
2017	19.66	31.77	1033.30
2018	18.88	31.54	625.20
2019	18.73	31.48	551.00

4.1 Binga and Kariba - Annual Mean Maximum Temperatures

4.1.1 Homogeneity test

The homogeneity of the annual mean maximum temperature data for Binga and Kariba was assessed using Pettitt's test. According to the test results, Binga's p-value is 0.54, above the 0.05 significance level, indicating that the time series underwent no sudden changes. Therefore, Binga's annual mean maximum temperature data is regarded as homogeneous, as shown in Figure 4.1 below. In contrast, Kariba Pettitt's test yielded a p-value of 0.01 below the 0.05 significance level. This result indicates a statistically significant shift in the mean annual maximum temperature, with an identified change point in 1997, as shown in Figure 4.2.

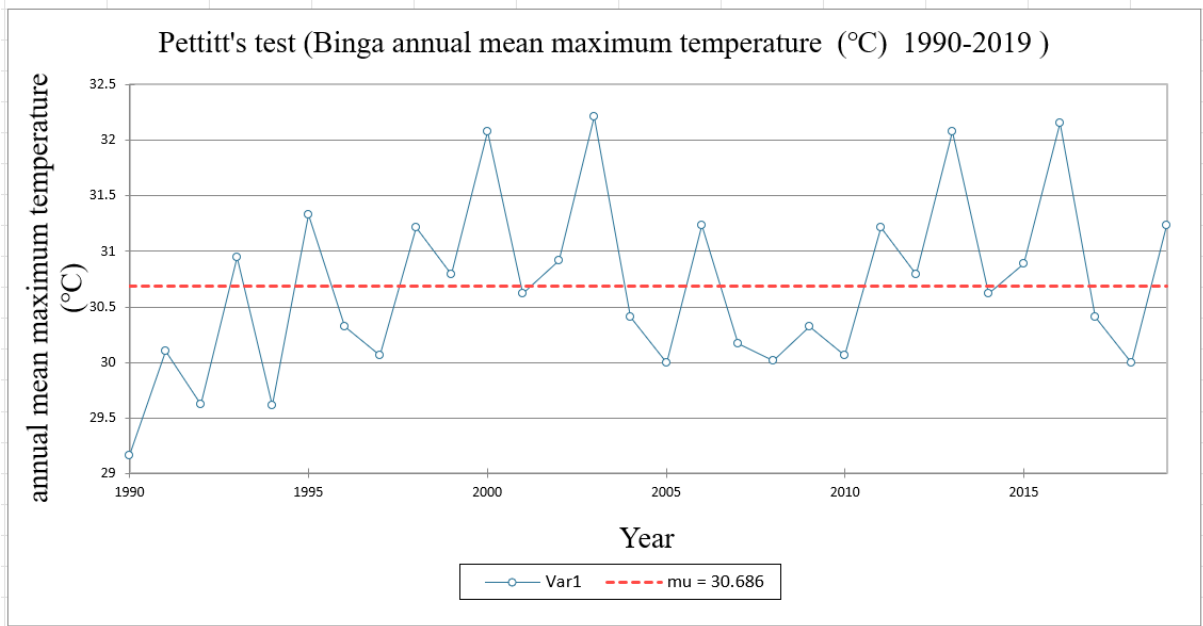


Figure 4.1: Binga annual mean maximum temperature 1990-2019

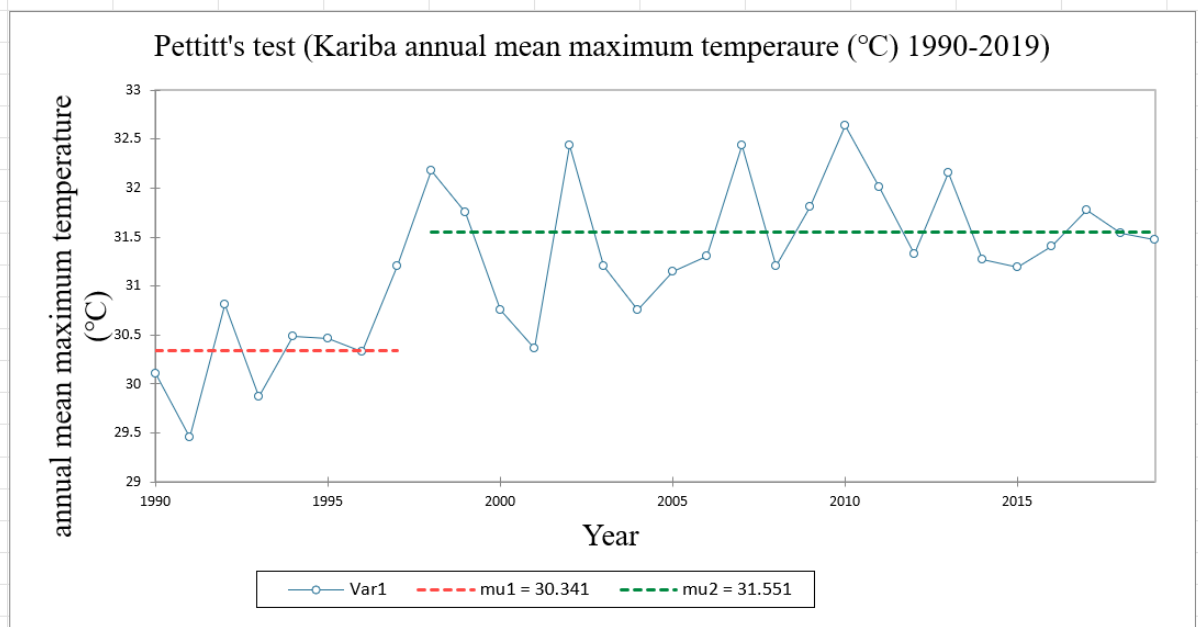


Figure 4.2: Kariba annual mean maximum temperature 1990-2019

4.1.2 Trend Analysis

The Mann-Kendall (MK) and Sen's Slope tests were conducted to analyse the trend and magnitude of annual mean maximum temperatures at Binga and Kariba stations. The results indicate that the two-tailed p-value (0.16) for Binga exceeds the 5% significance level (0.05), suggesting no statistically significant trend in annual mean maximum temperature at a 95% confidence level. However, despite the lack of statistical significance, the positive Sen's slope

value (0.029) indicates a slightly increasing tendency in annual mean maximum temperature over the study period (1990–2018) as shown in Figure 4.3.

For Kariba, the MK test results show a two-tailed p-value of 0.266 for the pre-change period (1990–1997) with a corresponding Sen's slope of 0.16, indicating a weakly increasing trend, albeit statistically insignificant as shown in Figure 4.4. In the post-change period (1998–2019), the p-value was 0.50, with a slope value of 0.02, suggesting no significant trend and only a marginal increase in temperature, as shown in Figure 4.5. These results, as presented in Tables 4.3 and 4.4, indicate that while both stations exhibit slight warming trends, the trends are not statistically significant at the 5% significance level.

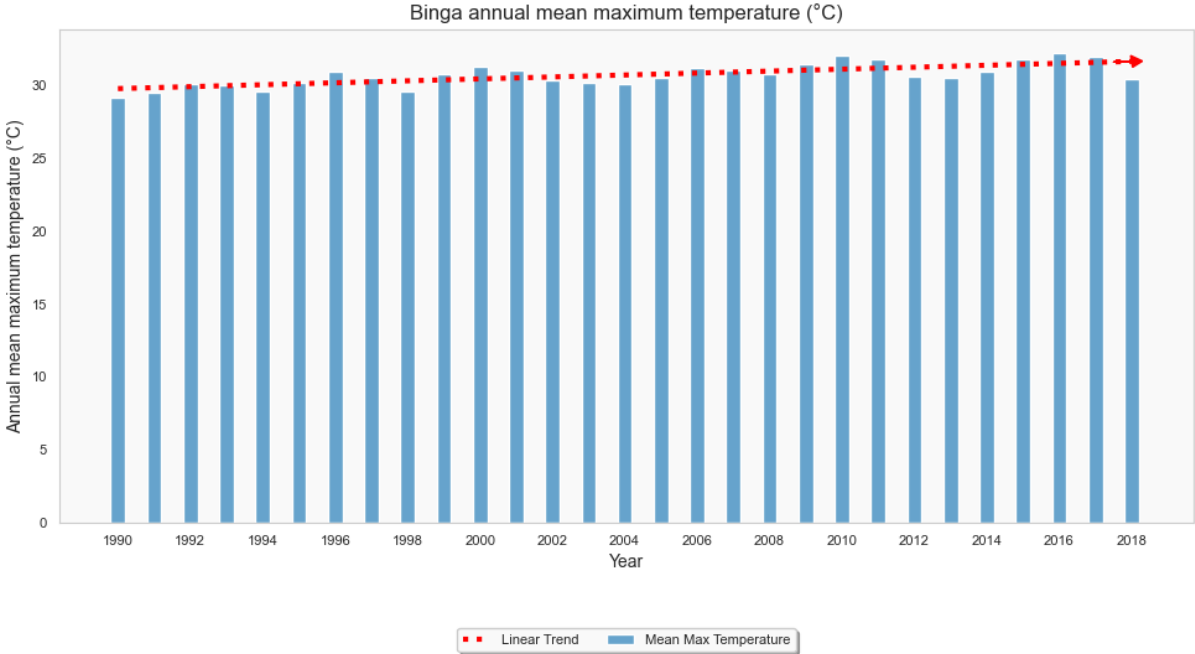


Figure 4.3: Binga annual mean maximum temperature (1990-2018)

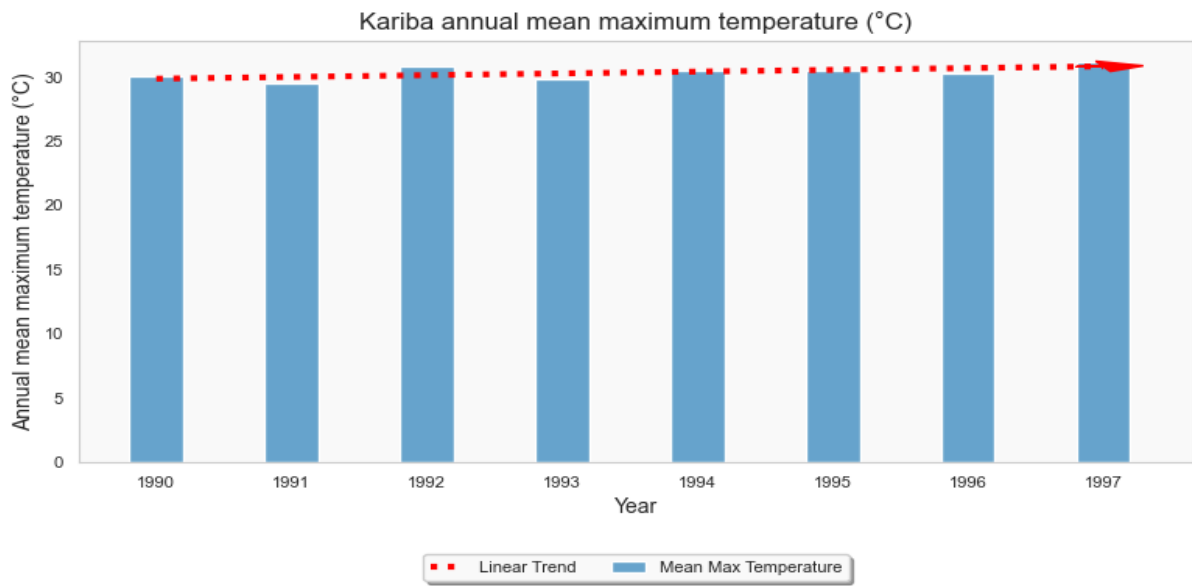


Figure 4.4: Kariba annual mean maximum temperature (1990-1997)

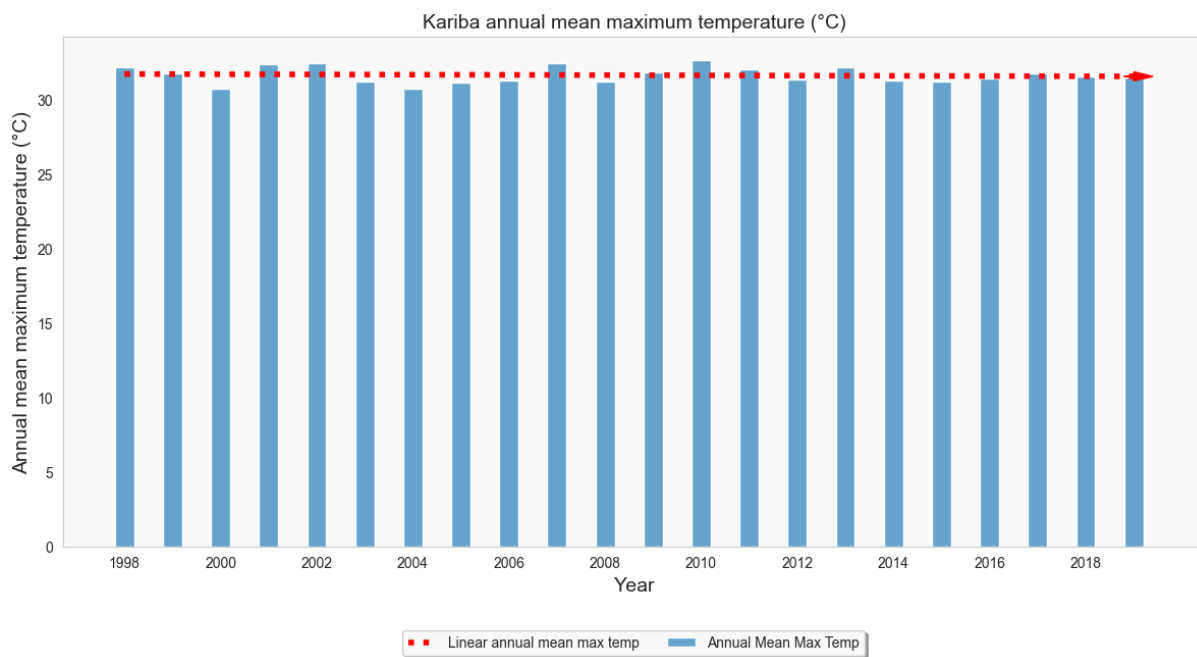


Figure 4.5: Kariba annual mean maximum temperature 1998-2019

Table 4.3: Homogeneity test for Binga and Kariba annual mean maximum temperature

Type of test	Parameter of Interest	Pre-test homogeneity p-value	Segmented data p-values	Year	Station name
Pettitt's test	P	0.54		1990-2019	Binga
Pettitt's test	P	0.01	0.66	1990-1997	Kariba
			0.83	1998-2019	

Table 4.4: Trend analysis for Binga and Kariba annual mean maximum Temperature

Type of test	Parameter of Interest	Annual mean maximum temperature p-value	Year	Station name
MK test	p-value	0.16	1990-2019	Binga
Sen's slope	slope	0.03		
MK test	p-value	0.27	1990-1997	Kariba
		0.50	1998-2019	
Sen's slope	slope	0.16	1990-1997	
		0.02	1998-2019	

4.2 Binga and Kariba - Annual Mean Minimum Temperatures

4.2.1 Homogeneity test

Binga and Kariba's annual mean minimum temperatures were tested for homogeneity using Pettitt's test at a 5% significance level with a 95% confidence interval. The test results in Table 4.5 indicate p-values of 0.02 for both stations, suggesting a statistically significant shift in annual mean minimum temperature during the study period (1990–2019). The identified breakpoints occurred in 1998 for Binga and 1997 for Kariba, as shown in Figures 4.6 and 4.7. Each station's annual mean minimum temperature datasets were segmented into two periods to account for these abrupt shifts. For Binga, the pre-change period spans 1990–1998, while the

post-change period covers 1999–2019. Similarly, Kariba's dataset was divided into a pre-change period (1990–1997) and a post-change period (1998–2019). These segmented datasets were then used for subsequent Mann-Kendall (MK) and Sen's Slope trend analysis.

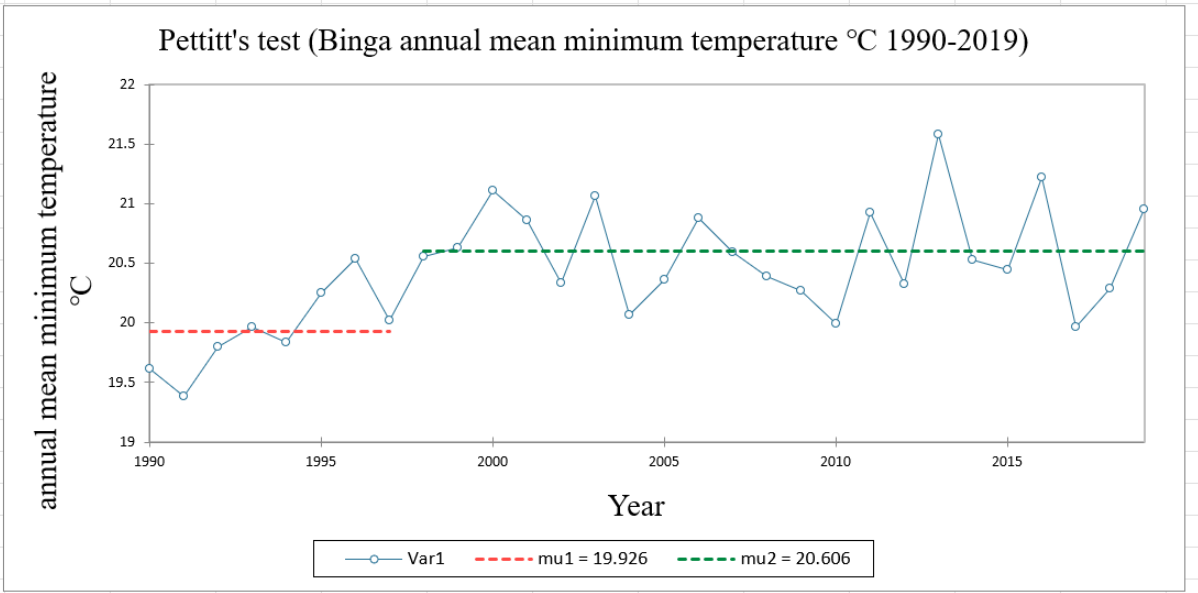


Figure 4.6: Binga homogeneity test annual mean minimum temperature 1990-2019

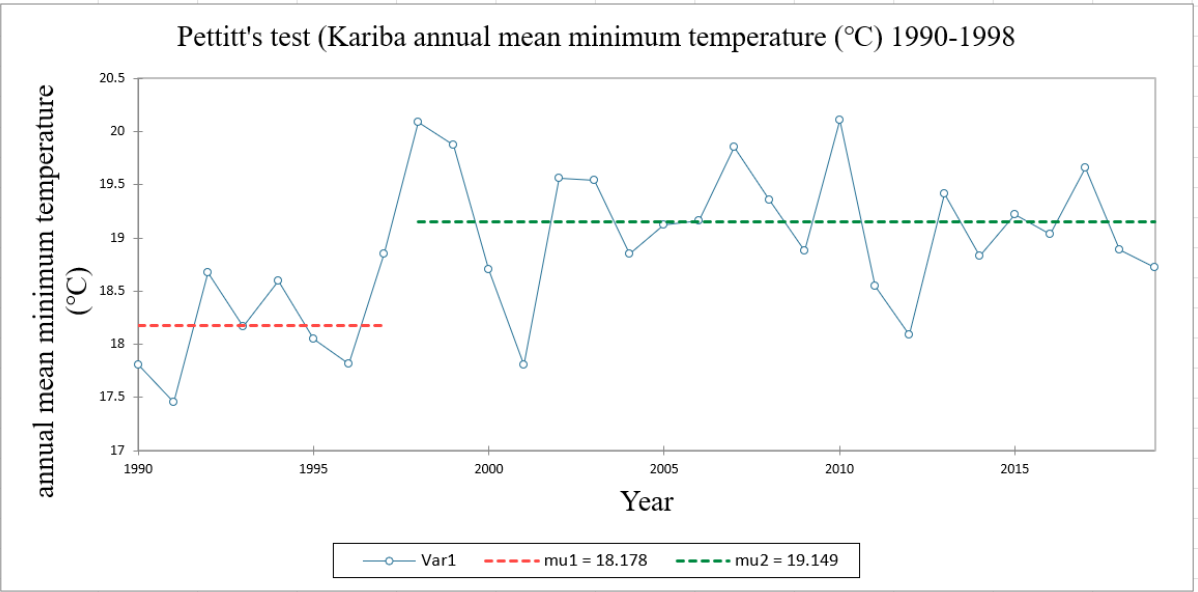


Figure 4.7: Kariba homogeneity test annual mean minimum temperature (1990-2019)

4.2.2 MK and Sen's Slope Trend Analysis for Annual Minimum Temperatures

Trend analysis was conducted on two data segments for Binga and Kariba's annual mean minimum temperatures, covering the pre-change (1990–1998) and post-change (1999–2019) periods. For Binga, the Mann-Kendall (MK) test for the pre-change period (1990–1998) yielded a p-value of 0.004 and a Sen's slope value of 0.15, as shown in Table 4.6. These results indicate a statistically significant warming trend in annual mean minimum temperature. However, in the post-change period for Binga station (1999–2019), the MK test produced a p-value of 0.61, suggesting no statistically significant trend. The corresponding Sen's slope value (-0.01) indicates a slight decreasing tendency, though not statistically significant.

For Kariba, the MK test results for the pre-change period (1990–1997) showed a p-value of 0.39 and a Sen's slope value of 0.08, indicating no statistically significant trend but a slightly increasing tendency in annual mean minimum temperature. In the post-change period (1998–2019), the MK test yielded a p-value of 0.31 and a Sen's slope value of -0.03, suggesting a very slight decreasing trend, which is also not statistically significant. Overall, the results summarised in Table 4.6 indicate that while Binga experienced a statistically significant warming trend before 1998, both stations exhibited no significant annual mean minimum temperature trends in the later period, as shown in Figures 4.8, 4.9, 4.10, and 4.11 below.

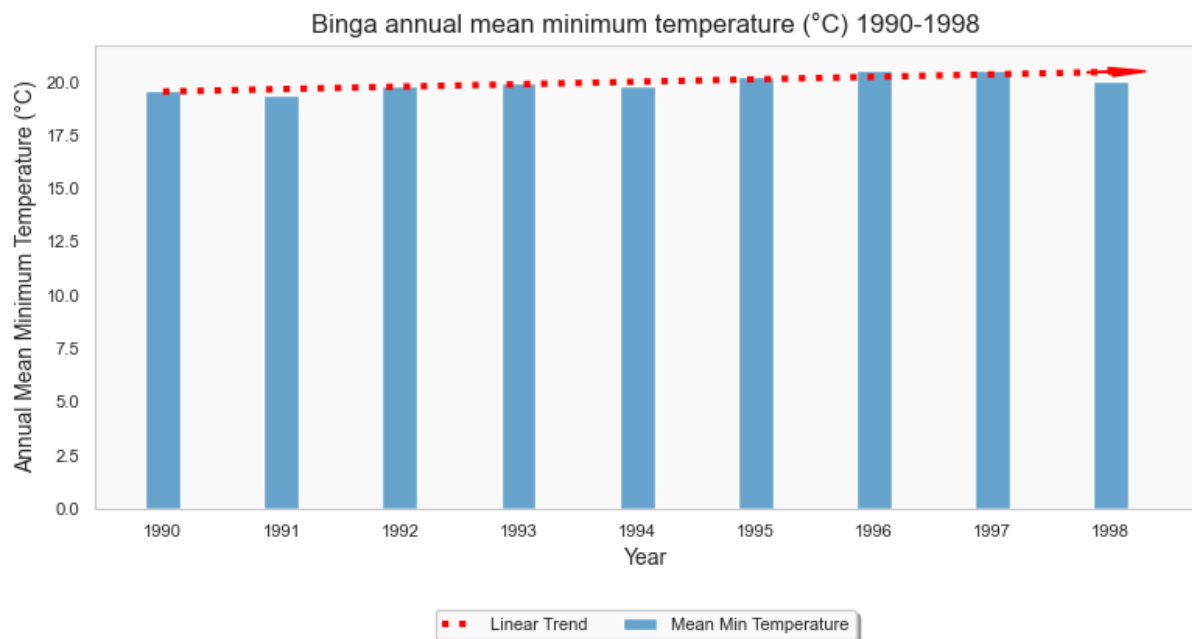


Figure 4.8: Binga annual mean minimum temperature (°C) 1990-1998

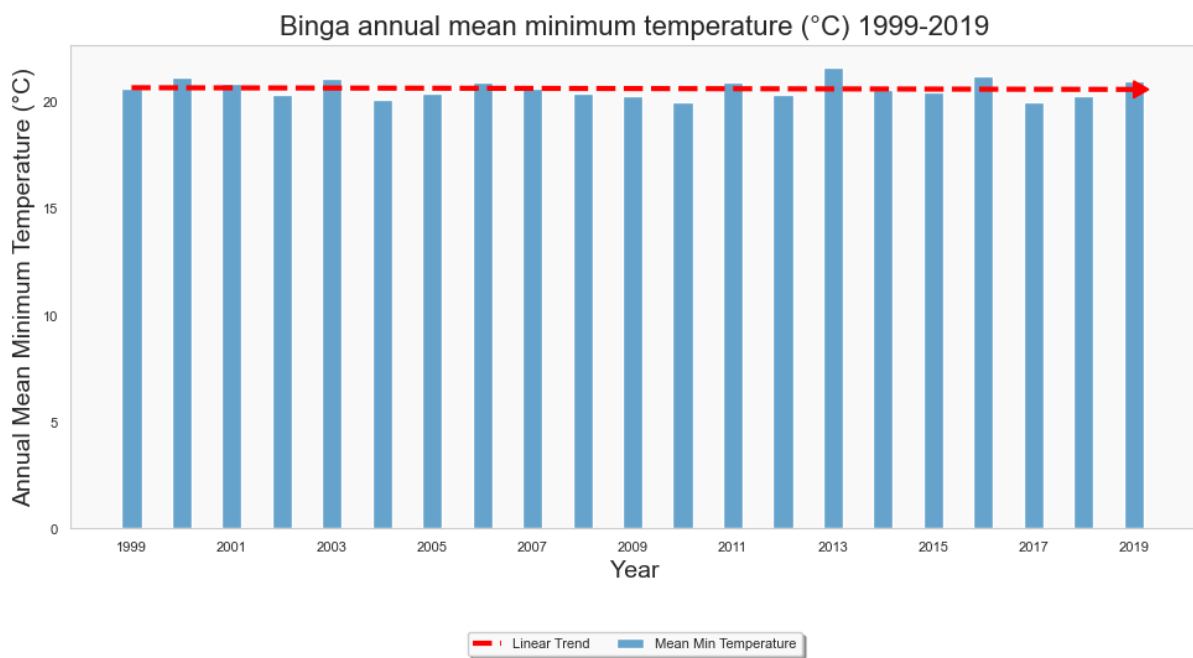


Figure 4.9: Binga annual mean minimum temperature (°C) 1999-2019

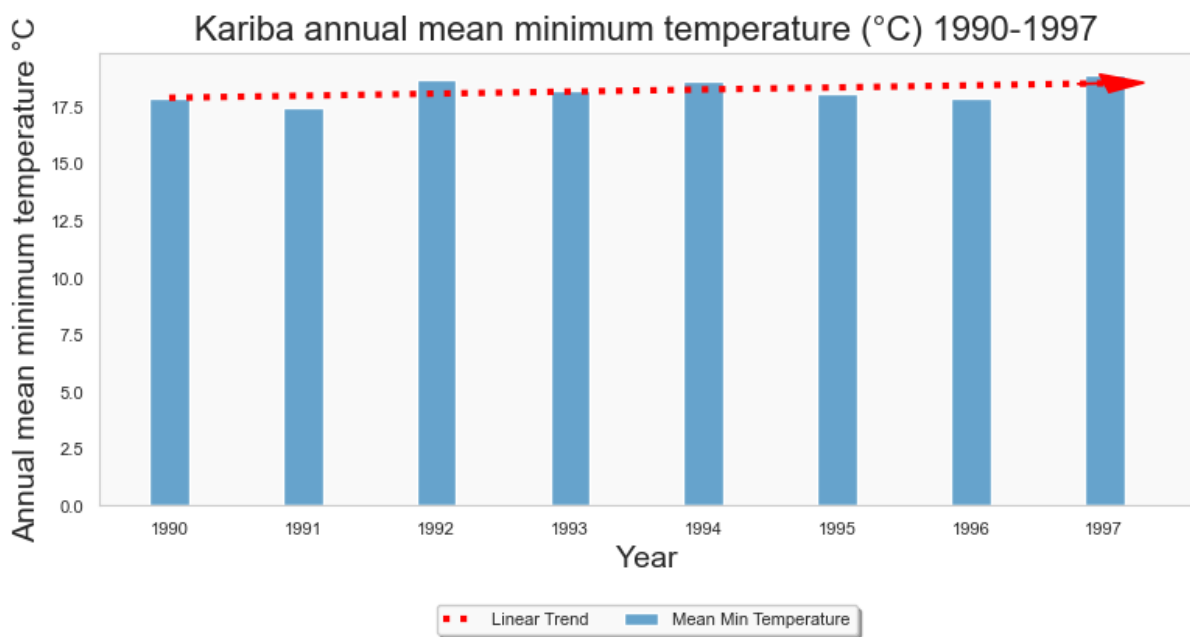


Figure 4.10: Kariba annual mean minimum temperature (°C) 1990-1997

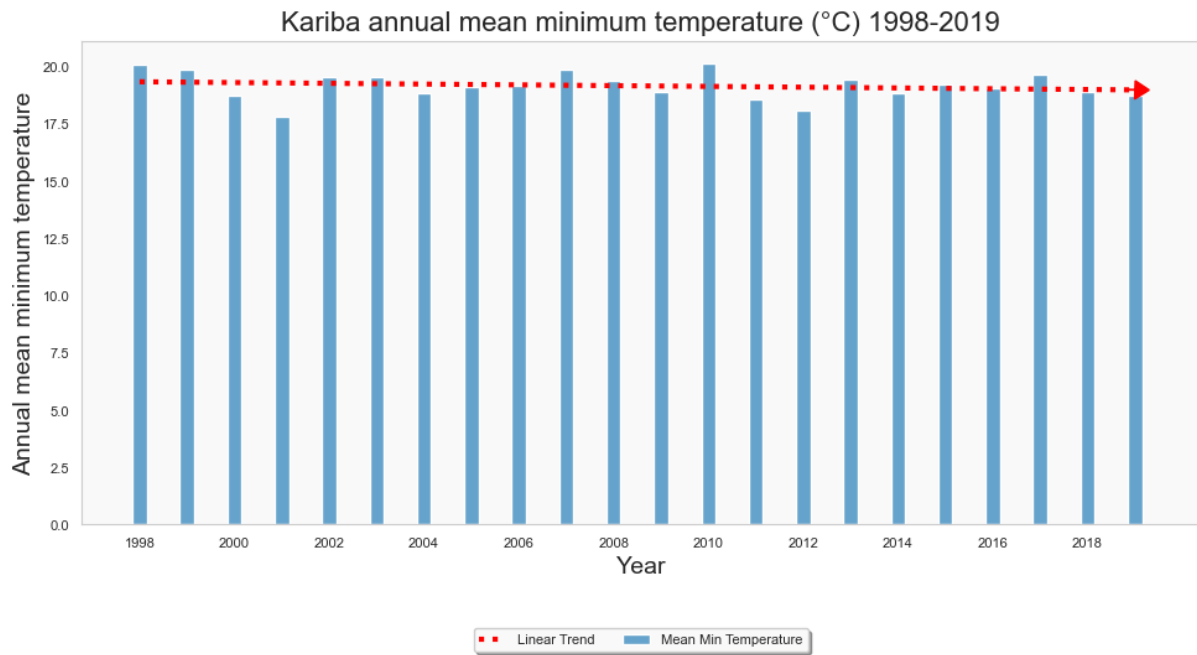


Figure 4.11: Kariba annual mean minimum temperature (°C) 1998-2019

Table 4.5 Homogeneity test for Binga and Kariba annual mean minimum temperature (°C)

Type of test	Parameter of Interest	Pre-Test Homogeneity p-value	Segmented data p-value	Year	Station Name
Pettitt's test	P	0.02	0.06	1990-1998	Binga
			0.52	1999-2019	
Pettitt's test	P	0.02	0.30	1990-1997	Kariba
			0.91	1998-2019	

Table 4.6 Trend analysis for Binga and Kariba annual mean minimum temperature (°C)

Type of test	Parameter of Interest	P-value	Year	Station name
MK test	p-value (two-tailed)	0.004	1990-1998	Binga
		0.60	1999-2019	
Sen's slope	slope	0.15	1990-1998	
		-0.01	1999-2019	
MK test	p-value (two-tailed)	0.39	1990-1997	Kariba
		0.31	1998-2019	
Sen's slope	slope	0.08	1990-1997	
		-0.03	1998-2019	

4.3 Precipitation for Binga and Kariba

4.3.1 Homogeneity test for total annual precipitation and seasonal precipitation (1990-2019)

The homogeneity of total precipitation at Binga station for the study period (1990–2019) was assessed using Pettitt's test, with the resulting p-values presented in Table 4.7. A seasonal homogeneity test was also conducted for the November–March (NDJFM) rainfall period to enhance the analysis. The p-values for total annual and seasonal precipitation at Binga station exceeded the significance threshold of 0.05, indicating that the dataset is homogeneous as shown in Figure 4.12, and suitable for trend analysis using the Mann-Kendall (MK) test and Sen's slope estimator. At Kariba station, Pettitt's test for total annual precipitation returned a p-value of 0.04, suggesting a statistically significant abrupt change in precipitation patterns around 1995 as shown in Figure 4.15. Consequently, the dataset was segmented before applying the MK test and Sen's slope estimator to assess trends and magnitudes accurately.

However, Pettitt's test for Kariba's total seasonal (NDJFM) precipitation yielded a p-value of 0.07, which is above the 0.05 significance threshold. This result indicates that the seasonal precipitation data is homogeneous as shown in Figure 4.13 and does not require segmentation before trend analysis.

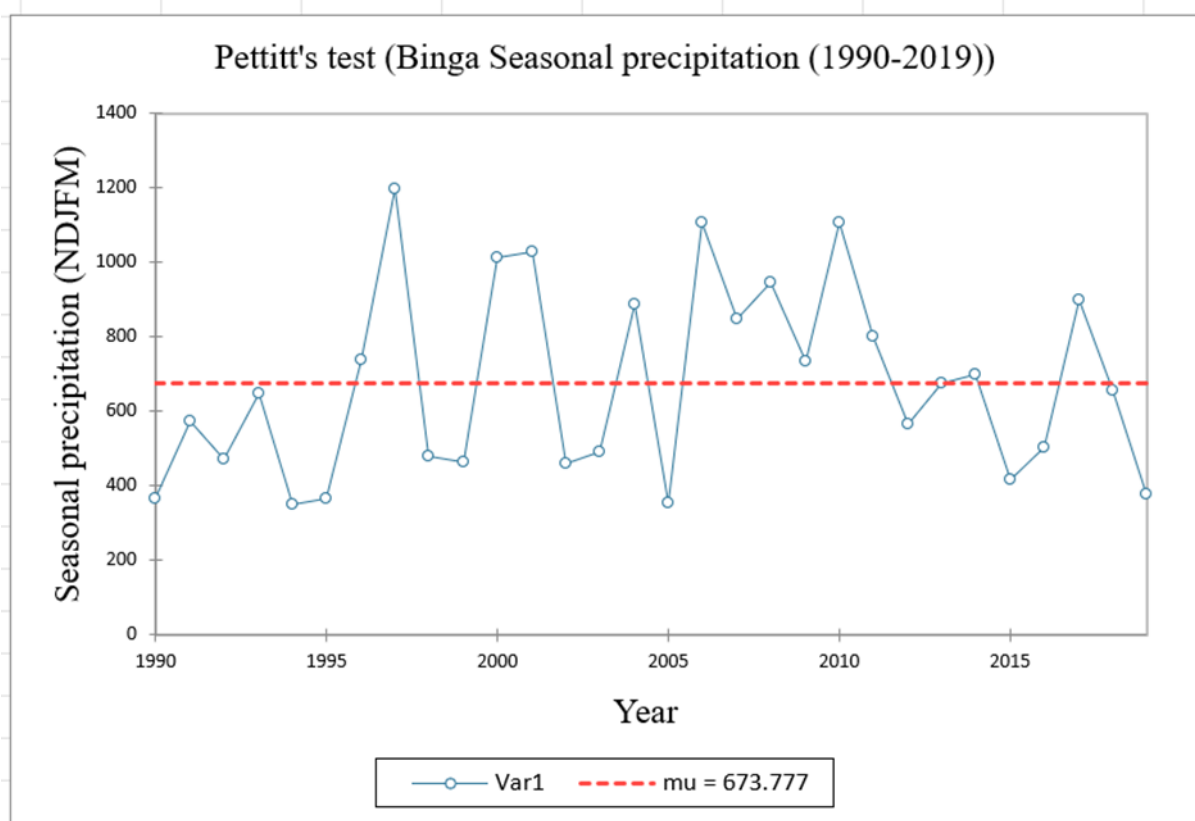


Figure 4.12: Binga seasonal precipitation homogeneity test 1990-2019

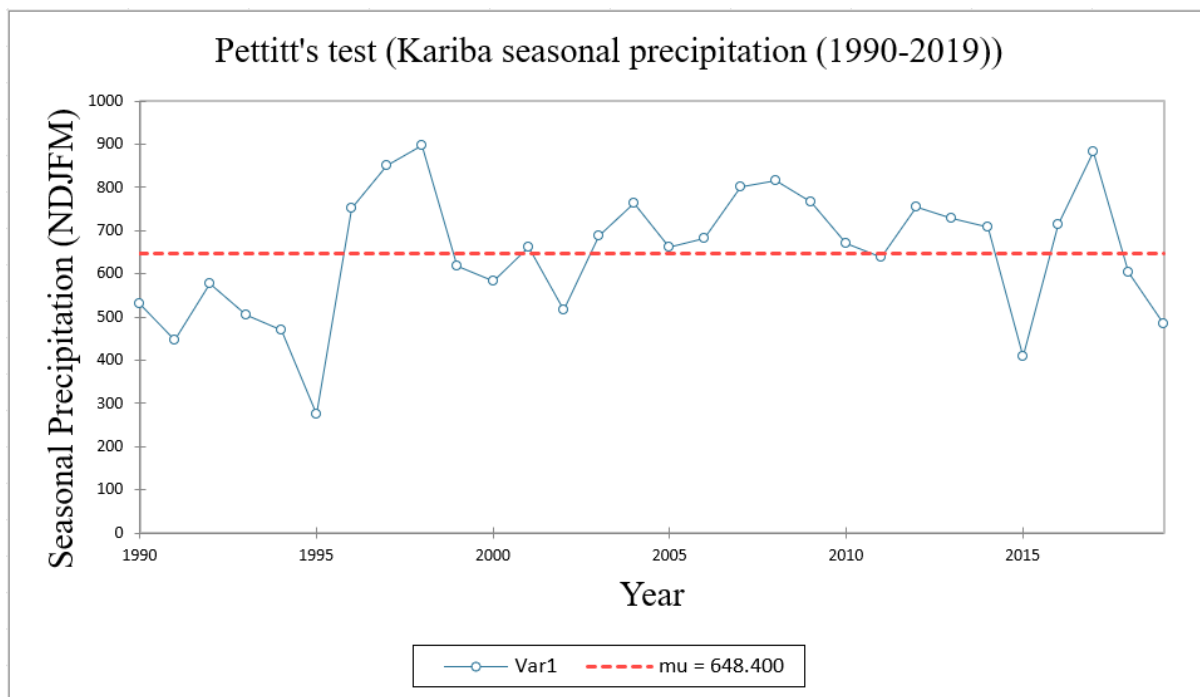


Figure 4.13: Kariba seasonal precipitation homogeneity test 1990-2019

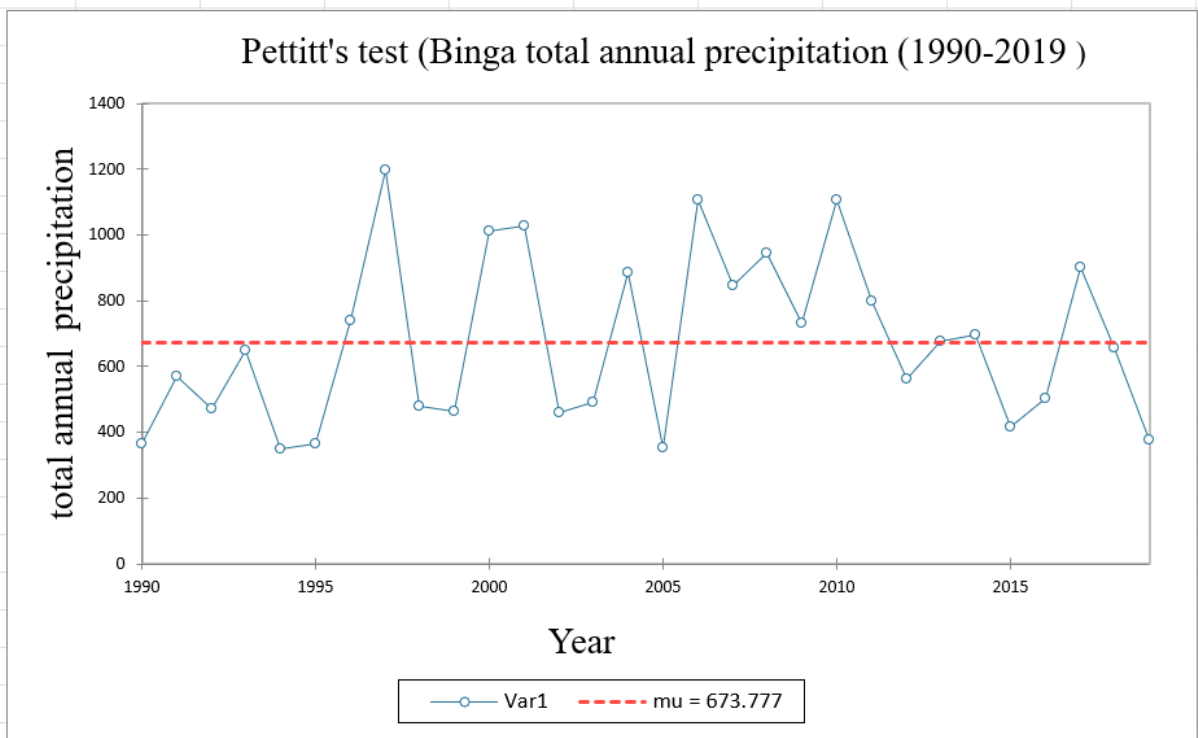


Figure 4.14: Binga total annual precipitation (1990-2019)

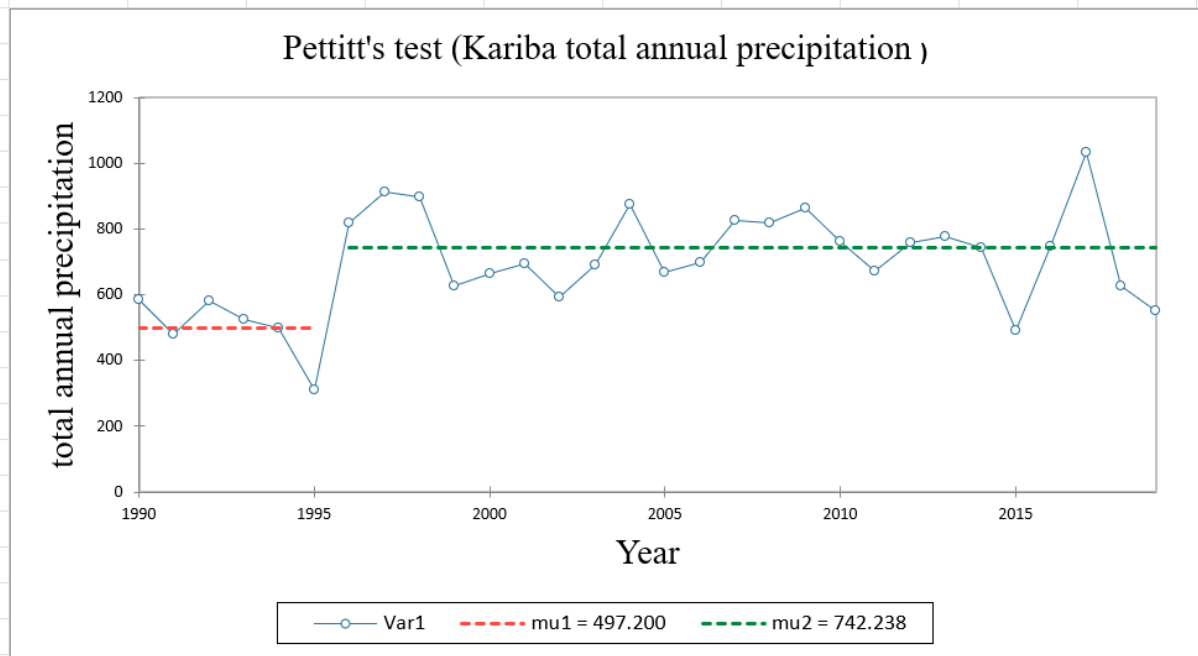


Figure 4.15: Kariba total annual precipitation (1990-2019)

4.3.2 Trend analysis for annual total precipitation and seasonal precipitation for Binga and Kariba Stations (1990-2019)

The results of the Mann-Kendall (MK) and Sen's slope trend analysis for annual total precipitation and seasonal total precipitation at Binga and Kariba are presented in Table 4.8. At Binga station, the MK p-values for total annual precipitation (0.48) and seasonal precipitation (0.41) exceed the significance threshold of 0.05, indicating no statistically significant trends. However, Sen's slope estimator suggests a positive increasing trend as shown in Figure 4.17, with slope values of 3.2 for annual precipitation and 2.7 for seasonal precipitation shown in Figure 4.16.

For Kariba, the MK p-value for total annual precipitation is 0.13 for 1990–1995 and 0.36 for 1996–2019. The trend analysis for 1990–1995 indicates a decline in annual precipitation as shown in Figure 4.19, but the trend is not statistically significant, as reflected by the MK p-value. However, the substantial negative Sen's slope value of -42.10 suggests a notable downward tendency. Similarly, for 1996–2019, the decreasing trend remains statistically insignificant at the 5% level as shown in Figure 4.20, with a smaller negative slope value of -4.11, indicating a less pronounced decline in total annual precipitation.

Regarding seasonal precipitation (NDJFM) at Kariba, the MK p-value of 0.13 suggests that the observed increasing trend, as shown in Figure 4.18, is not statistically significant at the 5% level. However, the positive Sen's slope value of 5.95 indicates a slight upward trend in total seasonal precipitation from 1990–2019.

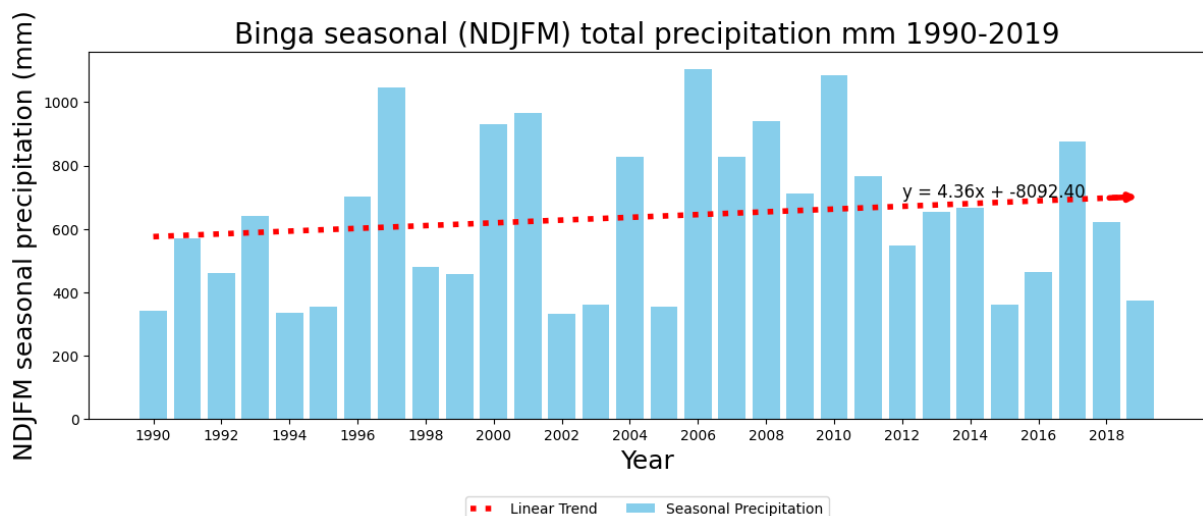
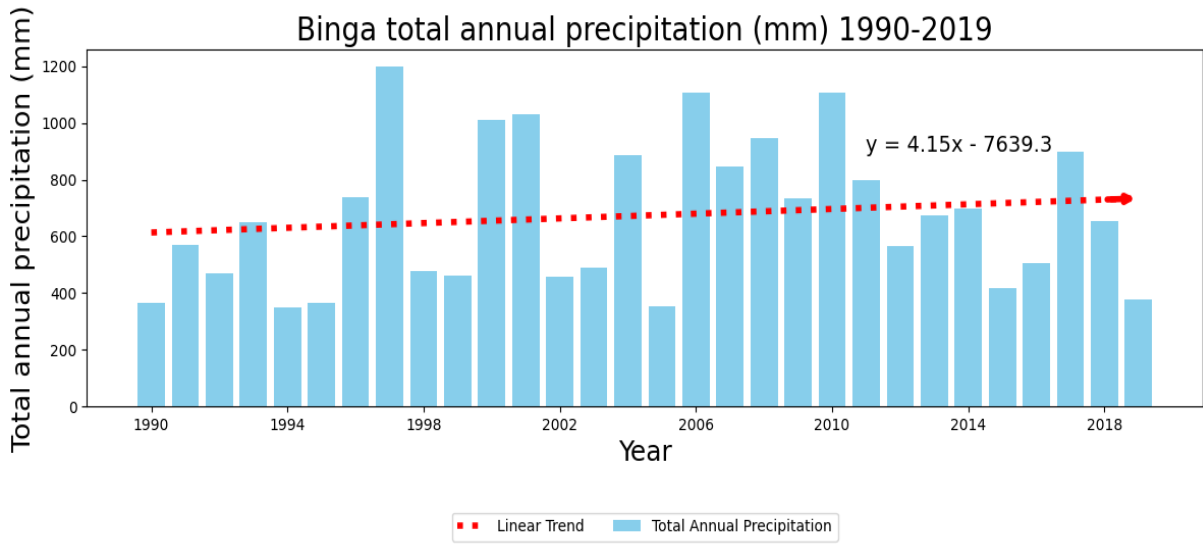
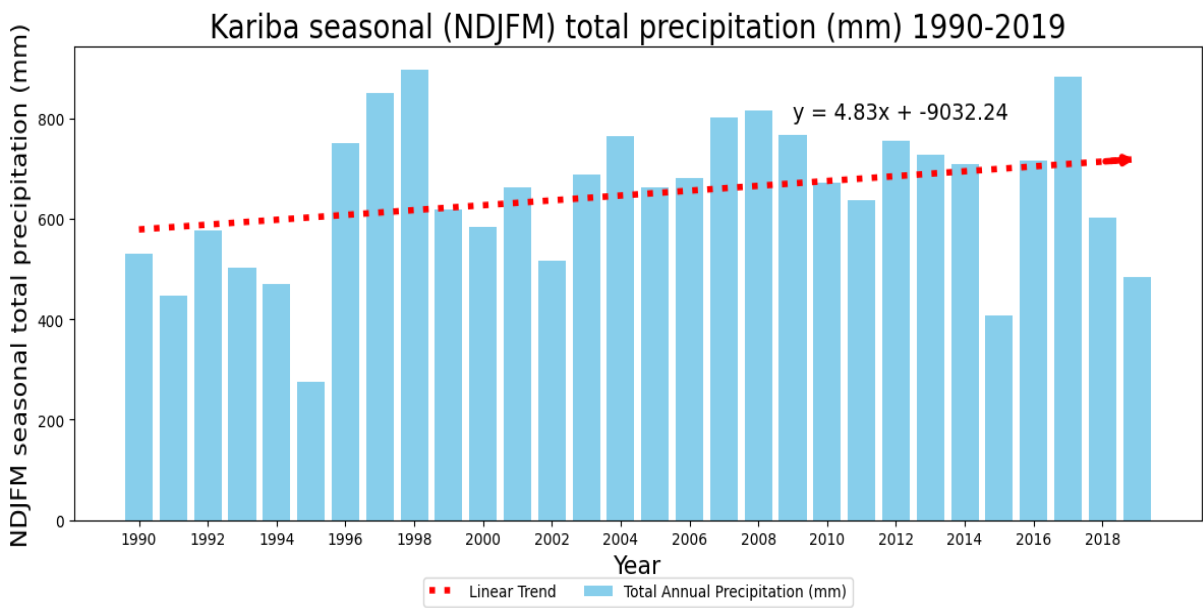


Figure 4.16: Binga seasonal total precipitation (NDJFM) 1990-2019



Data estimated from image.

Figure 4.17: Binga total annual precipitation 1990-2019



Data estimated from image.

Figure 4.18: Kariba seasonal (NDJFM) total precipitation 1990-2019

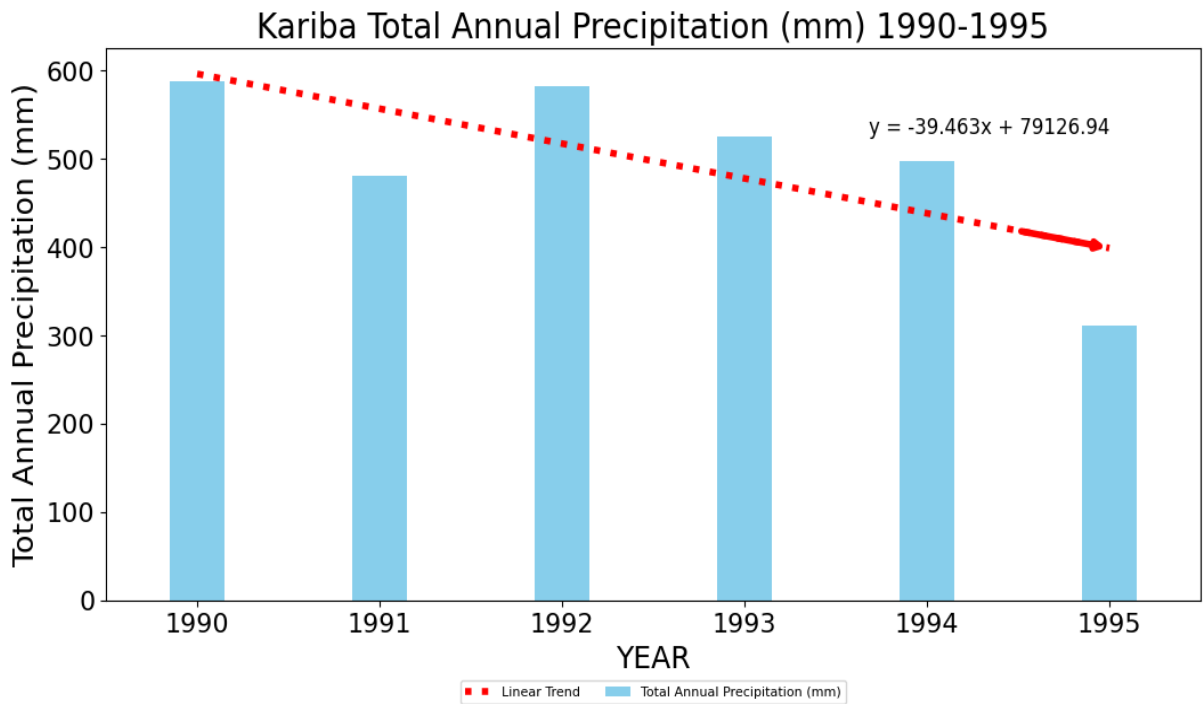


Figure 4.19: Kariba total annual precipitation 1990-1995

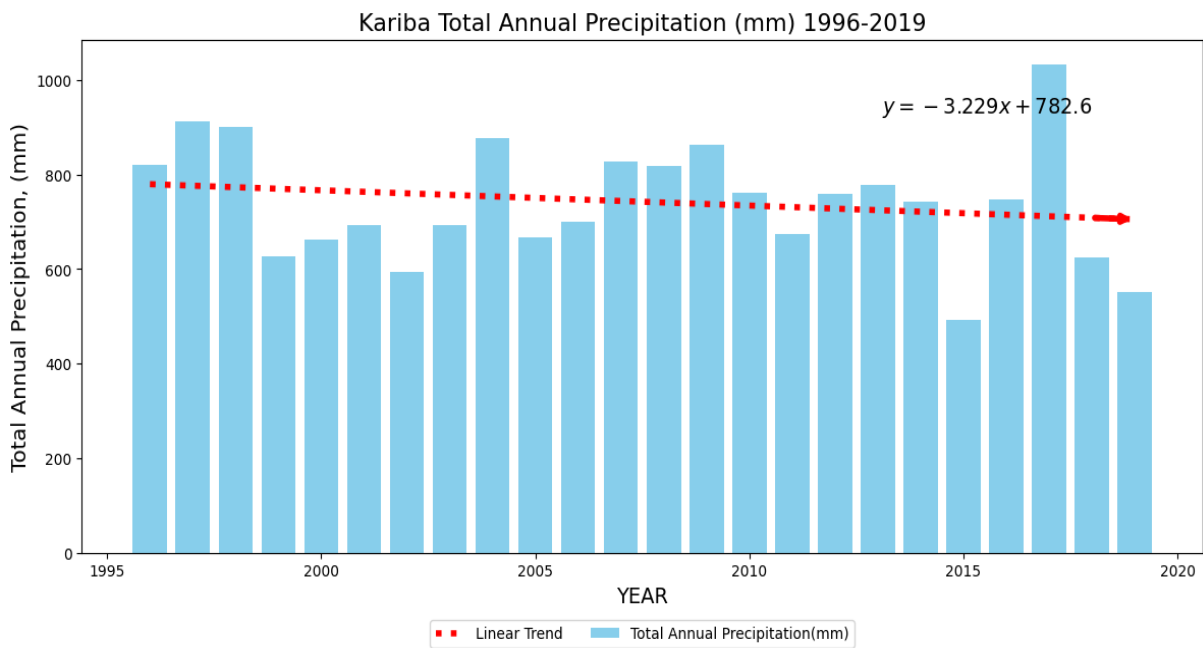


Figure 4.20: Kariba total annual precipitation 1996-2019

Table 4.7 Binga and Kariba annual total precipitation and seasonal precipitation (NDJFM) Homogeneity test from 1990-2019

Type of test	Parameter of interest	Year	Annual total precipitation	Seasonal total precipitation (NDJFM)	Station Name
Pettitt's test	P-value	1990-2019	0.39	0.49	Binga
Pettitt's test	P-value	1990-2019	0.04	0.07	Kariba

Table 4.8 Binga and Kariba seasonal and annual total precipitation MK and Sens Slope trend analysis from 1990-2019

Type of test	Parameter of Interest	Year	Annual total precipitation	Seasonal total precipitation	Station Name
MK test	p-value	1990-2019	0.48	0.41	Binga
Sen's Slope	slope	1990-2019	3.20	2.70	
MK test	p-value	1990-1995	0.13	0.13	Kariba
		1996-2019	0.36		
Sen's test	slope	1990-1995	-42.10	5.95	
		1996-2019	-4.11		

4.4 Trend Analysis from the satellite data from NASA POWER for 8 meteorological stations

Homogeneity test and Mann-Kendall trend analysis for the Annual mean maximum temperature for eight meteorological stations in the Kariba subbasin were performed. All the data sets from the eight stations had Pettitt's test P-value more significant than the significance level alpha of 0.05, showing that the data sets were homogenous. Five stations (Bulawayo Airport, Gokwe, Livingstone, Victoria Falls, and Kasane) exhibited negative slope values, indicating a slight cooling, and the remaining three stations (Gweru, Hwange National Park, and Kwekwe) exhibited positive slope values, indicating a slight warming trend, as shown in Table 4.9 below. The Mann-Kendall trend analysis revealed that the trends were not statistically significant at a 95% confidence level and significant level, despite five stations exhibiting negative slope values and the remaining three exhibiting positive values. Figure 4.21 shows the Annual mean maximum temperature variations for the eight meteorological stations in the Kariba subbasin.

Homogeneity test and Mann-Kendall trend analysis analysed the Annual mean minimum temperature for the eight meteorological stations in the Kariba subbasin. All the data sets from the eight stations had Pettitt's test P-values more significant than the significance level alpha of 0.05 shown in Table 4.10, showing that the data sets were homogenous. All eight stations (Bulawayo Airport, Gokwe, Livingstone, Victoria Falls, Kasane, Gweru, Hwange National Park, and Kwekwe) showed positive slope values, indicating a slight warming trend. Despite these positive slope values from the station's annual mean minimum data, the Mann-Kendall trend analysis results from the stations showed that the trends are not statistically significant at a 95% confidence level. Figure 4.22 represents the Annual mean minimum temperature variations for eight meteorological stations in the Kariba subbasin.

The total annual precipitation of the eight meteorological stations in the Kariba sub was analysed using a homogeneity test and Mann-Kendall trend analysis. Pettitt p-values for all the eight meteorological stations were more significant than 5%, the significance level; hence, all the data from the eight stations were homogenous. All the stations show positive Sens slope values, indicating a slight increase in the total annual precipitation trend, as shown in Table 4.11. Seven stations out of the eight stations (Bulawayo Airport, Gokwe, Livingstone, Victoria Falls, Gweru, Hwange National Park, and Kwekwe) had values more significant than the significance level alpha of 5% exempt for one station, Kasane (0.04), which had a p value less than significance level alpha showing that a trend exists to the total precipitation trend for

Kasane station. Livingstone and Victoria Falls show a potential increasing trend approaching statistical significance. Most stations except Kasane station show no statistically significant trends in the total annual precipitation. Figure 4.23 represents the variations in Annual total precipitation for eight meteorological stations in the Kariba subbasin.

Table 4.9: Results of the Pettitt’s homogeneity, Mann–Kendall, and Sens slope trend test on Annual mean maximum temperature

Station	Dataset Source	Pettitt’s P-value (two-tailed)	Mann-Kendall P-value (two-tailed test)	Sens slope value
Bulawayo Airport, ZI	NASA Power	0.19	0.83	-0.005
Gokwe, ZI	NASA Power	0.89	0.97	-0.003
Gweru, ZI	NASA Power	0.57	1	0.004
Hwange national park, ZI	NASA Power	0.79	0.91	0.004
Livingstone, ZA	NASA Power	0.50	0.16	-0.03
Victoria Falls, ZI	NASA Power	0.82	0.24	-0.025
Kwekwe, ZI	NASA Power	0.23	0.88	0.003
Kasane, BC	NASA Power	0.47	0.164	-0.03

Table 4.10: Results of the Pettitt’s homogeneity, Mann–Kendall, and Sens slope trend test on Annual mean minimum temperature

Station	Dataset	Pettitt’s P-value (two-tailed)	Mann-Kendall P-value (two-tailed test)	Sens slope value
Bulawayo Airport, ZI	NASA Power	0.80	0.11	0.02
Gokwe, ZI	NASA Power	0.70	0.25	0.02
Gweru, ZI	NASA Power	0.77	0.23	0.02
Hwange national park, ZI	NASA Power	0.40	0.40	0.01
Livingstone, ZA	NASA Power	0.70	0.60	0.008
Victoria Falls, ZI	NASA Power	0.52	0.40	0.012
Kwekwe, ZI	NASA Power	0.60	0.225	0.013
Kasane, BC	NASA Power	0.70	0.592	0.008

Table 4.11: Results of the Pettitt’s homogeneity, Mann–Kendall-trend, and Sens slope test on Annual total precipitation

Station	Dataset	Pettitt’s P-value (two-tailed)	Mann-Kendall P-value (two-tailed test)	Sen’s slope value
Bulawayo Airport, Zi	NASA Power	0.63	0.67	1.26
Gokwe, Zi	NASA Power	0.16	0.86	0.66
Gweru, Zi	NASA Power	0.55	0.62	1.12
Hwange national park, Zi	NASA Power	0.26	0.59	1.41
Livingstone, Za	NASA Power	0.31	0.06	5.53
Victoria Falls, Zi	NASA Power	0.30	0.06	5.53
Kwekwe, Zi	NASA Power	0.54	0.69	1.85
Kasane, BC	NASA Power	0.08	0.04	7.03

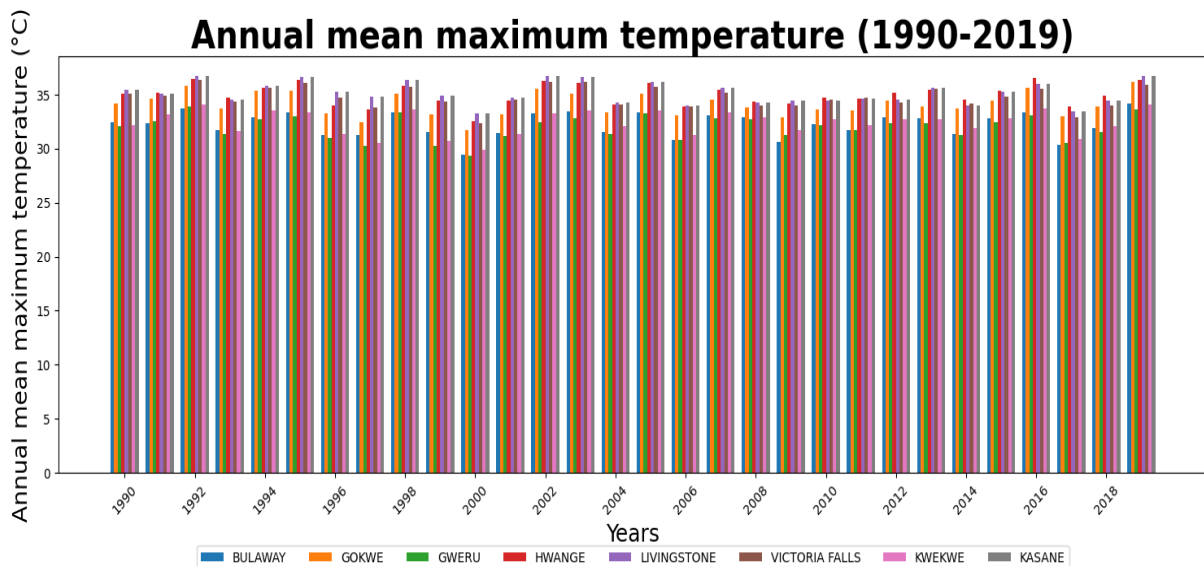


Figure 4.21: Annual mean maximum temperature for eight meteorological stations in the Kariba subbasin

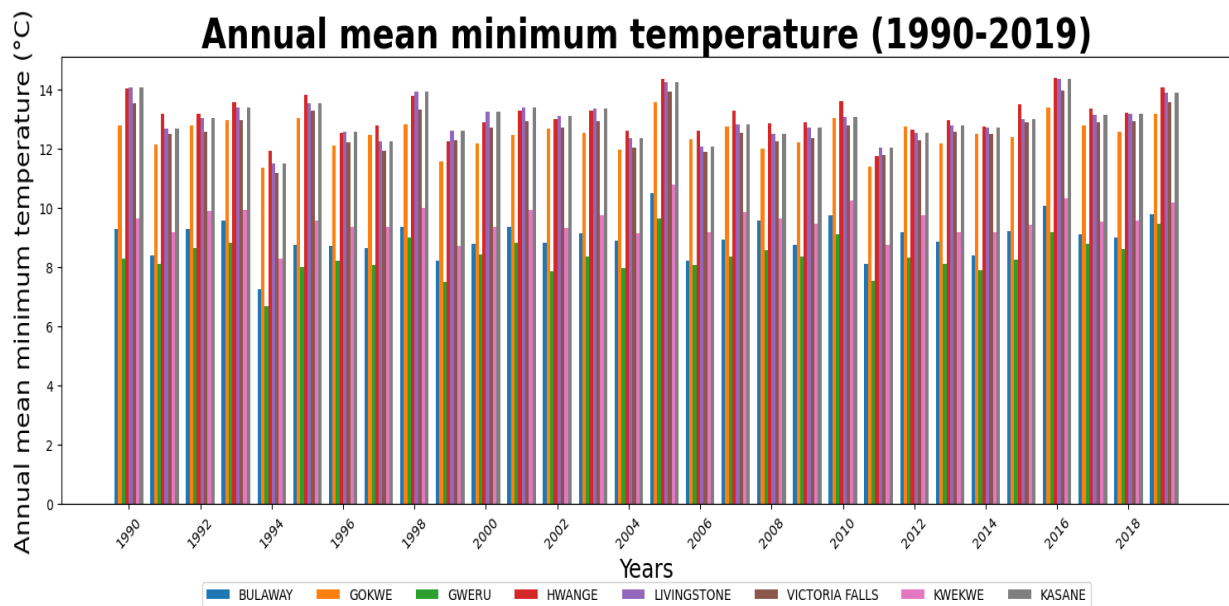


Figure 4.22: Annual mean minimum temperature for eight meteorological stations in the Kariba subbasin

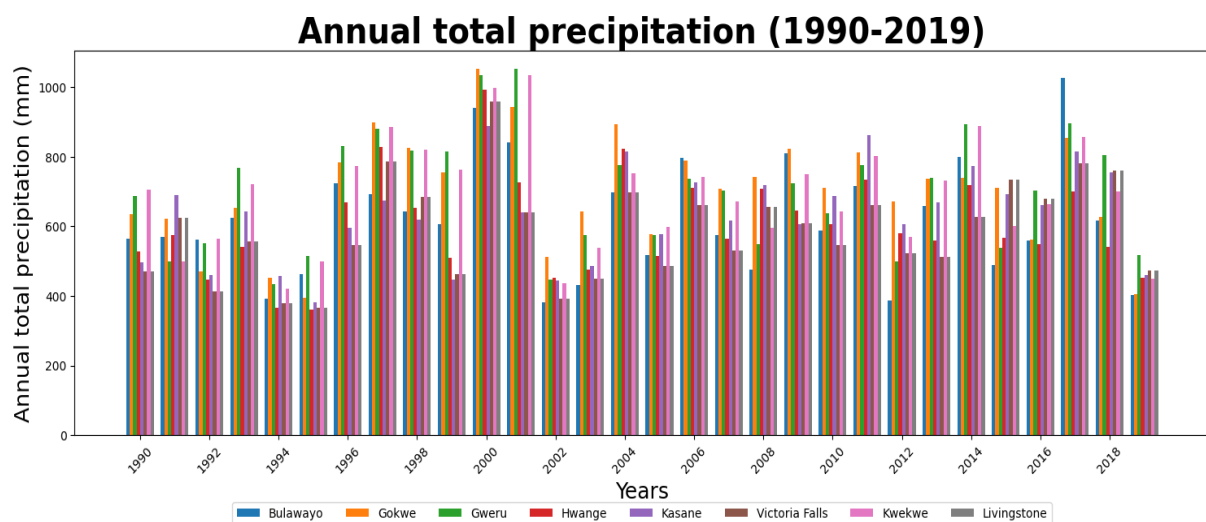


Figure 4.23: Annual total precipitation for eight meteorological stations in the Kariba subbasin

4.5 River Flow

River flow data were obtained from the Zambezi River Authority for three key locations: Ngonye Rapids (Sioma Falls), Chavuma Mission (130400), and Victoria Falls, Big Tree Station. The discharge data for Chavuma Mission and Victoria Falls (Big Tree Station) spanned the entire study period from 1990 to 2019, as both gauging stations were established well before 1990. For Ngonye Rapids, the discharge data available for analysis started in 2005, 15 years after 1990, following the station's establishment in 2004. While this gap could have posed a

challenge, the data available from Ngonye Rapids was sufficient to understand the annual mean discharge trends at this gauging station, as shown in Table 4.12.

Table 4.12: Annual mean discharge at Chavuma, Ngonye, and Victoria Falls

Year	Ngonye Rapids (Sioma Falls) (m³/s)	Chavuma Mission (m³/s)	Victoria Falls (Big Tree Station) (m³/s)
1990		281.44	586
1991		519.26	804
1992		348.14	528
1993		611.74	896
1994		297.78	612
1995		305.90	442
1996		209.48	390
1997		414.75	588
1998		1001.88	1104
1999		662.94	1074
2000		432.26	885
2001		755.28	1227
2002		482.17	839
2003		680.50	1097
2004		700.87	1337
2005	888.47	356.84	691
2006	1441.59	463.97	987
2007	1223.60	840.13	1471
2008	1220.25	530.74	1317
2009	1417.15	813.66	1519
2010	1596.05	1030.37	1703
2011	1622.18	1115.67	1692
2012	1218.71	700.76	1236
2013	1303.52	695.86	1349
2014	1287.09	795.71	1354
2015	1028.42	402.85	760
2016	1025.61	799.26	1034
2017	1023.21	508.64	1068
2018	1524.38	986.49	1551
2019	1397.89	255.59	537

4.5.1 Ngonye Rapids gauging station (Sioma Falls)

4.5.1.1 Homogeneity test

The annual mean discharge data obtained for the Ngonye Rapids (Sioma Falls) hydro gauging station were tested for homogeneity at a 5% significance level. The p-value associated with the annual mean discharge data, as shown in Table 4.10, exceeds the significance level of 0.05. Therefore, we conclude that the river flow data is homogeneous as shown in Figure 4.24.

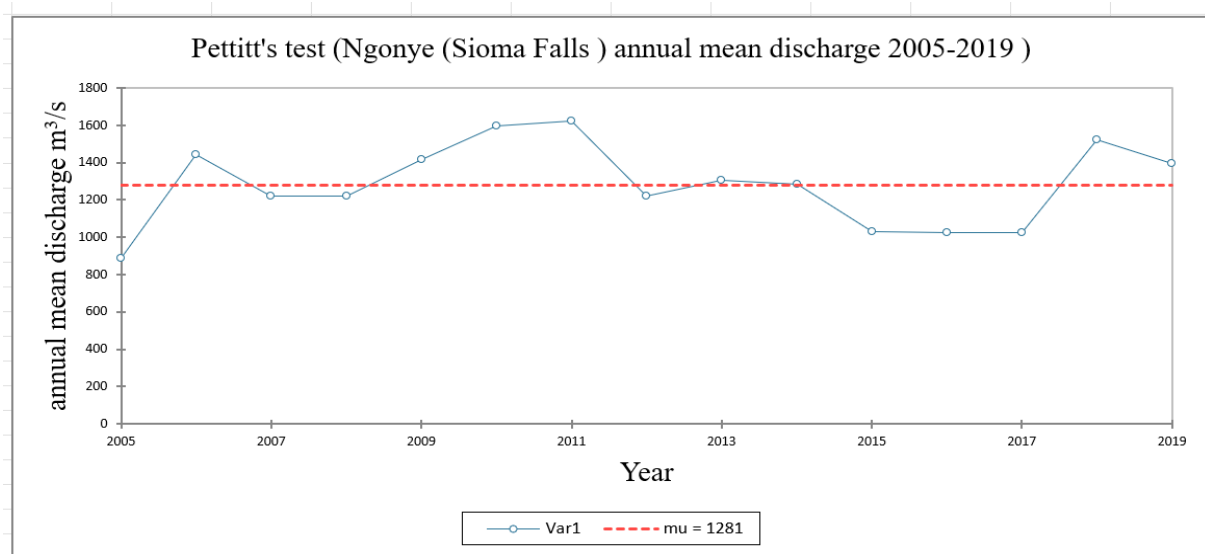


Figure 4.24: Homogeneity test for Ngonye (Sioma Falls) annual mean discharge 2005-2019

4.5.1.2 Trend analysis for annual mean discharge Ngonye Rapids (Sioma Falls)

The annual mean discharge data for Ngonye Rapids from 2005 to 2019 were analysed using the Mann-Kendall (MK) trend test and Sen's slope estimator to assess the trend and magnitude of change at a 5% significance level and a 95% confidence interval. The results, presented in Table 4.11, show that the MK p-value (0.77) exceeds the significance threshold ($\alpha = 0.05$), indicating no statistically significant trend in discharge. Despite the lack of statistical significance, the negative Sen's slope value (-2.40) suggests a potential declining trend in discharge at Ngonye Rapids (Sioma Falls).

The lowest recorded annual mean discharge was in 2005, at 888.47 m³/s, likely due to the 2004/2005 drought. In contrast, the highest discharge was recorded in 2011 at 1,622.18 m³/s, followed closely by 2010 with 1,596.05 m³/s shown in Figure 4.25. The inter-annual variability of discharge at Ngonye Rapids station was 773.71 m³/s, the difference from the minimum

discharge recorded in 2005 (888.47 m³/s) and the maximum discharge recorded in 2011 (1622.18 m³/s).

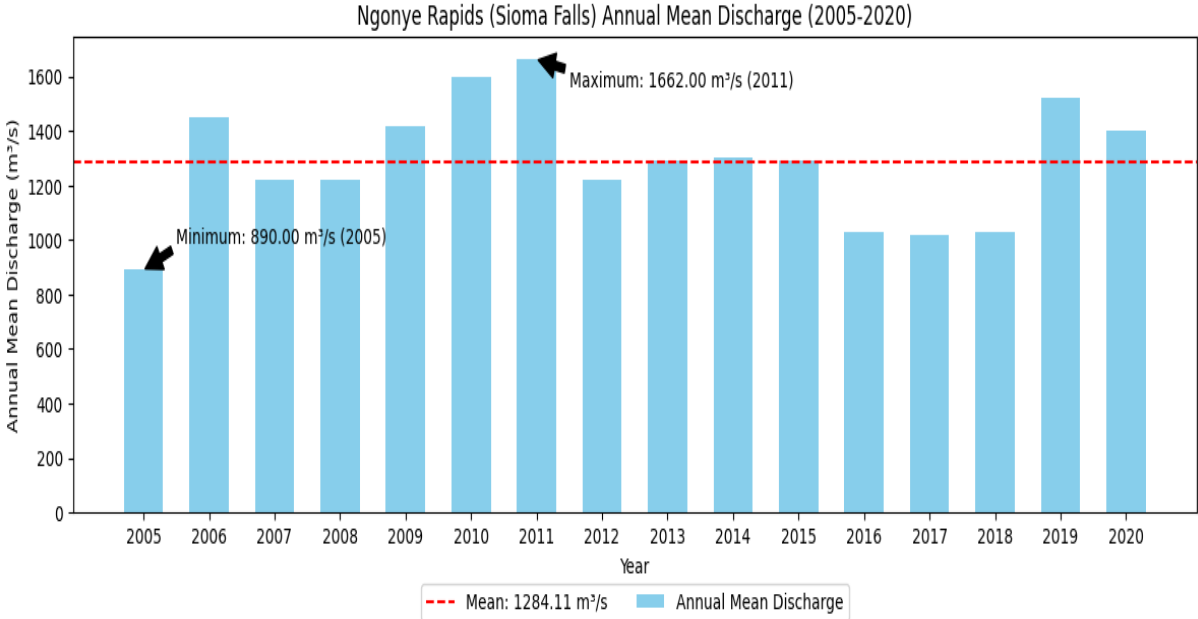


Figure 4.25: Trend analysis for Ngonye (Sioma Falls) annual mean discharge 2005-2019

4.5.2 Chavuma Mission Gauging Station

4.5.2.1 Homogeneity test

At a 5% significance level, the Chavuma station's river flow data from 1990 to 2019 were put through a homogeneity test. The analysis revealed a notable shift in the behaviour of the time series data during this period. Consequently, the data were divided into two distinct segments, as shown in Table 10: the pre-change period, which spans from 1990 to 1997, and the post-change period, which spans from 1998 to 2019, shown in Figure 4.26. The minimum discharge recorded at Chavuma station was 255.59 m³/s in 2019, and the maximum discharge was recorded in 1115.67 m³/s in 2011.

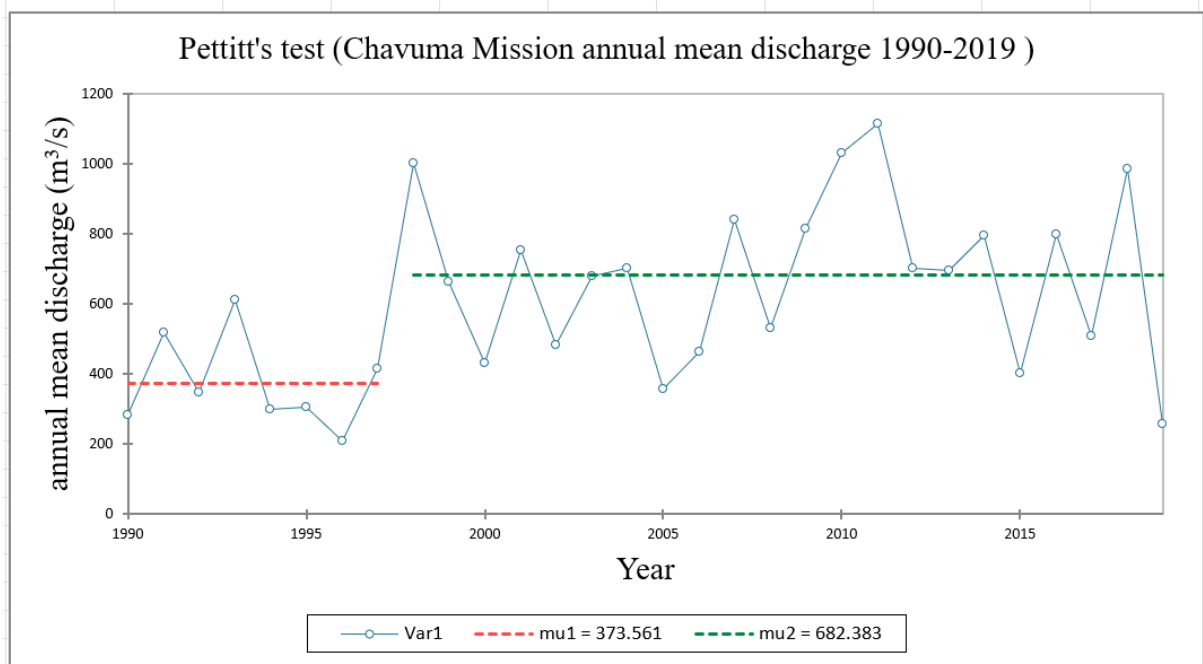


Figure 4.26: Homogeneity test for Chavuma Mission annual mean discharge 1990-2019

4.5.2.2 Trend analysis for Chavuma Mission annual mean discharge

We conducted a trend analysis of the annual mean discharge data for the Chavuma Mission gauging station using the Mann-Kendall (MK) trend test and Sen's slope magnitude test, with a 5% significance level and a 95% confidence interval. The data sets were divided into segments 1990–1997 and 1998–2019 to identify any significant trends in the mean annual discharge for these periods. For the 1990–1997 period, a slightly decreasing trend was observed (Sen's slope -13.04) as shown in Figure 4.27; however, the p-value (two-tailed test) exceeds the significance threshold (0.05), indicating that the trend is not statistically significant. The lowest annual mean discharge for the period 1990-1997 was recorded in 1996 and was 209.48m³/s, and for the period 1998-2019, the lowest discharge was in 2019, which coincides with the (2018-2019) drought experienced in Southern Africa (Bradshaw et al., 2022). In the 1998–2019 period, despite a slight upward trend shown in Figure 4.28, Sen's slope = 2.25, the p-value (0.87) shows that the trend is also not statistically significant. Figure 4,27 shows inter-annual variability in annual mean discharge at Chavuma mission station for the period 1990-1997, with a fluctuation of 402.26 m3/s, the difference from the maximum discharge recorded in 1993 (611.74 m3/s) and the minimum discharge recorded in 1996 (209.48 m3/s). While the graph Figure 4.28 for Chavuma discharge for the study period 1998-2019 shows significant inter-annual variability in discharge with a fluctuation of 860.08 m3/s, the difference from the highest recorded discharge in 2011 (1115.67 m3/s) and the minimum recorded discharge in 2019 (255.59 m3/s).

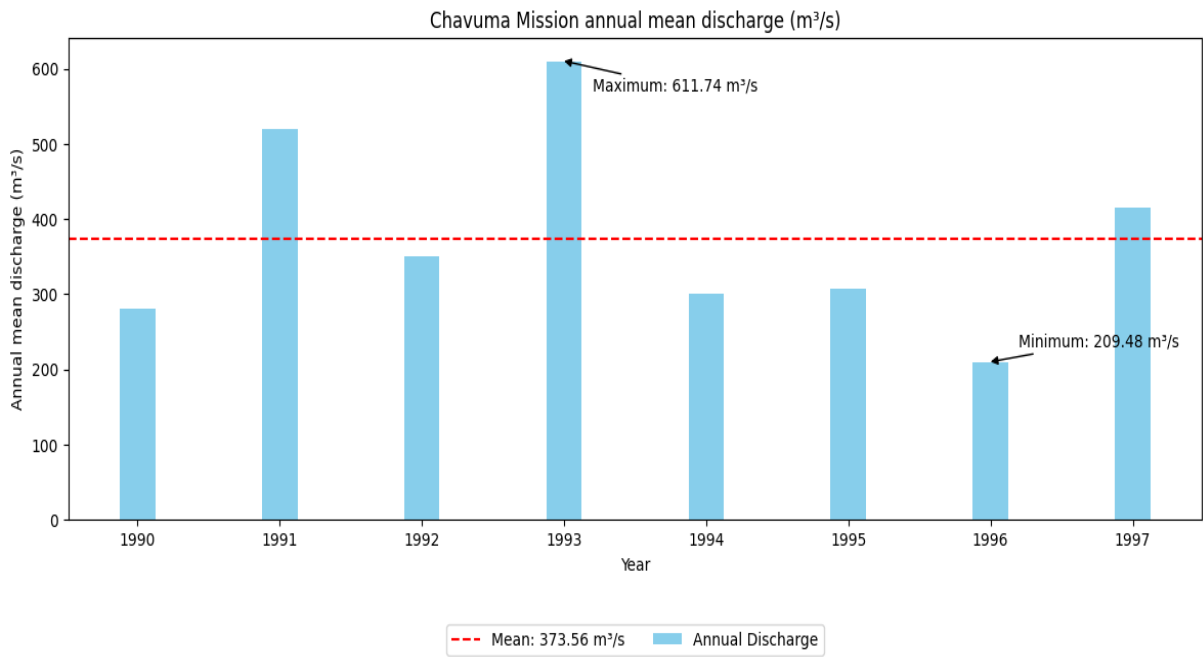


Figure 4.27: Trend analysis for Chavuma Mission station annual mean discharge 1990-1997

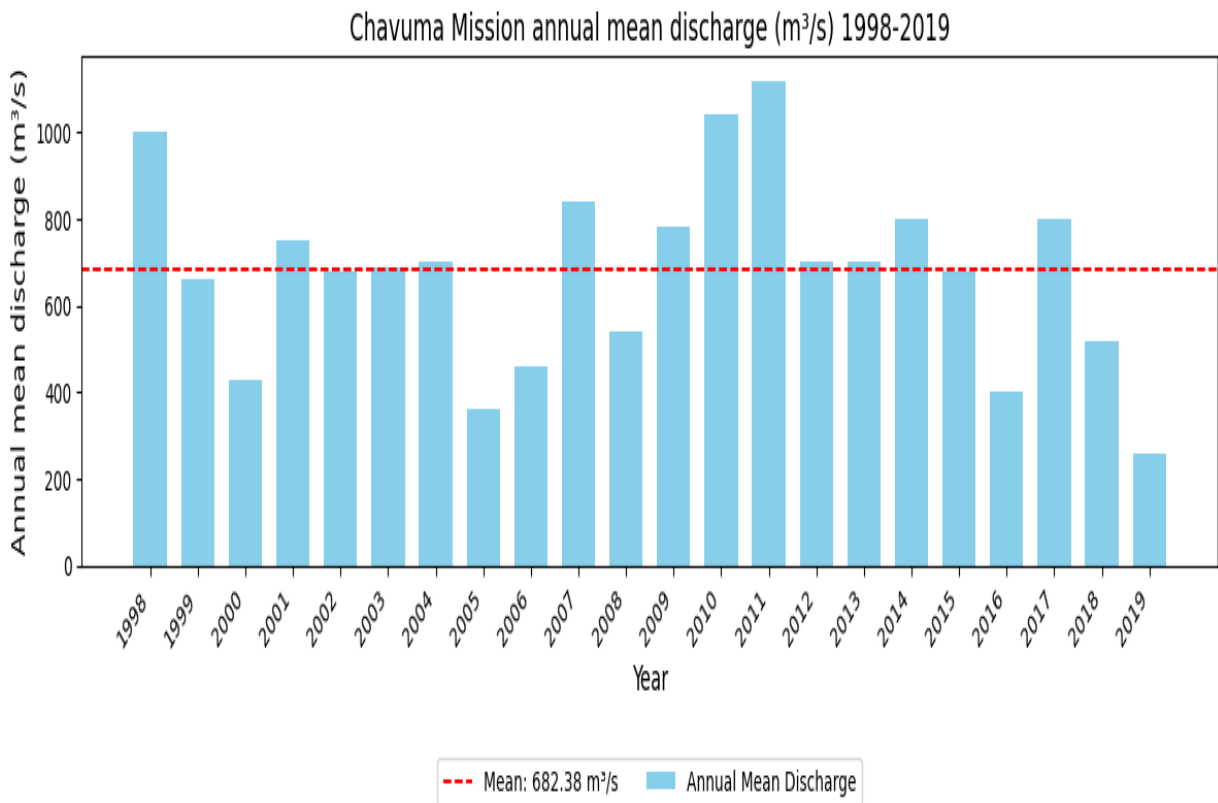


Figure 4.28: Trend analysis for Chavuma Mission station annual mean discharge 1998 -2019.

4.5.3 Victoria Falls (Big Tree Station)

4.5.3.1 Homogeneity test

The annual mean river flow data for Victoria Falls (Big Tree Station) from 1990 to 2019 were assessed for homogeneity at a 5% significance level. The analysis revealed a notable shift in the behaviour of the annual mean discharge during this period, as shown in Figure 4.29. As a result, the data were divided into two distinct segments. The pre-change period (1990–1997) showed a two-tailed p-value exceeding the significance level ($\alpha = 0.05$), indicating that the annual mean discharge was homogeneous during this period. Similarly, the post-change period (1998–2019) also yielded a two-tailed p-value greater than the significance level ($\alpha = 0.05$), confirming the homogeneity of the data in this later period shown in Table 4.13.

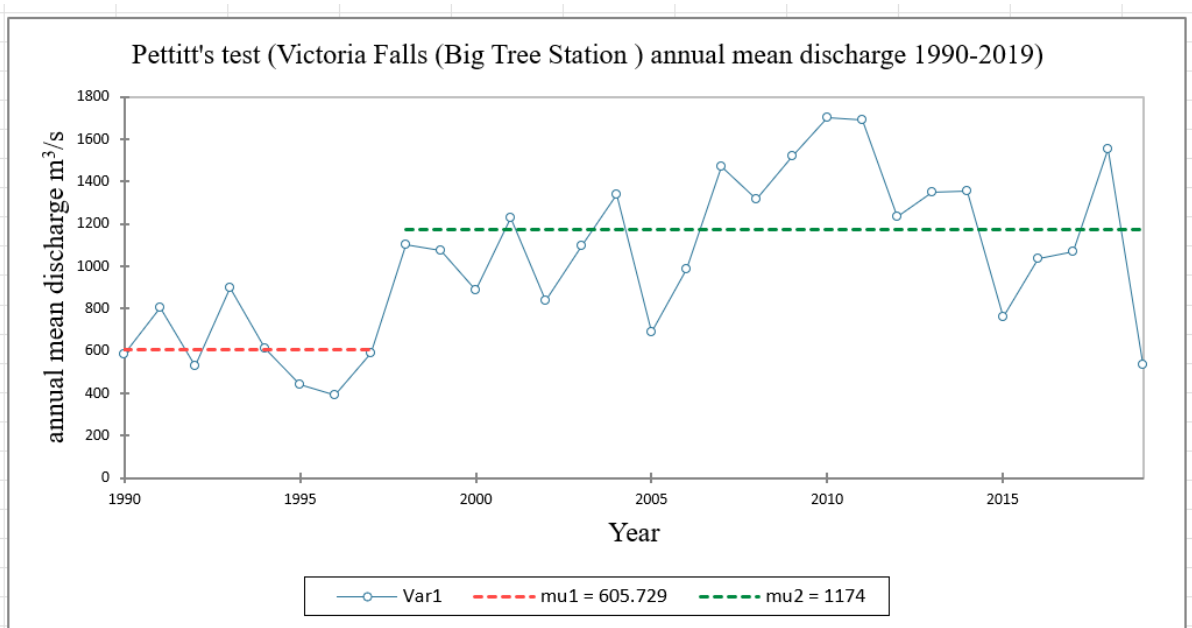


Figure 4.29: Homogeneity test for Victoria Falls (Big Tree Station) annual mean discharge 1990-2019

4.5.3.2 Trend analysis for Victoria Falls (Big Tree Station annual mean discharge) 1990-2019

The Mann-Kendall (MK) test was applied to analyse trends in the annual mean discharge at Victoria Falls (Big Tree Station) over two segmented periods: the pre-change period (1990–1997) shown in Figure 4.29 and the post-change period (1998–2019) shown in Figure 4.30, at a 5% significance level and 95% confidence interval. The p-value for the pre-change period

(0.39) exceeds the significance threshold (0.05), indicating that the observed trend is not statistically significant, as shown in Table 4.14. However, the negative Sen's slope value (-31.04) suggests a decreasing trend in discharge at an average rate of -31.04 m³/s. Similarly, the p-value for the post-change period (0.50) confirms the absence of statistical significance, while Sen's slope value (9.31) indicates a slightly increasing trend in discharge. The lowest recorded annual mean discharge at Victoria Falls (Big Tree Station) occurred in 2019, measuring 537.41 m³/s, coinciding with a severe drought in the Southern African region. (Mupepi & Matsa, 2021). Figure 4.30 shows the fluctuations in annual mean discharge at Victoria Falls from 1990 to 1997, showing some fluctuations in the Zambezi River flow. The function from the highest recorded discharge to the lowest for this period, 1990-1997, was 506.6 m³/s, as shown in Figure 4.30. In Figure 4.31, the study period 1998-2019 shows inter-annual variability in annual mean discharge recorded at the Victoria Falls gauging station, with a fraction of 1165.95 m³/s from the maximum recorded discharge in 2010 (1703.36m³/s) to the minimum recorded discharge in 2019 (537.41m³/s), which resulted in a decline in water levels in Lake Kariba and power cuts for both Zambia and Zimbabwe.

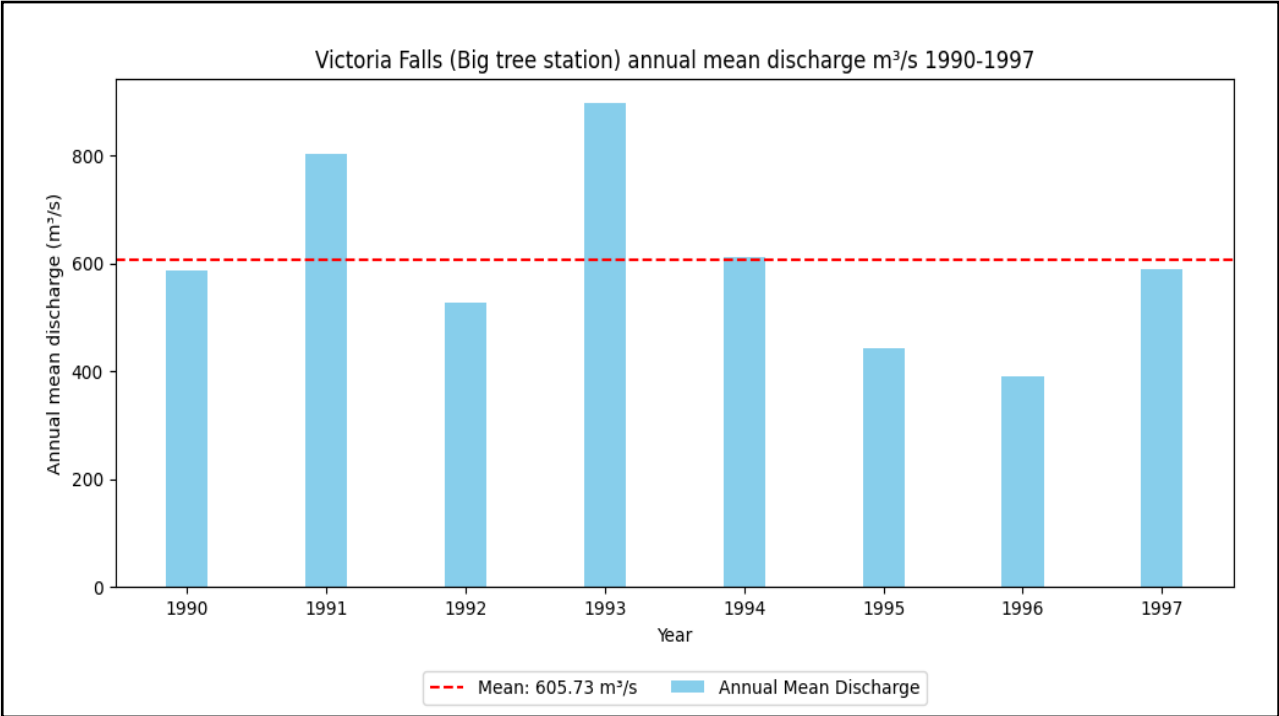


Figure 4.30: Victoria Falls (Big Tree station) annual mean discharge (m³/s) 1990-2019

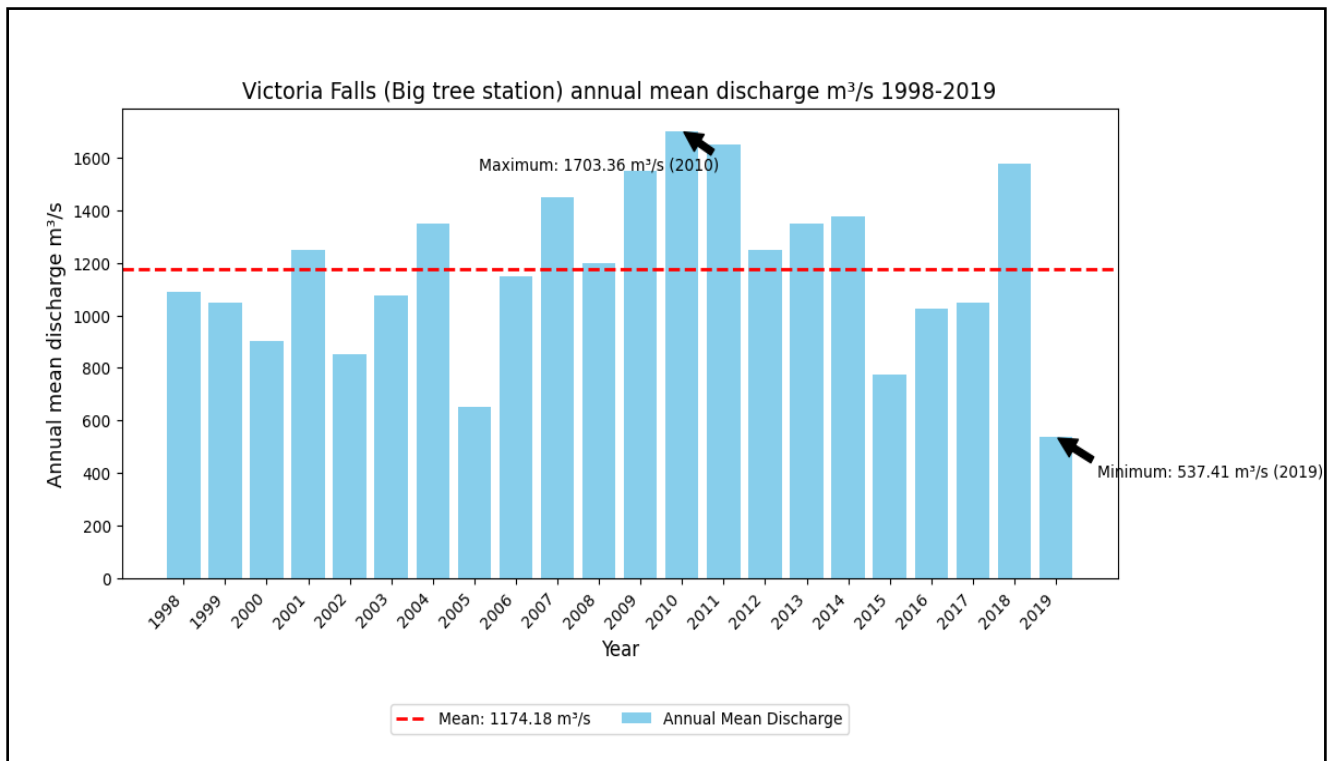


Figure 4.31: Victoria Falls (Big Tree station) annual mean discharge (m³/s) 1998-2019

Table 4.13: Homogeneity test for Chavuma, Ngonye Rapids (Sioma Falls), and Victoria Falls (Big Tree Station) 1990-2019

Station	Type of test	Parameter of interest	Year	p-value (Two-tailed)
Chavuma	Pettitt	P	1990-1997	0.94
			1998-2019	0.85
Ngonye Rapids (Sioma Falls)	Pettitt	P	2005-2019	0.68
Victoria Falls (Big Tree Station)	Pettitt	P	1990-1997	0.52
			1998-2019	0.36

Table 4.14: MK trend test for annual mean river flow for Chavuma Mission Station, Ngonye Rapids (Sioma Falls), Victoria Falls (Big Tree Station)

Type of test	Parameter of Interest	Year	p-value	Station name
MK test	p-value (two-tailed)	1990-1997	0.90	Chavuma Mission Station
		1998-2019	0.87	
MK test	p-value (two-tailed)	1990-2019	0.77	Ngonye Rapids (Sioma Falls)
MK test	p-value (two-tailed)	1990-1997	0.39	Victoria Falls (Big Tree Station)
		1998-2019	0.50	

Table 4.15: Magnitude of trend (Sen's slope test) for annual mean river flow for Chavuma Mission Station, Ngonye Rapids (Sioma Falls), Victoria Falls (Big Tree Station)

Type of test	Parameter of Interest	Year	Slope-Value	Station name
Sen's Slope	slope-value	1990-1997	-13.04	Chavuma Mission Station
		1998-2019	2.25	
Sen's Slope	slope-value	1990-2019	-2.40	Ngonye Rapids (Sioma Falls)
Sen's Slope	slope-value	1990-1997	-31.04	Victoria Falls (Big Tree Station)
		1998-2019	9.31	

4.5.4 Lake Kariba reservoir levels from 1990-2019

Hydropower production at the Kariba South Hydropower Station is closely linked to the water supply in Lake Kariba. Water from the Kariba reservoir enters intake tunnels and penstocks, which direct it to turbines connected to generators below. The turbines convert the kinetic energy of the flowing water into mechanical energy. Water levels in the lake, which are impacted by evaporation rates, precipitation patterns, and upstream inflows, directly affect the electricity produced. When abundant water is available, the turbines can run at maximum capacity, producing the most power. In contrast, prolonged droughts, decreased precipitation,

and changes in upstream river flows can reduce water levels, impairing the turbines' ability to generate electricity.

4.5.4.1 Homogeneity test annual mean water levels for Lake Kariba

We conducted a homogeneity test on Lake Kariba's annual mean water levels using Pettitt's test at a 5% significance level. The 1990-2019 annual mean water levels data results indicated a significant change point in 1998, shown in Figure 4.32. Consequently, we divided the water level data into two segments: the pre-change period, covering 1990-1998, and the post-change period, spanning 1999-2019.

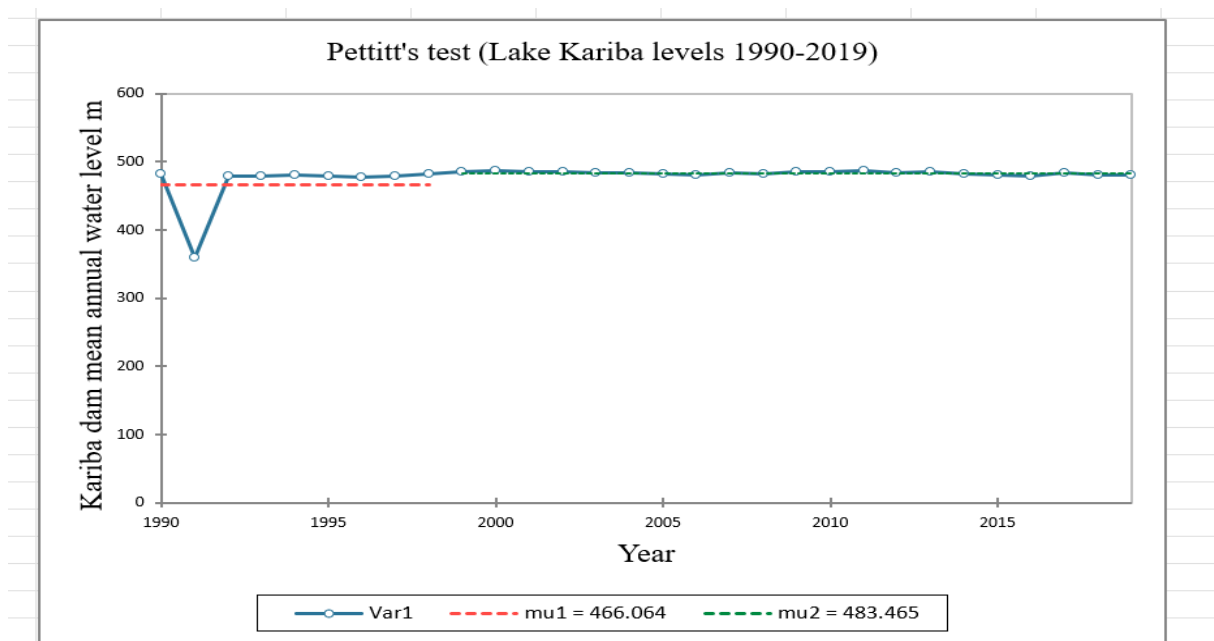


Fig 4.32: Homogeneity test for Lake Kariba mean annual water level

4.5.4.2 Mann-Kendall trend test for Annual Mean Water Levels for Lake Kariba

The Mann-Kendall (MK) trend analysis was performed to assess changes in Lake Kariba's water levels between the pre-change period (1990-1998) shown in Figure 4.33 and the post-change period (1999-2019) shown in Figure 4.35 at a 5% significance level and 95% confidence interval. Sen's slope estimator was applied to determine the magnitude of the observed trends. The MK p-value (0.60) for the pre-change period (1990–1998) shows that the trend is not statistically significant; however, the positive slope value of 0.12 points to a modest but not significant upward trend, as shown in Table 4.16. Conversely, the MK p-value (0.02) indicates a statistically significant trend at the 5 percent level for the post-change period (1999–2019). The negative slope value of -0.24 reflects a significant decrease in Lake Kariba's

average annual water level during this period, as shown in Table 4.16. The annual mean water level for Lake Kariba from 1990 to 1999 was 89% above the mean level (466.06m); the lowest yearly water level (359.56m) was recorded in 1991, which was the only value below the mean level (466.06m). The annual water level for Lake Kariba for the period 1999-2019 shows significant fluctuations of approximately 7.45 meters from the highest lake levels recorded of 486.83m in 2011 to 479.38m in 2016. The fluctuation in water level in the Lake can impact the capacity of hydropower generation capacity of the KSHS, which has a minimum operating level of 475.5m.

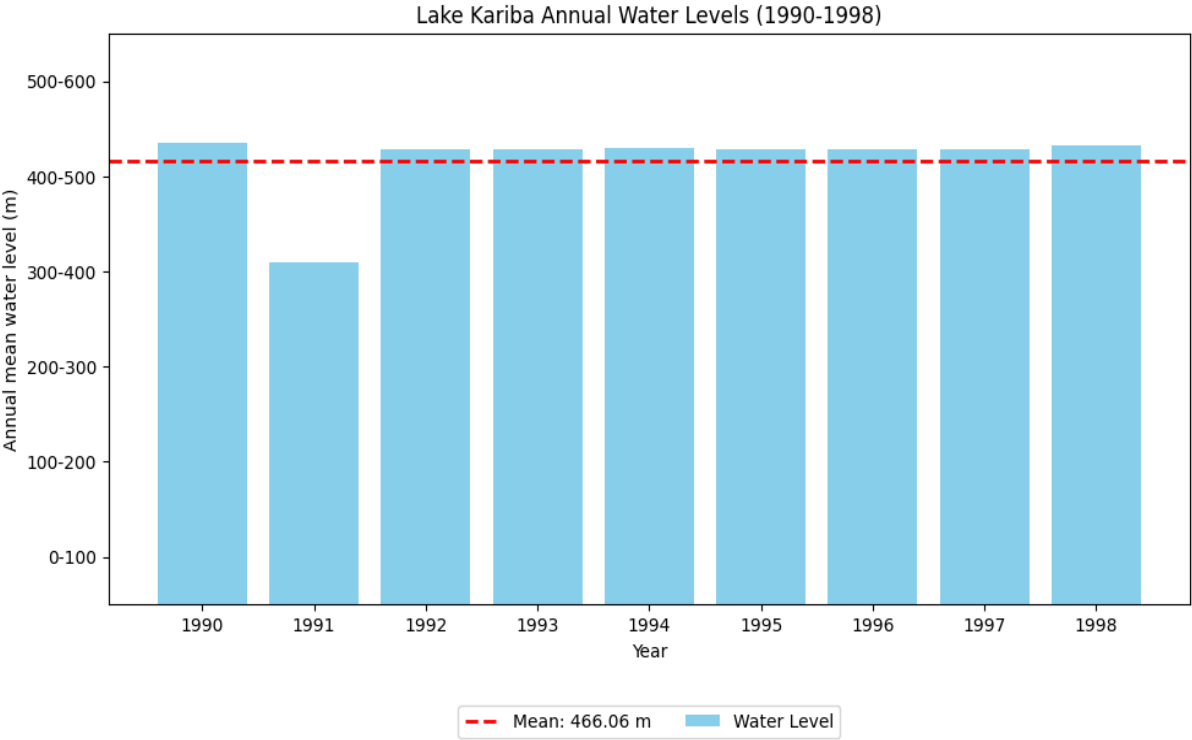


Fig 4.33: Mann-Kendall trend test for Lake Kariba annual mean water level (1990-1998)

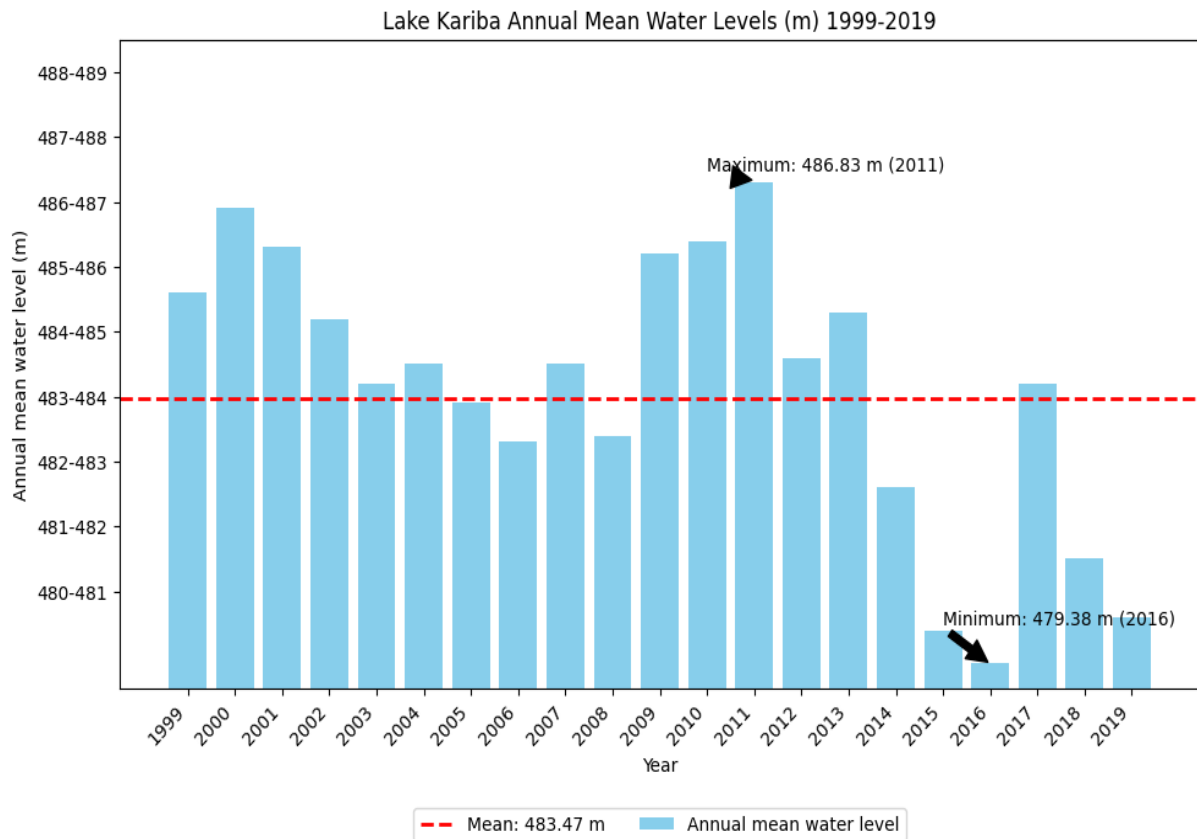


Fig 4.34: Mann-Kendall trend test for Lake Kariba annual mean water level (1999-2019)

Table 4.16: Lake Kariba Pettitt's homogeneity test, Mann-Kendall, and Sen's slope trend test

Type of test	Parameter of Interest	Value	Year
Pettitt's test	p-value (Two-tailed)	0.001	1990-2019
MK test	p-value (Two-tailed)	0.60	1990-1998
		0.02	1999-2019
Sen's slope	Slope-value	0.12	1990-1998
		-0.24	1999-2019

4.5.5 Effective Live Storage

Maintaining consistent electricity production at the Kariba South Hydropower Station requires efficient live storage, particularly during dry spells when water inflows are minimal. Live storage serves as a crucial buffer against climate variability, enabling controlled water release to sustain generation capacity. Sufficient storage is essential to meet energy demands while accommodating the erratic river inflows exacerbated by climate change. The minimum live

storage required for hydropower generation at Kariba is 0.053 BCM, with the full supply live storage totalling 64.7984 BCM. However, the sustainability of hydropower production may be threatened by insufficient live storage due to increased evaporation, sedimentation, and disruptions in precipitation patterns.

The highest recorded effective live storage between 1990 and 2023 was 60.1519 billion cubic meters (BCM) on December 31, 2010. In contrast, the lowest adequate live storage was recorded at 0.4983 BCM on July 31, 2022. When storage levels fall below this threshold, hydropower generation at Kariba Station is significantly impacted, potentially leading to a complete shutdown, as observed in 2022 (Cyril Zenda, 2024). Throughout this period, the live storage has never reached the full supply live storage level. Figure 4.35 illustrates a cyclic pattern of highs and lows, indicating seasonal variations in upstream rainfall patterns within the Kariba Subbasin and water inflows into the Kariba Reservoir. During peak storage levels, Kariba Station experienced high and stable power generation. However, during low effective live storage periods, such as in 1992, 1996, and 2022, power generation was severely affected, resulting in load shedding and power outages.

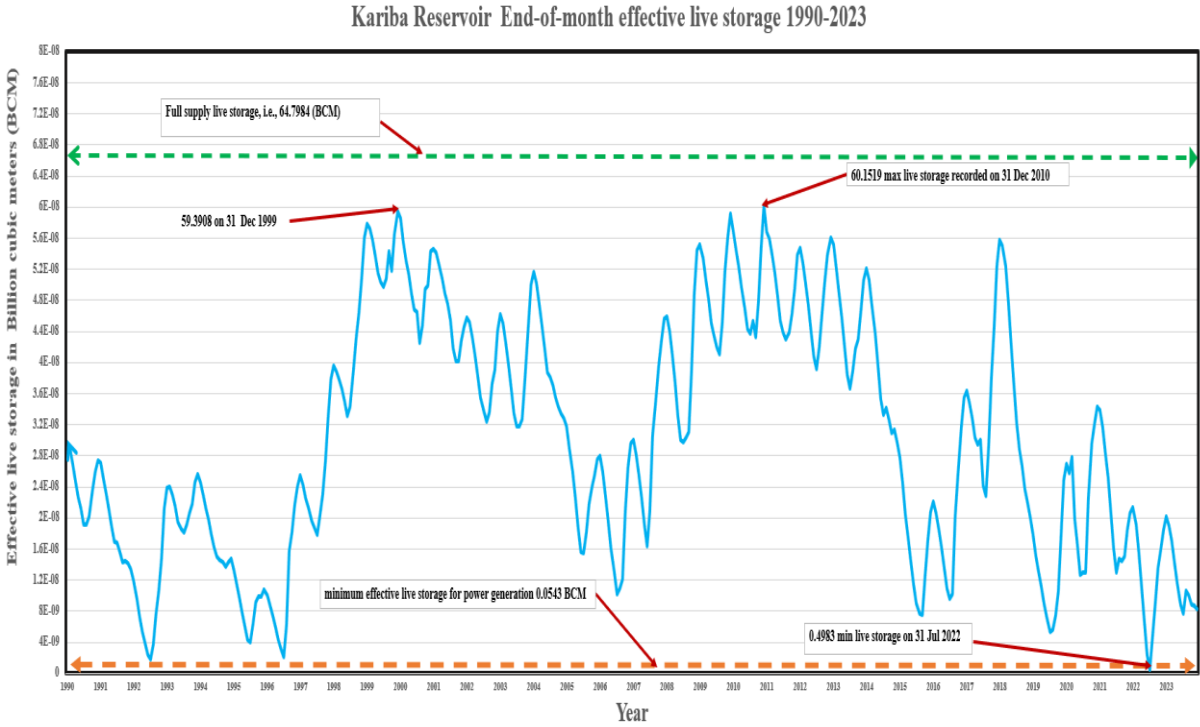


Figure 4.35: Kariba Effective live storage in billion cubic meters BCM 1990-2023

4.5.6 Future Projections

4.5.6.1 Projected Annual Mean Maximum Temperature

The projected annual mean maximum temperature under the SSP245 scenario shown in Figure 4.33 ranges between approximately 28°C and 34°C, with a relatively stable increase over time. Although the models and ensemble mean under SSP245 show year-to-year fluctuations reflecting natural climate variability, no strong, sustained upward trend exists. Projections on annual maximum temperature indicate that maximum temperatures will remain relatively stable from 2041 to 2065, as shown in Figure 4.36, with only a slight increase in the projected annual mean maximum temperature. The projected annual mean temperature range for the four models over the study period ranges from 29.66 °C to 36.76 °C. In contrast, the mean maximum temperature under the SSP585 scenario Figure 4.37 shows a consistent rise across all four models (CNRM-CM6, IPSL-CM6A-LR, MIROC6, MPI-ESM1-2-LR) and the ensemble mean. The ensemble mean indicates a warming of 2-3°C between 2041 and 2070, with individual models suggesting a higher potential increase. The near-term projections (2041-2045) show relative stability with a slight upward trend, but from 2045 onwards, the rate of warming accelerates, indicating a pronounced increase as the century progresses. This trend aligns with the findings of Almazroui et al. (2020), who projected an increase of 1.5°C (2.3°C) under SSP245 and 1.8°C (4.4°C) under SSP585 for Africa. The projected annual mean maximum temperature under SSP585 585 will range from 27.56 °C to 34.18 °C. According to Moses (2024), under the SSP585 scenario, a significant rise in temperatures is expected throughout the 21st century for Southern Africa. The significant warming under SSP585 increases the risk of hydropower generation at the Kariba South Hydropower Station because of increased water demand, higher evaporation rates, and possible changes in precipitation patterns. Firm adaptation plans and potentially different approaches to water management are required in this situation.

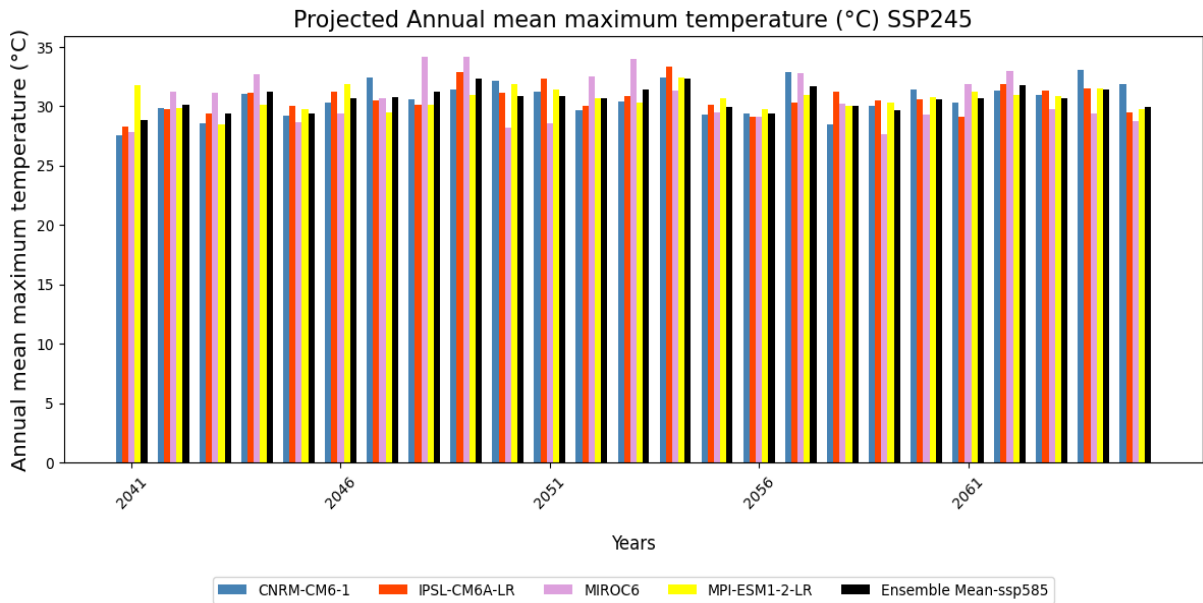


Fig 4.36: Projected annual mean maximum temperature (°C) SSP245 2041-2065

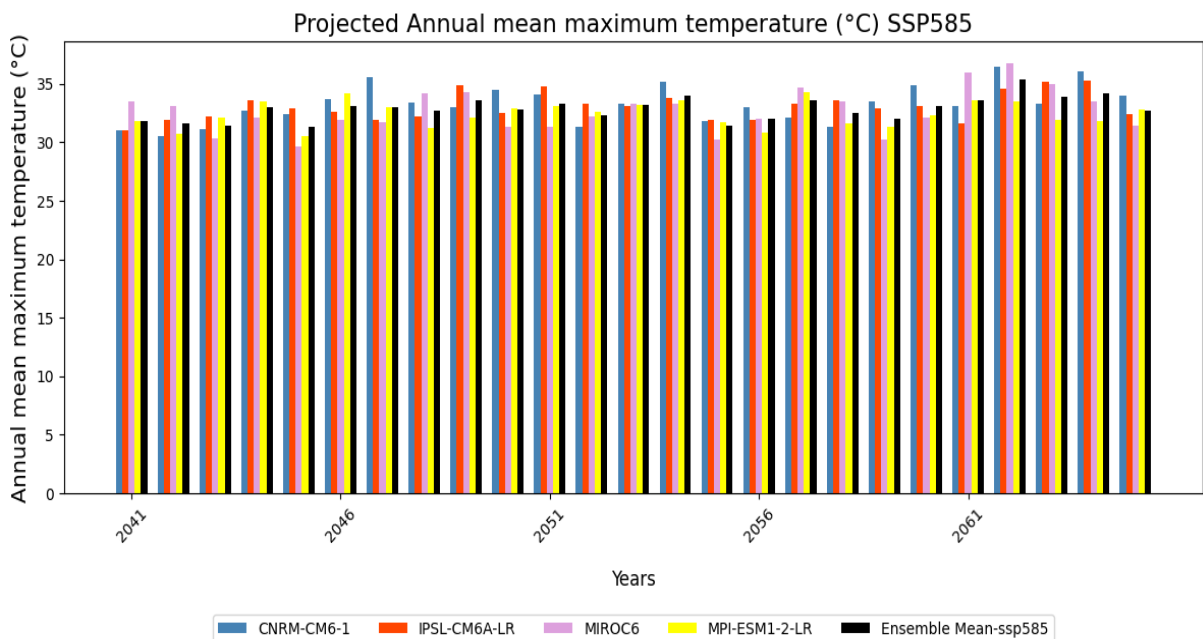


Fig 4.37: Projected annual mean maximum temperature (°C) SSP585 2041-2065

4.5.6.2 Projected Annual Mean Minimum Temperature

The projected annual mean minimum temperature under SSP245, as shown in Figure 4.38, reveals year-to-year fluctuations across the four models, with the ensemble mean reflecting natural climate variability. The projected annual mean minimum temperature under SSP245 will range from 18.30 °C to 22.14°C. Annual mean minimum temperatures are expected to remain stable from 2041 to 2065, with only a slight potential increase. Similarly, the annual

mean minimum temperature under SSP585 shows a relatively stable trend shown in Figure 4.39, though with a subtle upward drift, with the projected annual mean minimum temperature ranging from 18.52 °C to 22.52 °C. The ensemble suggests a gradual increase over the period, albeit less pronounced than under SSP585. Higher minimum temperatures can increase evaporation rates from water bodies, particularly Lake Kariba, which reduces water availability in an already water-scarce region. Reduced water flow in rivers along the Kariba catchment due to increased evaporation and changed precipitation patterns is anticipated to lower reservoir levels and possibly reduce the Kariba South Hydropower Station's capacity to generate hydropower.

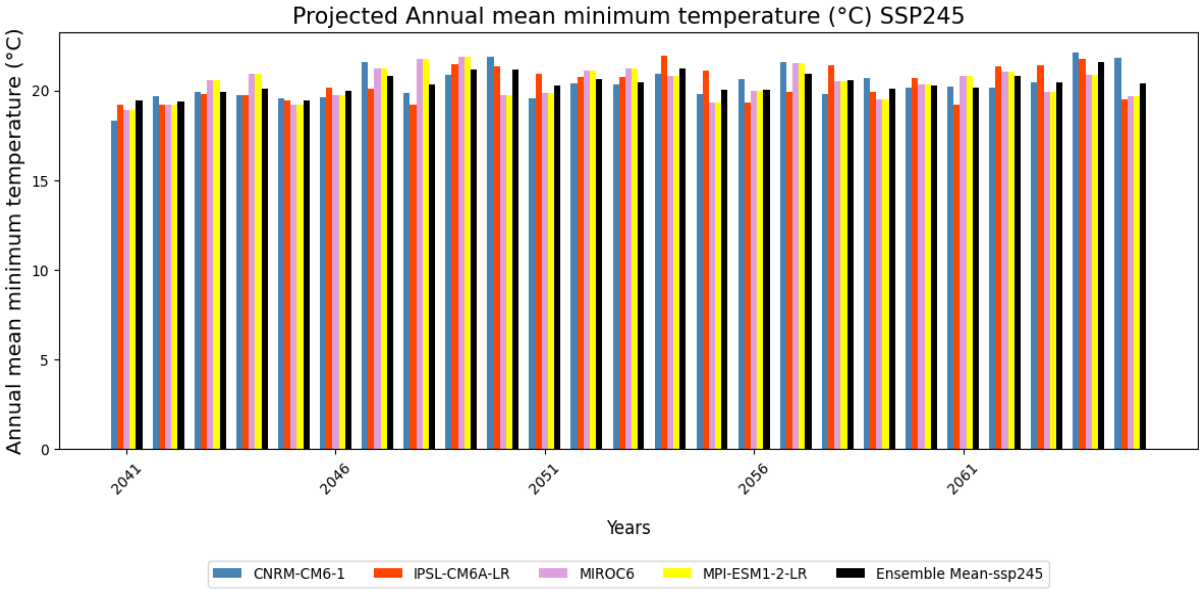


Fig 4.38: Projected annual mean minimum temperature (°C) SSP245 2041-2065

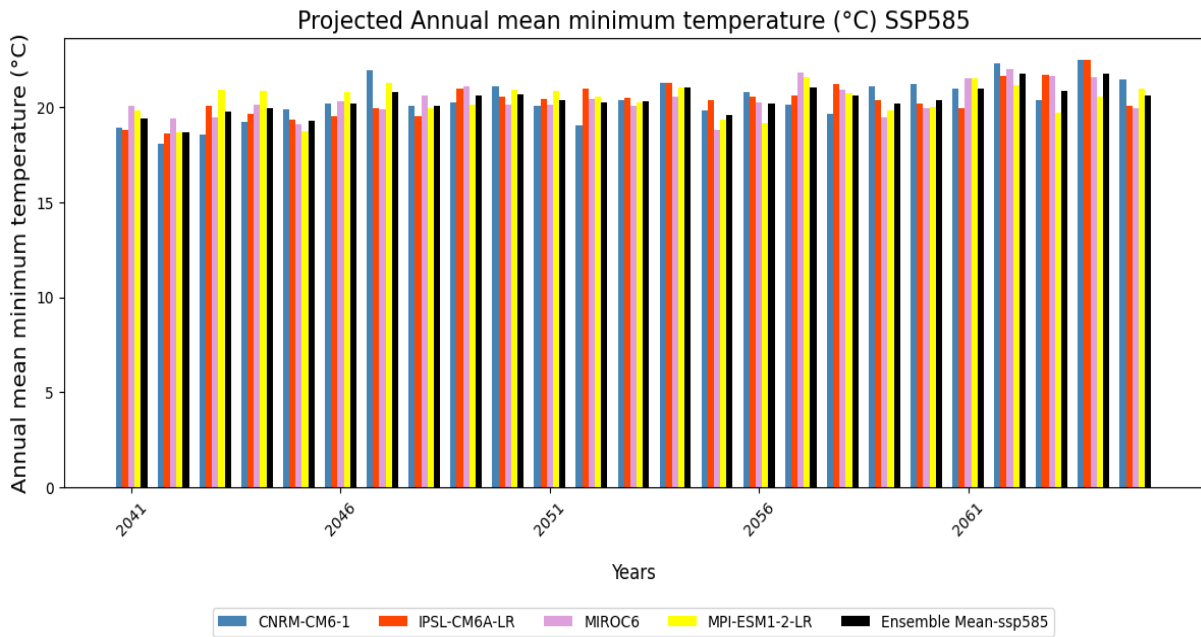


Fig 4.39: Projected annual mean minimum temperature (°C) SSP585 2041-2065

4.5.6.3 Projected Total Annual Precipitation

The projected precipitation patterns across the four GCMs indicate a reduction in annual precipitation under SSP2-4.5 and SSP5-8.5. These findings align with the results of Bobde et al. (2024), who utilized CMIP6 models to project regional changes in mean and extreme precipitation over Africa. The ensemble means of the four GCMs under SSP2-4.5 and SSP5-8.5 show a slight decrease in annual precipitation over Southern Africa. This projected decline in precipitation directly affects river discharge, as reduced rainfall diminishes inflows into the Zambezi River, ultimately lowering the water levels in the Kariba reservoir.

Figures 4.40 and 4.41 below illustrate the projected precipitation patterns for the Kariba Subbasin during the near future period (2041-2060) and the far future period (2061-2080) under SSP2-4.5 and SSP5-8.5. The northern and eastern parts of the Kariba subbasin show some areas of extremely high precipitation, while the southern part exhibits low precipitation for all models under both scenarios. The maps for the periods 2040-2060 and 2061-2080 under SSP2-4.5 and SSP5-8.5 highlight significant spatial variability in projected precipitation across the Kariba Subbasin. The slight decrease in precipitation under SSP2-4.5 will directly affect water availability, posing challenges to the reliance on hydropower for electricity generation in Zimbabwe. However, under SSP5-8.5, the projected observed decline in mean precipitation over Southern Africa will exacerbate climate change extremes, such as prolonged observed

meteorological droughts, and observed increase in the intensity but decrease in duration leading to pluvial flooding severely impacting reservoir storage levels and hydropower output at the Kariba South Hydropower Station (IPCC,2021b).

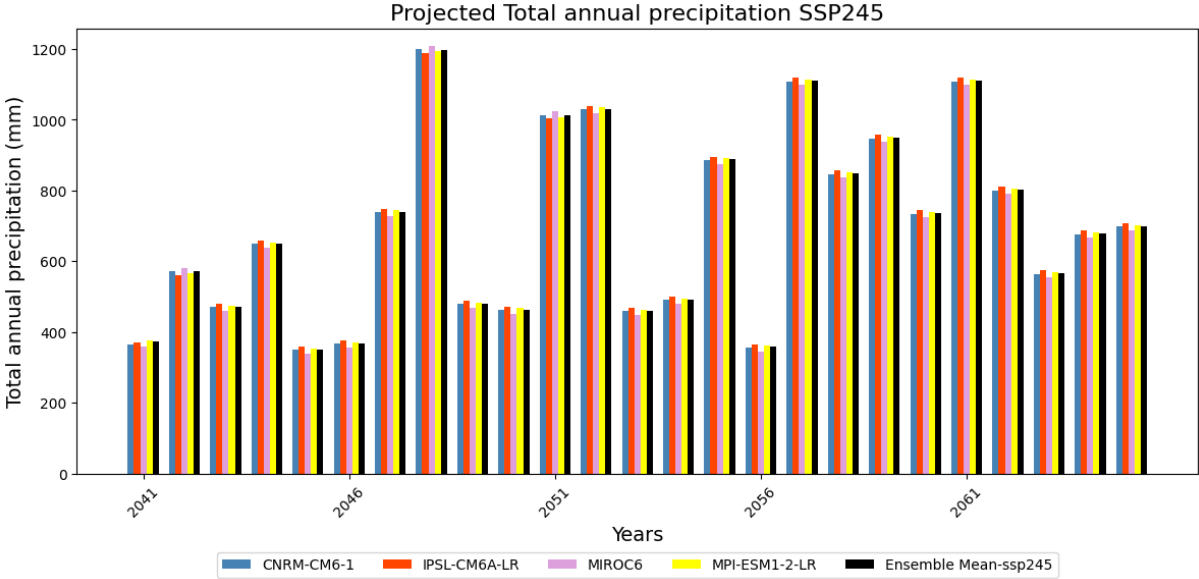


Figure 4.40: Projected future precipitation for the Kariba subbasin under 4 GCM models for the period 2041-2065

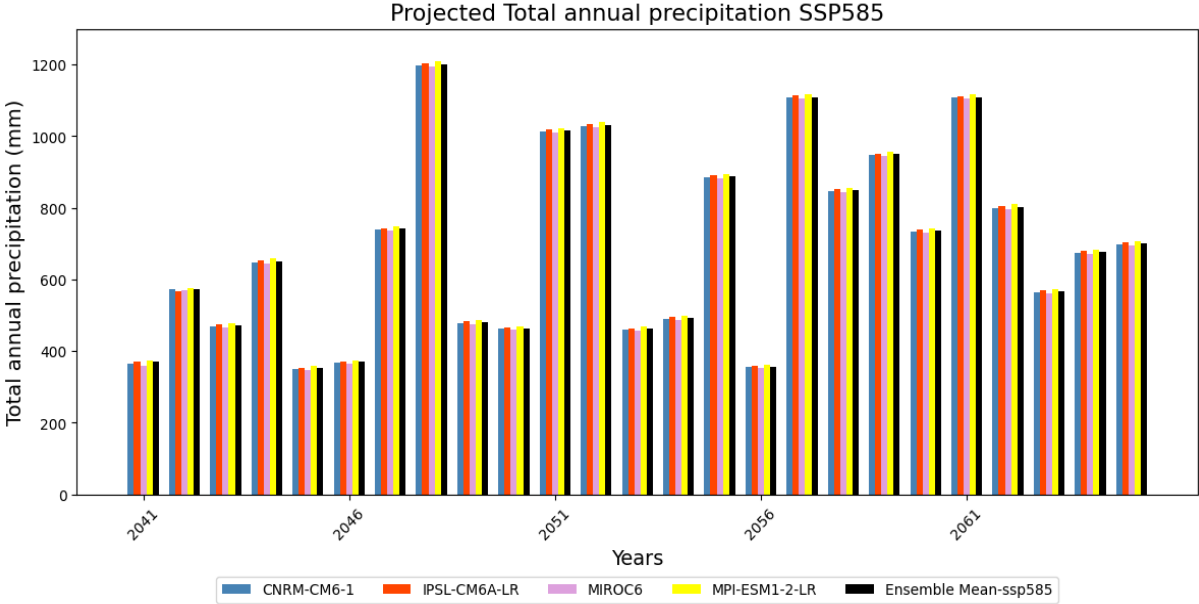


Figure 4.41: Projected Future precipitation for the Kariba subbasin under 4 GCM models for the period 2041-2061.

CHAPTER FIVE

CONCLUSION AND RECOMMENDATIONS

5.1 Conclusion

This study assessed the impact of climate change on the electricity-generating capacity of the Kariba South Hydropower Station, located in the Kariba subbasin, one of the thirteen subbasins of the Zambezi River basin. The research analysed historical trends in climate parameters, focusing on annual total precipitation, total precipitation during the rainy season, annual mean maximum temperature, and annual mean minimum temperature. It also examined future minimum and maximum temperature and precipitation projections for the Kariba Subbasin from a total of ten stations. Additionally, the study investigated hydrological trends in discharge/river flow from 1990-2019 at key locations, including Chavuma Mission, Victoria Falls (Big Tree Station), and from 2005-2019 for Ngonye Sioma Falls. The study further addressed the overall water availability at Lake Kariba and its implications for hydropower generation at the Kariba South Hydropower Station during the study period, that is, 1990-2019, and for future hydropower generation.

The annual mean maximum temperature was one of the parameters examined in this study. Temperature affects hydrological processes such as evaporation rates, runoff production, and total water availability. Results from the analysis of the annual mean maximum temperature in the study area indicate that the annual mean maximum temperature at Binga station increased from 1990 to 2019. However, this trend was not statistically significant. Similarly, Kariba station showed an increasing mean yearly maximum temperature trend, but this trend was not statistically significant. Results from the analysis of the annual mean maximum temperature from the NASA Power satellite data reviewed mixed results, with five out of the eight satellite stations exhibiting negative slope values, indicating a slight decrease in the annual mean maximum temperature, and three stations exhibiting positive slope values, indicating a slight increase in mean maximum. All the results from the eight stations from NASA Power satellite reviewed had no statistical significance at a 95 % confidence level and 5% significance level. The results suggest that the mean maximum temperature has been relatively stable during the study period 1990-2019.

An analysis of ground-based meteorological data for the annual mean minimum temperature for Binga from 1990-1998 showed a warming trend. In contrast to the period from 1999-2019, which showed a cooling trend. Kariba's annual mean minimum temperature from 1990-1997 exhibited a slight increase, while the period from 1998-2019 showed a very slight decrease, with no statistical significance in the trend. Examination of the annual mean minimum temperature from all eight satellite stations from the NASA POWER data exhibited positive slope values; however, the Mann-Kendall revealed no statistical significance in the trends at all the stations at a 95% confidence level and 5% significance level. Results from the NASA Power satellite stations reinforce the observations from ground stations (Binga and Kariba), suggesting that despite the positive slope values or localized or short-term fluctuations, the overall annual mean minimum temperature trend shows no significant change over the observed period.

The annual total precipitation and seasonal precipitation analysis for ground-based meteorological stations in the Kariba subbasin revealed positive trends of 3.2 mm/year for annual precipitation and 2.7 mm/year for seasonal precipitation at the Binga ground-based meteorological station. However, the trends were not statistically significant. The Kariba subbasin's annual and seasonal precipitation demonstrated non-significant positive and negative trends. In contrast, for Kariba, the Sen's slope negative slope values for total annual precipitation suggest a decreasing trend, while the seasonal precipitation (NDJFM) revealed a positive slope value from 1990-2019) and a positive Sen's slope value of 5.95 for seasonal total precipitation indicating an increasing trend. Despite these values, the annual and seasonal total precipitation trends were not statistically significant. Examination of the total annual precipitation of all satellite stations from NASA POWER exhibited positive Sen's slope for all stations (Bulawayo Airport, Gokwe, Gweru, Hwange National Park, Livingstone, Victoria Falls, Kasane, and Kwekwe). This widespread indication of increasing annual precipitation across the broader region is notable. However, consistent with the ground-based findings for the Kariba subbasin, the Mann-Kendall trend test revealed that most of these positive trends were not statistically significant at the 95% confidence level and 5% significance level. Only Kasane station had a statistically significant trend with a p-value of 0.4.

The river flow trends from the three hydro gauging stations, Chavuma Mission, Ngonye Rapids, and Victoria Falls, provide insights into river flow trends along the Zambezi River, which affect water availability in reservoirs such as Lake Kariba. The results from trend analysis of river flow from these hydro gauging stations for the study period 1990-2019 indicate that the changes

are not statistically significant within the analysed timeline. Natural variability, upstream water management factors, land use changes, and other factors affecting river flow may cause these trends' lack of statistical significance within the timeline; a more thorough investigation into these factors may be necessary.

Lake Kariba's effective live storage from 1990 to 2019 displays significant variations, highlighting the dynamic storage capacity of Lake Kariba. The end-of-month live storage minimum was 0.4983 billion cubic meters in July 2022, and it peaked at 60,1519 billion cubic meters in December 2010. Results from the analysis of effective live storage of Lake Kariba show that effective live storage for Kariba has multiple times fallen to near the minimum effective live storage required for hydropower generation at the Kariba South hydropower Station, which is 0.543 BCM. Overall, the research on efficient live storage demonstrates how susceptible the Kariba South Hydropower plants' hydropower generation is to drying out or extended dry spells. Effective water management techniques are essential for the Kariba South hydropower station to operate dependably.

Although longer-term changes in hydrological cycles and increased evaporation from Lake Kariba reservoir can have an impact on hydropower, the absence of statistically significant warming trends in annual mean maximum temperature between 1990 and 2019 raises the possibility that thermal stresses on the Kariba reservoir and the Kariba South Hydropower Station power plant as a whole may not have been the main factor during this study period. Climate variability can be attributed to changes in hydropower generation. Despite some signs of wet seasons within the subbasin, the precipitation trends from NASA POWER's ground-based and satellite stations from 1990 to 2019 showed no statistically significant changes, indicating stability in the subbasin's precipitation trends.

5.2 RECOMMENDATION

To properly evaluate how future climate change will affect hydrology and water resources trends in the Kariba subbasin, research should extend the study period beyond 1990-2019; this helps in understanding long-term trends in river flow and precipitation. This method will simplify identifying long-term historical trends in hydrological and climatic patterns in the subbasin. Future studies using GCMs should use an increased number of GCMs suitable for impact assessment of the Kariba subbasin, as this helps in capturing a range of possible future climate conditions, reducing reliance on a few GCM projections that might be

biased. These GCMs differ in their sensitivity to atmospheric processes, land-atmosphere interaction, and greenhouse gas emissions. The Kariba South Hydropower Station (KSHS) needs long-term datasets of more than 30 years of hydrological parameters (river flow), hydropower generation data, and key climatic parameters (temperature and precipitation) to evaluate the effects of climate change on hydropower generation. These datasets provide critical insights into how climate change has affected power generation at KSHS over time. The study also recommends that meteorological records in Zimbabwe should be made available for free or at a discounted rate to researchers contributing to the broader scientific knowledge base. Providing these records at a reduced or no cost would encourage innovation and well-informed decision-making while advancing research on important topics like climate change and its effects. Hydropower generation data also needs to be made available for researchers trying to work on climate change impact assessments on these infrastructures, which are critical to the energy domain of Zimbabwe. In domains like climate science and hydropower, where long-term datasets are required to make significant inferences and implement practical solutions, researchers must have access to such data.

REFERENCES

- Ajiboye, F. (2013). Small hydro power potential capacity estimation for provision of rural electricity in Nigeria. *Acta Technica Corvininensis - Bulletin of Engineering*, 6(2), 117–120.
- Almazroui, M., Saeed, F., Saeed, S., Nazrul Islam, M., Ismail, M., Klutse, N. A. B., & Siddiqui, M. H. (2020). Projected Change in Temperature and Precipitation Over Africa from CMIP6. *Earth Systems and Environment*, 4(3), 455–475. <https://doi.org/10.1007/s41748-020-00161-x>.
- Anaza, S. O., Abdulazeez, M. S., Yisah, Y. A., Yusuf, Y. O., Salawu, B. U., & Momoh, S. U. (2017). *Micro Hydro-Electric Energy Generation—An Overview*. American Journal of Engineering Research (AJER), 6, 5–12. www.ajer.org.
- Bailey, M., & Dorothy. (2020). *Climate Profiles of Countries in Southern Africa : Zimbabwe. 2021, 2016–2021*.
- Basson, J. (2011). *Kariba South Extension Project Janus Basson*. <https://www.esi-africa.com/wp-content/uploads/>.
- Bhardwaj, S. (2015). *Climate Modelling: Basics Lecture at APN-TERI Student Seminar*.
- Bhowmik, R. Das, Sankarasubramanian, A., Sinha, T., Patskoski, J., Mahinthakumar, G., & Kunkel, K. E. (2017). Multivariate downscaling approach preserving cross correlations across climate variables for projecting hydrologic fluxes. *Journal of Hydrometeorology*, 18(8), 2187–2205. <https://doi.org/10.1175/JHM-D-16-0160.1>.
- Bradshaw, C. D., Pope, E., Kay, G., Davie, J. C. S., Cottrell, A., Bacon, J., Cosse, A., Dunstone, N., Jennings, S., Challinor, A., Chapman, S., Birch, C., Sallu, S. M., King, R., & Macdiarmid, J. (2022). Unprecedented climate extremes in South Africa and implications for maize production. *Environmental Research Letters*, 17(8). <https://doi.org/10.1088/1748-9326/ac816d>.
- Caron, J., & Markusen, J. R. (2016). *Zambezi River Basin Atlas*.
- Chan, D., & Wu, Q. (2015). Significant anthropogenic-induced changes of climate classes since 1950. *Scientific Reports*, 5(4), 1–8. <https://doi.org/10.1038/srep13487>.
- Chilkoti, V., Boliseti, T., & Balachandar, R. (2017). Climate change impact assessment on hydropower generation using multi-model climate ensemble. *Renewable Energy*, 109, 510–517. <https://doi.org/10.1016/j.renene.2017.02.041>.
- Davidson, O. (2014). Summary for Policymakers Summary for Policymakers. *International Panel on Climate Change, April 2007*, 1–161.
- Davis-Reddy, C. L., & Vincent, K. (2017). *Climate Change Handbook for Southern Africa Climate*.
- Demory, M. E., Berthou, S., Fernández, J., Sørland, S. L., Brogli, R., Roberts, M. J., Beyerle, U., Seddon, J., Haarsma, R., Schär, C., Buonomo, E., Christensen, O. B., Ciarlo, J. M., Fealy, R., Nikulin, G., Peano, D., Putrasahan, D., Roberts, C. D., Senan, R., ... Vautard, R. (2020).

European daily precipitation according to EURO-CORDEX regional climate models (RCMs) and high-resolution global climate models (GCMs) from the High-Resolution Model Intercomparison Project (HighResMIP). *Geoscientific Model Development*, 13(11), 5485–5506. <https://doi.org/10.5194/gmd-13-5485-2020>.

Diop, S., Scheren, P., & Niang, A. (2021). Climate change and water resources in Africa. In S. D. · P. S. · A. Niang (Ed.), *Climate Change and Water Resources in Africa: Perspectives and Solutions Towards an Imminent Water Crisis*. © Springer Nature Switzerland AG 2021. https://doi.org/10.1007/978-3-030-61225-2_15.

Ebi, K. L., Vanos, J., Baldwin, J. W., Bell, J. E., Hondula, D. M., Errett, N. A., Hayes, K., Reid, C. E., Saha, S., Spector, J., & Berry, P. (2020). Extreme Weather and Climate Change: Population Health and Health System Implications. *Annual Review of Public Health*, 42, 293–315. <https://doi.org/10.1146/annurev-publhealth-012420-105026>.

Eden, J. M., & Widmann, M. (2014). Downscaling of GCM-simulated precipitation using model output statistics. *Journal of Climate*, 27(1), 312–324. <https://doi.org/10.1175/JCLI-D-13-00063.1>.

Edwards, P. N. (2011). History of climate modeling. *Wiley Interdisciplinary Reviews: Climate Change*, 2(1), 128–139. <https://doi.org/10.1002/wcc.95>.

Eyring, V., Bony, S., Meehl, G. A., Senior, C. A., Stevens, B., Stouffer, R. J., & Taylor, K. E. (2016). Overview of the Coupled Model Intercomparison Project Phase 6 (CMIP6) experimental design and organization. *Geoscientific Model Development*, 9(5), 1937–1958. <https://doi.org/10.5194/gmd-9-1937-2016>.

FAO, F. and A. O. of the U. N. (2016). AQUASTAT Country Profile –Zimbabwe. *Food and Agriculture Organization of the United Nations (FAO)*, 21. <http://www.fao.org/3/i9842en/I9842EN.pdf>.

Frischen, J., Meza, I., Rupp, D., Wietler, K., & Hagenlocher, M. (2020). Drought risk to agricultural systems in Zimbabwe: A spatial analysis of hazard, exposure, and vulnerability. *Sustainability (Switzerland)*, 12(3). <https://doi.org/10.3390/su12030752>.

Gan, T. Y., Ito, M., Hülsmann, S., Qin, X., Lu, X. X., Liang, S. Y., Rutschman, P., Disse, M., & Koivusalo, H. (2016). Possible climate change/variability and human impacts, vulnerability of drought-prone regions, water resources, and capacity building for Africa. *Hydrological Sciences Journal*, 61(7), 1209–1226. <https://doi.org/10.1080/02626667.2015.1057143>.

Gettelman, A., & Rood, R. B. (2016). Demystifying Climate Models: A User's Guide to Earth System Models. In *Earth Systems Data and Models* (Vol. 2).

Gillett, N. P., Kirchmeier-Young, M., Ribes, A., Shiogama, H., Hegerl, G. C., Knutti, R., Gastineau, G., John, J. G., Li, L., Nazarenko, L., Rosenbloom, N., Seland, Ø., Wu, T., Yukimoto, S., & Ziehn, T. (2021). Constraining human contributions to observed warming since the pre-industrial period. *Nature Climate Change*, 11(3), 207–212. <https://doi.org/10.1038/s41558-020-00965-9>.

Giorgi, F. (2019). Thirty Years of Regional Climate Modeling: Where Are We and Where Are We Going Next? *Journal of Geophysical Research: Atmospheres*, 124(11), 5696–5723. <https://doi.org/10.1029/2018JD030094>.

- Goharian, E., Burian, S. J., Bardsley, T., & Strong, C. (2016). Incorporating Potential Severity into Vulnerability Assessment of Water Supply Systems under Climate Change Conditions. *Journal of Water Resources Planning and Management*, 142(2), 1–12. [https://doi.org/10.1061/\(asce\)wr.1943-5452.0000579](https://doi.org/10.1061/(asce)wr.1943-5452.0000579).
- Goosse, H., Barriat, P. Y., Lefebvre, W., Loutre, M. F., & Zunz, V. (2010). Chapter 3 . Modelling the climate system. *Introduction to Climate Dynamics and Climate Modelling*, 59–86.
- Government of Zimbabwe. (2016). *Zimbabwe third national communication to the United Nations Framework Convention on Climate Change*.
- Government of Zimbabwe. (2020). *Government of Zimbabwe Zimbabwe Long-term Low Greenhouse Gas Emission Development Strategy (2020-2050)*.
- Gumbo, A. D., Kapangaziwiri, E., Chikoore, H., & Pienaar, H. (2021). Assessing water resources availability in headwater sub-catchments of Pungwe River Basin in a changing climate. *Journal of Hydrology: Regional Studies*, 35(May), 100827. <https://doi.org/10.1016/j.ejrh.2021.100827>.
- Hagemann, S., Chen, C., Clark, D. B., Folwell, S., Gosling, S. N., Haddeland, I., Hanasaki, N., Heinke, J., Ludwig, F., Voss, F., & Wiltshire, A. J. (2013). Climate change impact on available water resources obtained using multiple global climate and hydrology models. *Earth System Dynamics*, 4(1), 129–144. <https://doi.org/10.5194/esd-4-129-2013>.
- Hamududu, B. H., & Killingtveit, Å. (2016). Hydropower production in future climate scenarios; the case for the Zambezi River. *Energies*, 9(7), 1–18. <https://doi.org/10.3390/en9070502>.
- Hoesly, R. M., Smith, S. J., Feng, L., Klimont, Z., Janssens-Maenhout, G., Pitkanen, T., Seibert, J. J., Vu, L., Andres, R. J., Bolt, R. M., Bond, T. C., Dawidowski, L., Kholod, N., Kurokawa, J. I., Li, M., Liu, L., Lu, Z., Moura, M. C. P., O'Rourke, P. R., & Zhang, Q. (2018). Historical (1750-2014) anthropogenic emissions of reactive gases and aerosols from the Community Emissions Data System (CEDS). *Geoscientific Model Development*, 11(1), 369–408. <https://doi.org/10.5194/gmd-11-369-2018>.
- Hughes, D. A., & Farinosi, F. (2020). Assessing development and climate variability impacts on water resources in the Zambezi River basin: Simulating future scenarios of climate and development. *Journal of Hydrology: Regional Studies*, 32, 100763. <https://doi.org/10.1016/j.ejrh.2020.100763>.
- IEA. (2020). World Energy Outlook 2020 – Analysis. *OECD International Energy Agency, October*, 1–810. <https://www.iea.org/reports/world-energy-outlook-2020>.
- IHA. (2022). Hydropower Status Report. *International Hydropower Association*, 52. <https://www.hydropower.org/publications/2022-hydropower-status-report>.
- IPCC. (1990). Climate and water. In *Eos, Transactions American Geophysical Union* (Vol. 71, Issue 12). <https://doi.org/10.1029/90EO00112>.
- IPCC. (2014). Climate Change 2014 Synthesis Report. In *Journal of Crystal Growth* (Vol. 218, Issue 2). [https://doi.org/10.1016/S0022-0248\(00\)00575-3](https://doi.org/10.1016/S0022-0248(00)00575-3).

IPCC. (2021a). IPCC press release - Climate change widespread, rapid, and intensifying - IPCC. *IPCC Intergovernmental Panel on Climate Change, August 2021*, 1–6.

Intergovernmental Panel on Climate Change (IPCC). (2021). *Regional fact sheet – Africa*. In *Climate change 2021: The physical science basis. Contribution of Working Group I to the Sixth Assessment Report of the Intergovernmental Panel on Climate Change* (Fact Sheet No. 6). https://www.ipcc.ch/report/ar6/wg1/downloads/factsheets/IPCC_AR6_WGI_Regional_Fact_Sheet_Africa.pdf

Intergovernmental Panel on Climate Change (IPCC). (2021b). *Regional fact sheet - Africa*. In *Climate change 2021: The physical science basis* (6th Assessment Report, p. 2). IPCC. https://www.ipcc.ch/report/ar6/wg1/downloads/factsheets/IPCC_AR6_WGI_Regional_Fact_Sheet_Africa.pdf.

IPPC. (2014). Summary for Policymakers Summary for Policymakers. *International Panel on Climate Change*, 1–161. <http://ebooks.cambridge.org/ref/id/CBO9781107415416A011>.

Ivey, J. (2018). Southern Africa. *The British Empire: A Historical Encyclopedia: Volumes 1-2*, 1–2(May), 238–240. https://doi.org/10.1163/9789004367630_044.

Jang, S., & Kavvas, M. L. (2015). Downscaling Global Climate Simulations to Regional Scales: Statistical Downscaling versus Dynamical Downscaling. *Journal of Hydrologic Engineering*, 20(1), 1–18. [https://doi.org/10.1061/\(asce\)he.1943-5584.0000939](https://doi.org/10.1061/(asce)he.1943-5584.0000939).

Jiang, D., & Wang, K. (2019). The role of satellite-based remote sensing in improving simulated streamflow: A review. *Water (Switzerland)*, 11(8), 10–14. <https://doi.org/10.3390/w11081615>.

Jubb, I., Canadell, P., & Dix, M. (2013). Representative Concentration Pathways. Australian Government, Department of the Environment. *Australian Climate Change Science Program*, 75(June, 2010), 1–19.

Kamal, S., Jan, A., Ullah, M., Ali, A., & Khan, S. (2021). Impact of Affordable and Clean Energy (SDG 7) on Significant SDGs. *International Journal of Engineering Works*, 8(03), 103–111. <https://doi.org/10.34259/ijew.21.803103111>.

Karamouz, M., Nazif, S., & Zahmatkesh, Z. (2013). Self-Organizing Gaussian-Based Downscaling of Climate Data for Simulation of Urban Drainage Systems. *Journal of Irrigation and Drainage Engineering*, 139(2), 98–112. [https://doi.org/10.1061/\(asce\)ir.1943-4774.0000500](https://doi.org/10.1061/(asce)ir.1943-4774.0000500).

Kariba South Power Station. (n.d.). *Zimbabwe Power Company*, from <https://www.zpc.co.zw/powerstations/2/kariba-south-power-station>. Accessed on November 18, 2024.

Kattsov, V., Federation, R., Reason, C., Africa, S., Uk, A. A., Uk, T. A., Baehr, J., Uk, A. B., Catto, J., Canada, J. S., & Uk, A. S. (2013). Evaluation of climate models. *Climate Change 2013 the Physical Science Basis: Working Group I Contribution to the Fifth Assessment Report of the Intergovernmental Panel on Climate Change*, 9781107057, 741–866. <https://doi.org/10.1017/CBO9781107415324.020>.

Killingtveit, Å. (2018). Hydropower. In *Managing Global Warming: An Interface of Technology and Human Issues*. <https://doi.org/10.1016/B978-0-12-814104-5.00008-9>.

- Kling, H., Stanzel, P., & Preishuber, M. (2014). Impact modelling of water resources development and climate scenarios on Zambezi River discharge. *Journal of Hydrology: Regional Studies*, 1, 17–43. <https://doi.org/10.1016/j.ejrh.2014.05.002>.
- Kotlarski, S., Keuler, K., Christensen, O. B., Colette, A., Déqué, M., Gobiet, A., Goergen, K., Jacob, D., Lüthi, D., Van Meijgaard, E., Nikulin, G., Schär, C., Teichmann, C., Vautard, R., Warrach-Sagi, K., & Wulfmeyer, V. (2014). Regional climate modeling on European scales: A joint standard evaluation of the EURO-CORDEX RCM ensemble. *Geoscientific Model Development*, 7(4), 1297–1333. <https://doi.org/10.5194/gmd-7-1297-2014>.
- Kuriqi, A., Pinheiro, A. N., Sordo-Ward, A., & Garrote, L. (2019). Flow regime aspects in determining environmental flows and maximising energy production at run-of-river hydropower plants. *Applied Energy*, 256, 113980. <https://doi.org/10.1016/j.apenergy.2019.113980>.
- Kusangaya, S., Warburton, M. L., Archer van Garderen, E., & Jewitt, G. P. W. (2014). Impacts of climate change on water resources in southern Africa: A review. *Physics and Chemistry of the Earth*, 67–69, 47–54. <https://doi.org/10.1016/j.pce.2013.09.014>.
- Leggett, J., Pepper, W. J., & Swart, R. J. (1992). *Climate Change 1992: The Supplementary Report to the IPCC Scientific Assessment, Section A3 - Emissions Scenarios for the IPCC an Update*. 73–94.
- Mabhaudhi, T., Mpandeli, S., Nhamo, L., Chimonyo, V. G. P., Nhemachena, C., Senzanje, A., Naidoo, D., & Modi, A. T. (2018). Prospects for improving irrigated agriculture in Southern Africa: Linking water, energy and food. *Water (Switzerland)*, 10(12), 1–16. <https://doi.org/10.3390/w10121881>.
- Maraun, D., Wetterhall, F., Ireson, A. M., Chandler, R. E., Kendon, E. J., Widmann, M., Brienen, S., Rust, H. W., Sauter, T., Themel, M., Venema, V. K. C., Chun, K. P., Goodess, C. M., Jones, R. G., Onof, C., Vrac, M., & Thiele-Eich, I. (2010). Precipitation downscaling under climate change: Recent developments to bridge the gap between dynamical models and the end user. *Reviews of Geophysics*, 48(3), 1–34. <https://doi.org/10.1029/2009RG000314>.
- Mazvimavi, D., & Wolski, P. (2006). Long-term variations of annual flows of the Okavango and Zambezi Rivers. *Physics and Chemistry of the Earth*, 31(15–16), 944–951. <https://doi.org/10.1016/j.pce.2006.08.016>.
- Meinshausen, M., Nicholls, Z. R. J., Lewis, J., Gidden, M. J., Vogel, E., Freund, M., Beyerle, U., Gessner, C., Nauels, A., Bauer, N., Canadell, J. G., Daniel, J. S., John, A., Krummel, P. B., Luderer, G., Meinshausen, N., Montzka, S. A., Rayner, P. J., Reimann, S., ... Wang, R. H. J. (2020). The shared socio-economic pathway (SSP) greenhouse gas concentrations and their extensions to 2500. *Geoscientific Model Development*, 13(8), 3571–3605. <https://doi.org/10.5194/gmd-13-3571-2020>.
- Meixner, T., Manning, A. H., Stonestrom, D. A., Allen, D. M., Ajami, H., Blasch, K. W., Brookfield, A. E., Castro, C. L., Clark, J. F., Gochis, D. J., Flint, A. L., Neff, K. L., Niraula, R., Rodell, M., Scanlon, B. R., Singha, K., & Walvoord, M. A. (2016). Implications of projected climate change for groundwater recharge in the western United States. *Journal of Hydrology*, 534, 124–138. <https://doi.org/10.1016/j.jhydrol.2015.12.027>.
- Meyers, S. R., & Malinverno, A. (2018). Proterozoic Milankovitch cycles and the history of the

solar system. *Proceedings of the National Academy of Sciences of the United States of America*, 115(25), 6363–6368. <https://doi.org/10.1073/pnas.1717689115>.

Ministry of Environment, Climate, Tourism and Hospitality Industry. (2020). *Zimbabwe's First Biennial Update Report to the UNFCCC*. 82. <https://unfccc.int/documents/307389>.

Moran, E. F., Lopez, M. C., Moore, N., Müller, N., & Hyndman, D. W. (2018). Sustainable hydropower in the 21st century. *Proceedings of the National Academy of Sciences of the United States of America*, 115(47), 11891–11898. <https://doi.org/10.1073/pnas.1809426115>.

Moses, O. (2024). Projected changes in rainfall and temperature using CMIP6 models over the Okavango River basin, southern Africa. *Theoretical and Applied Climatology*, 155(6), 5337–5351. <https://doi.org/10.1007/s00704-024-04950-6>.

Mosley, L. M. (2015). Drought impacts on the water quality of freshwater systems: review and integration. *Earth-Science Reviews*, 140, 203–214. <https://doi.org/10.1016/j.earscirev.2014.11.010>.

Mphale, K., Adedoyin, A., Nkoni, G., Ramaphane, G., Wiston, M., & Chimidza, O. (2018). Analysis of temperature data over semi-arid Botswana: trends and break points. *Meteorology and Atmospheric Physics*, 130(6), 701–724. <https://doi.org/10.1007/s00703-017-0540-y>.

Muchuru, S., Botai, C. M., Botai, J. O., & Adeola, A. M. (2015). The hydrometeorology of the kariba catchment area based on the probability distributions. *Earth Interactions*, 19(4), 1–18. <https://doi.org/10.1175/EI-D-14-0019.1>.

Mukheibir, P. (2013). Potential consequences of projected climate change impacts on hydroelectricity generation. *Climatic Change*, 121(1), 67–78. <https://doi.org/10.1007/s10584-013-0890-5>.

Mwangala, B. B., Banda, K., Chimuka, L., Uchida, Y., & Nyambe, I. (2024). Analysis of streamflow and rainfall trends and variability over the Lake Kariba catchment, Upper Zambezi Basin. *Hydrology Research*, 55(7), 683–710. <https://doi.org/10.2166/nh.2024.122>.

Ndhlovu, G. Z., & Woyessa, Y. E. (2021). Evaluation of streamflow under climate change in the Zambezi River basin of Southern Africa. *Water (Switzerland)*, 13(21). <https://doi.org/10.3390/w13213114>.

Nguyen, P. L., Min, S. K., & Kim, Y. H. (2021). Combined impacts of the El Niño-Southern Oscillation and Pacific Decadal Oscillation on global droughts assessed using the standardized precipitation evapotranspiration index. *International Journal of Climatology*, 41(S1), E1645–E1662. <https://doi.org/10.1002/joc.6796>.

Oyerinde, G. T., Wisser, D., Hountondji, F. C. C., Odofoin, A. J., Lawin, A. E., Afouda, A., & Diekkrüger, B. (2016). Quantifying uncertainties in modeling climate change impacts on hydropower production. *Climate*, 4(3). <https://doi.org/10.3390/cli4030034>.

Palaniswami, S., & Muthiah, K. (2018). Change point detection and trend analysis of rainfall and temperature series over the Vellar River basin. *Polish Journal of Environmental Studies*, 27(4), 1673–1682. <https://doi.org/10.15244/pjoes/77080>.

Pedersen, J. T. S., van Vuuren, D., Gupta, J., Santos, F. D., Edmonds, J., & Swart, R. (2022).

- IPCC emission scenarios: How did critiques affect their quality and relevance, 1990–2022? *Global Environmental Change*, 75(April), 102538. <https://doi.org/10.1016/j.gloenvcha.2022.102538>.
- Perkins, S. E. (2015). A review on the scientific understanding of heatwaves- Their measurement, driving mechanisms, and changes at the global scale. *Atmospheric Research*, 164–165, 242–267. <https://doi.org/10.1016/j.atmosres.2015.05.014>.
- Pettitt. (1979). A Non-parametric Approach to the Problem. *Applied Statistics*, 28(2), 126–135.
- Post, E., Alley, R. B., Christensen, T. R., Macias-Fauria, M., Forbes, B. C., Gooseff, M. N., Iler, A., Kerby, J. T., Laidre, K. L., Mann, M. E., Olofsson, J., Stroeve, J. C., Ulmer, F., Virginia, R. A., & Wang, M. (2019). The polar regions in a 2°C warmer world. *Science Advances*, 5(12). <https://doi.org/10.1126/sciadv.aaw9883>.
- Räty, O., Räisänen, J., & Ylhäisi, J. S. (2014). Evaluation of delta change and bias correction methods for future daily precipitation: Intermodel cross-validation using ENSEMBLES simulations. *Climate Dynamics*, 42(9–10), 2287–2303. <https://doi.org/10.1007/s00382-014-2130-8>.
- Ray, S., Das, S. S., Mishra, P., & Al-Khatib, A. M. G. (2021). Time Series SARIMA Modelling and Forecasting of Monthly Rainfall and Temperature in the South Asian Countries. *Earth Systems and Environment*, 5(3), 531–546. <https://doi.org/10.1007/s41748-021-00205-w>.
- Rebecca Lindsey, & Luann Dahlman. (2023). Climate Change: Global Temperature. <https://www.climate.gov/news-features/understanding-climate/climate-change-global-temperature>, 1–5.
- Renewables - Energy System - IEA*. (n.d.). IEA. <https://www.iea.org/energy-system/renewables>. Accessed on 17 November 2024.
- Republic of Zimbabwe. (2021). Zimbabwe’s Second Voluntary National Review (VNR). *SDG Knowledge Platform. Voluntary National Reviews Database*, 1–144. <https://bit.ly/3zkajcy>.
- Sabater, S., Freixa, A., Jiménez, L., López-Doval, J., Pace, G., Pascoal, C., Perujo, N., Craven, D., & González-Trujillo, J. D. (2023). Extreme weather events threaten biodiversity and functions of river ecosystems: evidence from a meta-analysis. *Biological Reviews*, 98(2), 450–461. <https://doi.org/10.1111/brv.12914>.
- SAPP. (2021). *South African Power Pool - 2021 Annual Report*. 1–88.
- Schlosser, C. A., & Strzepek, K. (2015). Regional climate change of the greater Zambezi River Basin: a hybrid assessment. *Climatic Change*, 130(1), 9–19. <https://doi.org/10.1007/s10584-014-1230-0>.
- Schoof, J. T. (2013). Statistical downscaling in climatology. *Geography Compass*, 7(4), 249–265. <https://doi.org/10.1111/gec3.12036>.
- Serdeczny, O., Adams, S., Baarsch, F., Coumou, D., Robinson, A., Hare, W., Schaeffer, M., Perrette, M., & Reinhardt, J. (2017). Climate change impacts in Sub-Saharan Africa: from physical changes to their social repercussions. *Regional Environmental Change*, 17(6), 1585–1600. <https://doi.org/10.1007/s10113-015-0910-2>.

- Silvestro, F., Gabellani, S., Rudari, R., Delogu, F., Laiolo, P., & Boni, G. (2015). Uncertainty reduction and parameter estimation of a distributed hydrological model with ground and remote-sensing data. *Hydrology and Earth System Sciences*, *19*(4), 1727–1751. <https://doi.org/10.5194/hess-19-1727-2015>.
- Sirisena, T. A. J. G., Maskey, S., & Ranasinghe, R. (2020). Hydrological model calibration with streamflow and remote sensing-based evapotranspiration data in a data-poor basin. *Remote Sensing*, *12*(22), 1–24. <https://doi.org/10.3390/rs12223768>.
- Smitha, P. S., Narasimhan, B., Sudheer, K. P., & Annamalai, H. (2018). An improved bias correction method of daily rainfall data using a sliding window technique for climate change impact assessment. *Journal of Hydrology*, *556*, 100–118. <https://doi.org/10.1016/j.jhydrol.2017.11.010>.
- Spalding-Fecher, R., Chapman, A., Yamba, F., Walimwipi, H., Kling, H., Tembo, B., Nyambe, I., & Cuamba, B. (2016). The vulnerability of hydropower production in the Zambezi River Basin to the impacts of climate change and irrigation development. *Mitigation and Adaptation Strategies for Global Change*, *21*(5), 721–742. <https://doi.org/10.1007/s11027-014-9619-7>.
- Spalding-Fecher, R., Joyce, B., & Winkler, H. (2017). Climate change and hydropower in the Southern African Power Pool and Zambezi River Basin: System-wide impacts and policy implications. *Energy Policy*, *103*(December 2016), 84–97. <https://doi.org/10.1016/j.enpol.2016.12.009>.
- Tarroja, B., AghaKouchak, A., & Samuelsen, S. (2016). Quantifying climate change impacts on hydropower generation and implications on electric grid greenhouse gas emissions and operation. *Energy*, *111*, 295–305. <https://doi.org/10.1016/j.energy.2016.05.131>.
- Teutschbein, C., & Seibert, J. (2012). Bias correction of regional climate model simulations for hydrological climate-change impact studies: Review and evaluation of different methods. *Journal of Hydrology*, *456–457*, 12–29. <https://doi.org/10.1016/j.jhydrol.2012.05.052>.
- Teutschbein, C., & Seibert, J. (2013). Is bias correction of regional climate model (RCM) simulations possible for non-stationary conditions. *Hydrology and Earth System Sciences*, *17*(12), 5061–5077. <https://doi.org/10.5194/hess-17-5061-2013>.
- Teweldebrihan, M. D., & Dinka, M. O. (2024). The impact of climate change on the development of water resources. *Global Journal of Environmental Science and Management*, *10*(3), 1359–1370. <https://doi.org/10.22034/gjesm.2024.03.25>.
- Trenberth, K. E. (2018). Climate change caused by human activities is happening, and it already has major consequences. *Journal of Energy and Natural Resources Law*, *36*(4), 463–481. <https://doi.org/10.1080/02646811.2018.1450895>.
- Turner, S. W. D., & Voisin, N. (2022). Simulation of hydropower at subcontinental to global scales: A state-of-the-art review. *Environmental Research Letters*, *17*(2). <https://doi.org/10.1088/1748-9326/ac4e38>.
- Umugwaneza, A., Chen, X., Liu, T., Li, Z., Uwamahoro, S., Mind'je, R., Umwali, E. D., Ingabire, R., & Uwineza, A. (2021). Future climate change impact on the Nyabugogo catchment water balance in Rwanda. *Water (Switzerland)*, *13*(24), 1–18. <https://doi.org/10.3390/w13243636>.

- Van Vliet, M. T. H., Wiberg, D., Leduc, S., & Riahi, K. (2016). Power-generation system vulnerability and adaptation to changes in climate and water resources. *Nature Climate Change*, 6(4), 375–380. <https://doi.org/10.1038/nclimate2903>.
- Wan, W., Zhao, J., Popat, E., Herbert, C., & Döll, P. (2021). Analyzing the Impact of Streamflow Drought on Hydroelectricity Production: A Global-Scale Study. *Water Resources Research*, 57(4). <https://doi.org/10.1029/2020wr028087>.
- Welch, I. (2024). The IPCC Shared Socioeconomic Pathways (SSPs): Explained, Critiqued, Replaced. *SSRN Electronic Journal*, 54, 1–40. <https://doi.org/10.2139/ssrn.4681042>.
- World Bank Climate Change Knowledge Portal. (n.d.-c). <https://climateknowledgeportal.worldbank.org/country/zimbabwe> .Accessed on 16 November 2024.
- World Bank Group. (2021). Climate Risk Profile: Zimbabwe. *Usaid, December* 1–5.
- World Energy Council. (2015). World Energy Resources: Charting the Upsurge in Hydropower Development. *World Energy Council*, 70.
- Yoro, K. O., & Daramola, M. O. (2020). CO2 emission sources, greenhouse gases, and the global warming effect. In *Advances in Carbon Capture: Methods, Technologies and Applications*. Elsevier Inc. <https://doi.org/10.1016/B978-0-12-819657-1.00001-3>.
- Zambezi River Authority. (2021). *Zambezi River Authority 2021 Annual Report*.
- ZAMCOM. (2016). *Floods and Droughts in the Zambezi River Basin: What Can Be Done? 2*. http://zambezicommission.org/sites/default/files/publication_downloads/floods-and-drought-policy-brief.pdf.
- Zenda, C. (2024, August 29). Climate change: Zambia to shut down hydropower plant as Kariba dries up. *Down to Earth*. <https://www.downtoearth.org.in/africa/climate-change-zambia-to-shut-down-hydropower-plant-as-kariba-dries-up>.
- ZERA. (2016). *ZERA 2021Annual report*. 1–23 (Accessed on 10 Jan 2025).
- Zhao, T., Bennett, J. C., Wang, Q. J., Schepen, A., Wood, A. W., Robertson, D. E., & Ramos, M. H. (2017). How suitable is quantile mapping for postprocessing GCM precipitation forecasts? *Journal of Climate*, 30(9), 3185–3196. <https://doi.org/10.1175/JCLI-D-16-0652.1>.
- ZimStat. (2024). *Zimbabwe 2022 population and housing census report* (Vol. 1, Issue 1, pp. 1-259). ZimStat.
- Zorita, E., & Von Storch, H. (1999). The analog method as a simple statistical downscaling technique: Comparison with more complicated methods. *Journal of Climate*, 12(8 PART 2), 2474–2489. [https://doi.org/10.1175/1520-0442\(1999\)012<2474:tamaas>2.0.co;2](https://doi.org/10.1175/1520-0442(1999)012<2474:tamaas>2.0.co;2).

